

**Public Interest Energy Research (PIER) Program
FINAL PROJECT REPORT**

**ADVANCED LASER IGNITION
SYSTEM INTEGRATED ARICE
SYSTEM FOR DISTRIBUTED
GENERATION IN CALIFORNIA**

Prepared for: California Energy Commission
Prepared by: Argonne National Laboratory



MAY 2012
CEC-500-2012-043

Prepared by:

Primary Author(s):
Sreenath Gupta
Raj Sekar

Argonne National Laboratory
Argonne, IL, 60439

Contract Number: 500-02-022



Prepared for:

California Energy Commission

Avtar Bining, Ph.D.
Project Manager

Mike Gravely
Office Manager
Energy Systems Research Office

Laurie ten Hope
Deputy Director
RESEARCH AND DEVELOPMENT DIVISION

Robert P. Oglesby
Executive Director

DISCLAIMER

This report was prepared as the result of work sponsored by the California Energy Commission. It does not necessarily represent the views of the Energy Commission, its employees or the State of California. The Energy Commission, the State of California, its employees, contractors and subcontractors make no warrant, express or implied, and assume no legal liability for the information in this report; nor does any party represent that the uses of this information will not infringe upon privately owned rights. This report has not been approved or disapproved by the California Energy Commission nor has the California Energy Commission passed upon the accuracy or adequacy of the information in this report.

Acknowledgments

The authors thank the California Energy Commission for the funding, support and guidance for this project. The authors would also like to thank Mr. Ron Fiskum, Technology Manager of the Advanced Reciprocating Engine Systems Program at the United States Department of Energy for co-funding this project. We also record our appreciation for the interaction with Advanced Laser Ignition System Consortium partners.

Please cite this report as follows:

Gupta, Sreenath, and Raj Sekar (Argonne National Laboratory). 2008. *Advanced Laser Ignition System Integrated ARICE System for Distributed Generation in California*. California Energy Commission, PIER Environmentally Preferred Advanced Generation Program. CEC-500-2012-043.

Preface

The California Energy Commission's Public Interest Energy Research (PIER) Program supports public interest energy research and development that will help improve the quality of life in California by bringing environmentally safe, affordable, and reliable energy services and products to the marketplace.

The PIER Program conducts public interest research, development, and demonstration (RD&D) projects to benefit California.

The PIER Program strives to conduct the most promising public interest energy research by partnering with RD&D entities, including individuals, businesses, utilities, and public or private research institutions.

PIER funding efforts are focused on the following RD&D program areas:

- Buildings End-Use Energy Efficiency
- Energy Innovations Small Grants
- Energy-Related Environmental Research
- Energy Systems Integration
- Environmentally Preferred Advanced Generation
- Industrial/Agricultural/Water End-Use Energy Efficiency
- Renewable Energy Technologies
- Transportation

Advanced Laser Ignition Integrated ARICE System for Distributed Generation in California is the final report for the Advanced Laser Ignition Integrated Advanced Reciprocating Internal Combustion Engine (ARICE) System for Distributed Generation in California project Contract number 500-02-022 conducted by Argonne National Laboratory. The information from this project contributes to PIER's Environmentally Preferred Advanced Generation Program.

For more information about the PIER Program, please visit the Energy Commission's website at www.energy.ca.gov/research/ or contact the Energy Commission at 916-654-4878.

Table of Contents

Preface:	iii
Abstract	xiii
Executive Summary	1
1.0 Introduction.....	5
1.0 Introduction.....	5
1.1. Background	5
1.2. Fundamentals of Ignition	8
1.3. Why Laser Ignition?	9
1.4. ALIS Consortium.....	10
1.5. Goals and Objectives.....	11
2.0 (Task 2.2) Natural Gas-Air Ignition Experimental Study	13
2.1. Rationale for Task 2.2.....	13
2.2. Experimental Setup	14
2.2.1. Rapid compression machine.....	14
2.2.2. Laser ignition system	17
2.2.3. Conventional ignition system.....	17
2.2.4. Operational procedure.....	18
2.3. Results and Discussion	19
2.3.1. Test Matrix.....	19
2.3.2. Ignition Limits.....	20
2.3.5. Conclusions for Task 2.2.....	24
3.0 (Task 2.3) Design of ALIS Components	25
3.1. Goals and Objectives of Task 2.3	25
3.2. Laser System	28
3.3. Laser Plugs	31
3.4. High-Power Optical Multiplexer	34

3.4.1.	Electro-Optic Modulator (Pockels Cell)	34
3.4.2.	Rotating Mirror	35
3.4.3.	Flip-flop	37
3.5.	Fiber-Optic Delivery	38
3.5.1.	Solid core fibers.....	39
3.5.2.	Hollow Glass Waveguides (HGWs)	41
3.5.3.	Advanced air-core fibers	42
3.6.	Electronic Interface.....	43
3.7.	Results and Conclusions for Task 2.3	44
4.0	(Task 2.4) Single-Cylinder Laser Ignition Studies.....	47
4.1.	Statement of Work for Task 2.4	47
4.2.	Experimental Setup	48
4.2.1.	Single-Cylinder Engine.....	48
4.2.2.	Open-Path Laser Ignition Setup	50
4.2.3.	Fiber-coupled laser ignition setup	52
4.3.	Test Matrix.....	54
4.4.	Results and Discussion for Task 2.4.....	56
4.4.1.	Full Load Comparison (15 bar BMEP).....	58
4.4.2.	Part Load Comparison (10 bar BMEP)	62
4.4.3.	Fiber-Coupled Laser Ignition Results.....	64
4.5.	Conclusions for Task 2.4.....	65
5.0	(Task 2.5) Integrate ALIS and Refine for Performance on a Multi-Cylinder Engine..	67
5.1.	Engine and Natural Gas Fueling System Installation	67
5.1.1.	Multi-cylinder engine	67
5.1.2.	Natural Gas Fueling system.....	68
5.2.	ALIS Integration	69
5.2.1.	Mechanical integration	70
5.2.2.	Electronic Integration.....	72

5.2.3.	ALIS testing	75
6.0	(Task 2.6) Performance Testing of Integrated ALIS-ARICE System	79
6.1.	Statement of Work for Task 2.6	79
6.2.	Multi-Cylinder Engine Tests.....	79
7.0	(Task 2.7) Economic Evaluation for Feasibility	81
8.0	Summary and Conclusions	83
9.0	References	85
10.0	GLOSSARY.....	87

APPENDIX A: Advanced Laser Ignition System (ALIS) Consortium

APPENDIX B: Future High-Power Optical Multiplexing Technologies

List of Figures

	<u>Page</u>
Figure 1. Comparison of Maintenance Costs for Rich-Burn and Lean-Burn Engines.	6
Figure 2. Operational Region of a Typical Lean-Burn Engine. (Courtesy: SwRI)	7
Figure 3. Ignition Limits of a Typical Fuel-air System.	8
Figure 4. Schematic of a Capacitance Discharge Ignition (CDI) System.	9
Figure 5. ALIS Development Consortium	11
Figure 6. Ignition Limits of Methane-air Mixtures Established in a Static Chamber. Initial Mixture Temperature $\sim 22^{\circ}\text{C}$	14
Figure 7. Schematic of the Rapid Compression Machine.	16
Figure 8. A Picture of Argonne’s Rapid Compression Machine.....	16
Figure 9. Schematic of the Optical Arrangement in the Laser Ignition System.....	17
Figure 10. Conventional Ignition System Cart.	18
Figure 11. Typical Pressure Traces from RCM Operation; $P_1 = 1 \text{ bar}$, $\phi = 0.7$	20
Figure 12. Measured versus Calculated Peak Combustion Pressures for Various Methane-air Mixtures, $1.0 < P_1 < 3 \text{ bar}$ and $0.5 < \phi < 1.0$	20
Figure 13. Ignition Boundaries Determined by Using an RCM.....	21
Figure 14. Minimum Required Laser Energies (MRE) for a Lens Focal Length $f = 13 \text{ mm}$ and Laser Beam Quality of $M^2 \leq 5$	22
Figure 15. Minimum Required Laser Energies for $P_2 \approx 37.7 \text{ bar}$	22
Figure 16. Ignition Delays for CDI and Laser Ignition.....	23
Figure 17. Rates of Pressure Rise for CDI and Laser Ignition.	23
Figure 18. Schematic of the Laser-Per-Cylinder Concept.	26
Figure 19. Schematic of the Multiplexed Laser Concept.....	26
Figure 20. A Commercially-Available Diode Pumped Solid State Laser (DPSSL) Model: Centurion, Manufacturer: Big Sky Laser, Inc., 100 Hz, 45 mJ/pulse.	30
Figure 21. Ray Propagation Scheme inside a Laser Plug.....	32
Figure 22. Schematic of a Two-Lens Laser Plug.....	33
Figure 23. Schematic of a Pockels Cell-Based Multiplexer [18].....	34

Figure 24. Photograph of a Pockels Cell-Based Two-Channel Multiplexer.	35
Figure 25. Schematic of a Rotating Mirror Multiplexer.	36
Figure 26. Photograph of Argonne’s Rotating Mirror Multiplexer.	36
Figure 27. Schematic of a Flip-Flop Multiplexer.	37
Figure 28. (a) Schematic of Setup to Measure the Time Response of the Flip-Flop (b) A Typical Detector Response Curve.	37
Figure 29. Schematic of Laser Refocusing Scheme at the Distal End of the Optical Fiber.	39
Figure 30. Fiber Face Laser Intensity Distribution Profiles for an Injection Scheme Using (a) Plano-Convex Lens, (b) Combination of Axicon and Plano-Convex Lens.	40
Figure 31. The Refractive Index Distribution in Two Solid Core Fibers: (a) Step-Index Fiber, and (b) Gradient-Index Fiber.	41
Figure 32. (a) Schematic of the Cross-Section of a Hollow Glass Waveguide (HGW), and (b) A Photograph Showing Spark Generation Using HGW in the Lab.	42
Figure 33. (a) Schematic of the Cross-Section of a Multi-Layer Hollow Glass Waveguide, and (b) Photograph of an Air-Core Photonic Bandgap Fiber	43
Figure 34. Schematic Diagram of the Electronic Interface	44
Figure 35. Schematic of the Control Scheme of the BSCRE Single-Cylinder Engine Using SwRI’s RPECS	49
Figure 36. Photograph Showing the Installed Laser Plug in the Combustion Chamber.	51
Figure 37. Setup for the Open-Path Laser Ignition Tests on a Large-Bore, Single-Cylinder Bombardier BSCRE-04 Engine.	51
Figure 38. Layout of the Fiber-Coupled Laser Ignition System.	52
Figure 39. Fiber-Coupled Laser Ignition System as Mounted on the Bombardier BSCRE-04 Engine.	53
Figure 40. Arbitrary Cylinder Pressure and Heat Release Comparison to Clarify Nomenclature of Combustion Parameters.	57
Figure 41. COV of IMEP versus Equivalence Ratio (EQR) at a BMEP of 15 bar.	58
Figure 42. Combustion Stability with Conventional Spark Ignition at a BMEP of 15 bar.	59
Figure 43. Combustion Stability with Laser Ignition at a BMEP of 15 bar.	59
Figure 44. BSNO _x -Brake Thermal Efficiency Tradeoff at a BMEP of 15 bar.	61
Figure 45. Cylinder Pressure Comparison.	61

Figure 46. Cylinder Pressure and Heat Release Comparison.	62
Figure 47. COV of IMEP versus Equivalence Ratio at a BMEP of 10 bar.	63
Figure 48. BSNO _x -Brake Thermal Efficiency Trade-off at a BMEP of 10 bar.	63
Figure 49. A Comparison of Burn Durations for Different Modes of Ignition.	64
Figure 50. A Photograph of the Cummins QSK-19G Engine in one of the Engine Test Cells at Argonne National Laboratory	68
Figure 51. A Schematic of the Integrated ALIS	70
Figure 52. A schematic of the Integrated ALIS Shown Installed on One Cylinder of a Multi-Cylinder Engine.	71
Figure 53. Picture of the ALIS Assembly Mounted on Argonne’s QSK-19G Engine (Top View). Laser Head on the Right is not Shown.	72
Figure 54. (a) Schematic Representation of the use of Electronic Interface in a 6-cylinder Engine, (b) Schematic Representation of the use of Electronic Interface for Lab-Scale Testing.	73
Figure 55. Functional Representation of the Electronic Interface.	74
Figure 56. Timing Diagram for 1800 rpm Operation, red Pulses Trigger Laser Power Supply # 1 While Blue Pulses Trigger Laser Power Supply # 2.	74
Figure 57. Picture of the 6-Channel ALIS Assembly on the Test rig (Top View). Also Shown are the Laser, BNC 565 Pulser and the Electronic Interface. Laser Plugs are not Visible.	75
Figure 58. Picture of Misfire Detection System.	76
Figure 59. Data From one of the Long-Term Durability Tests.	77
Figure B1. (a) Photograph of a Galvanometer-Based System. Courtesy: Cambridge Technology, Inc. (b) Use of Galvanometer for Laser Scanning [28].	1
Figure B2. Photograph of a Piezo-Based Laser Scanner. Courtesy: Physique Instrumente.	2
Figure B3. (a) Photograph of a MEMS-Based Mirror Array, and (b) Texas Instrument’s Digital Mirror Device.	2

List of Tables

	<u>Page</u>
Table 1. Performance targets for advanced reciprocating internal combustion engines	5
Table 2. Performance Requirements of an Advanced Ignition System (Courtesy: Caterpillar, Cummins and Waukesha).....	28
Table 3. Performance Specifications of Some Commercially-Available Pulsed DPSSL	31
Table 4. Hollow Glass Waveguides Tested for High-Power Laser Transmission.....	41
Table 5. Specifications of SwRI's BSCRE Engine	50
Table 6. Test Matrix for Single-Cylinder Laser Ignition Studies.....	55

Abstract

The primary goal of this project was to develop and test an Advanced Laser Ignition System (ALIS) for improving efficiency and reducing engine-out emissions of oxides of nitrogen (NO_x) from natural gas-fueled reciprocating engines commonly used for distributed generation in California. The specific objective of the project was to design, develop and demonstrate an integrated ALIS on a multi-cylinder natural gas-fueled reciprocating engine meeting or exceeding California's Distributed Generation Emissions Standards.

Lean operation has been the preferred mode of operation for natural gas-fueled reciprocating engines as it allows low NO_x emissions and high overall efficiency. Laser ignition appears promising as it achieves ignition at high pressures and under lean conditions relatively easily. Lasers are becoming less expensive and more compact than before and are attractive means of ignition for engines.

Initially, the basic design requirements for laser ignition under typical in-cylinder conditions (temperature near 500 degrees Celsius, pressure under 77 bar) were established. Through fundamental ignition studies performed in a rapid compression machine, the characteristics of laser ignition and conventional spark ignition on methane-air mixtures were compared. The rapid compression machine studies demonstrated significant differences between the combustion processes associated with laser ignition and conventional spark ignition. Subsequent tests on a large-bore single-cylinder engine showed that laser ignition could potentially reduce NO_x emissions up to 70 percent. Alternately, for a given NO_x emissions level, laser ignition can enhance engine fuel conversion efficiency by 3 percentage points.

Various components required for ALIS were developed. A free-space laser transmission design approach was used due to non-availability of suitable fiber optics. The successfully developed components were integrated and optimized for use with a multi-cylinder engine. The integrated ALIS was tested for an extended period of time in the laboratory to prove system reliability. A brief engine test with ALIS was attempted in a test cell at Cummins Engine Company and the system integration issues were identified. Future work is expected to successfully demonstrate the performance and emissions benefits of Advanced Laser Ignition System operation in a multi-cylinder natural gas-fueled reciprocating engine suitable for distributed generation applications in California.

Keywords: Emissions, Engine, Ignition, Laser, Spark

Executive Summary

Introduction

With electric grid infrastructure capabilities lagging behind the ever-increasing power demands in California, Distributed Power Generation has come into vogue. Most of such installations are natural gas fueled internal combustion engines with either rich-burn (equivalence ratio, $\phi \sim 1.0$) or lean-burn ($\phi < 1.0$) operation. As these engines are operated round the clock throughout the year, component durability is of prime importance. Both engine manufacturers and facility operators have identified ignition to be the prime concern in these engines. The focus of this research effort was to evaluate one of the alternatives, laser ignition, in overcoming the shortcomings of conventional ignition.

Goals and Objectives

The primary goal of this project was to develop and test an Advanced Laser Ignition System to improve fuel conversion efficiencies and reduce engine-out emissions of oxides of nitrogen (NO_x) from natural gas-fueled reciprocating engines. The specific objectives of the project were:

1. Experimental studies to determine component design specifications.
2. Development of viable components for high-power laser transmission and their integration into the Advanced Laser Ignition System.
3. Integration and development of Advanced Laser Ignition System that meets industrial specifications.
4. Performance evaluation of an integrated Advanced Laser Ignition System on a multi-cylinder engine.
5. Demonstration of the integrated Advanced Laser Ignition System in meeting or exceeding California's Distributed Generation Emissions Standards.

Rationale

Lean operation has been the preferred mode of operation for natural gas-fueled reciprocating engines as it allows low emissions of NO_x and simultaneous high overall efficiencies. In these engines, the operating condition is often close to the point where the ignition boundary and the knock-limiting boundary crossover. While knocking is to a large extent determined by engine design, ignition of lean mixtures is limited by the mode of ignition. In light of such concerns, laser ignition appears promising as it achieves ignition at high pressures and under lean conditions relatively easily. With lasers becoming less expensive and more compact over the last decade, this mode of ignition is particularly attractive.

Approach

The project commenced with an exhaustive survey of the ignition literature. Following this literature review, fundamental ignition tests were performed on a Rapid Compression Machine to compare conventional spark ignition and laser ignition.

An initial survey of possible Advanced Laser Ignition System schemes was performed and two promising configurations were identified: (i) the laser-per-cylinder concept, and (ii) the multiplexed laser concept, wherein the output of a single laser is distributed over various cylinders. The latter concept was chosen as it promised low-cost and simplicity of thermal management. However, this concept required the development of three main components, namely, laser plugs, multiplexers and fiber-optic beam delivery. For breakdown to occur in gases, the required laser fluency at the focal point is of the order of 10^{12} Watts per Square Centimeter (W/cm^2). To achieve such peak fluencies, high-power laser pulses with peak power of several megawatts (MW) are required. Therefore, the main components of the Advanced Laser Ignition System must be designed to withstand such high power levels. Guidance was derived in the development of these components through (i) data from fundamental ignition studies conducted on the Rapid Compression Machine, and (ii) requirements of the advanced ignition system as specified by engine manufacturers. Specific details of the high-power components considered in the present project are described below:

Laser Plugs: A two-lens design that successfully meets the physical and functional requirements of a laser plug was developed. Adaptation of this design for various engine geometries is possible.

Multiplexers: Three schemes that distribute the output of a single laser among various cylinders were pursued: (i) an electro-optic switch, (ii) a rotating-mirror scheme, and (iii) a flip-flop switch. The first two schemes fell short of the requirements either due to high-cost or the inability to provide ignition timing variations in individual cylinders. The flip-flop scheme, however, proved effective in all respects.

Fiber Optic Beam Delivery: Through tests and analyses it was determined that the fiber optic delivery requirements are (i) low divergence at distal end, (ii) high-power laser transmission, and (iii) preservation of mode quality. Initial tests performed using solid core fibers showed that they are limited by the material damage threshold. Subsequent tests performed using Hollow Glass Waveguides showed that they are limited by mode shifts introduced by bending of the optical fibers. While photonic band-gap fibers appear promising, they are not readily available for tests and their development is expected to be expensive.

Electronic Interface: An electronic interface is required for the Advanced Laser Ignition System to communicate with the Electronic Control Unit of an engine for ignition timing coordination. In consultation with Argonne's industrial partner, Altronic, Inc., the timing modules from existing ignition systems were modified for the present purpose.

In parallel, the benefits of laser ignition were demonstrated in a single-cylinder research engine. For this purpose, a 9.5 inch bore, 11 liter displacement Bombardier single-cylinder engine at Southwest Research Institute was used. Tests were performed comparing conventional capacitance discharge spark ignition, free-space laser ignition, and fiber-coupled laser ignition.

The engine was operated at 10 bar and 15 bar Brake Mean Effective Pressure (BMEP) at 900 revolutions per minute (rpm). Sweeps of fuel-air equivalence ratio (from 0.5 to 0.65) and ignition timing (from 25 degrees Before Top Dead Center, to 8 degrees After Top Dead Center) were performed while adjusting the air boost to keep the mean power constant.

Results

Review of previously published ignition literature showed significant spread in data concerning the combustion behavior of natural gas-air mixtures with laser ignition. Subsequently, in the Rapid Compression Machine studies, methane-air mixtures under typical in-cylinder conditions (temperature ~ 500 degrees Celsius, pressure < 77 bar) were established and the characteristics of laser ignition and conventional spark ignition were compared. It was observed that laser ignition extends the lean operating limit of methane-air mixtures all the way to the lean flammability limit ($\phi_{II} = 0.5$), whereas conventional capacitance discharge ignition is limited (on an average) to mixtures richer than $\phi = 0.6$. Also, with laser ignition the flame spread was observed to be accelerated which is a very desirable trend when using lean mixtures as it enhances combustion efficiency. The observed trends of Minimum Required Energy (MRE) for successful laser ignition showed that a laser ignition system developed for $\phi = 0.65$ will successfully operate under all other possible lean operating conditions. Additionally, design parameters required for some of the components required for the Advanced Laser Ignition System were also obtained.

The following benefits were observed from the single-cylinder engine experiments performed with laser ignition:

- Extension of the lean misfire limit by about 10 percent at BMEPs of 10 and 15 bar,
- Increase of the overall burn rate, and
- Improved combustion stability at all comparable test points.

The combustion behavior described above, combined with optimization of engine parameters, was found to result in

- A reduction of brake specific NO_x (BSNO_x) emissions by ~ 70 percent at constant engine efficiency, or
- An increase in brake thermal efficiencies up to 3 percentage points, while maintaining BSNO_x emissions constant.

In view of the aforementioned benefits of laser ignition, efforts were directed at developing an integrated Advanced Laser Ignition System. Previously developed components were integrated into a single system while relying on a free-space laser beam delivery. Tests conducted in a laboratory environment showed the integrated system to have the required time response and performance.

Conclusions

In conclusion, the project titled “Advanced Laser Ignition Integrated ARICE System for Distributed Generation in California” produced important results of practical significance toward the development of an advanced laser ignition system for reciprocating engines.

Fundamental Rapid Compression Machine studies clearly showed the potential benefits of laser ignition compared to conventional spark ignition: (i) Laser ignition extended the lean operating limit of methane-air mixtures to the lean flammability limit ($\phi_{II} = 0.5$), and (ii) Combustion rates were accelerated with laser ignition.

Single-cylinder engine experiments performed with laser ignition realized the potential benefits evidenced in the Rapid Compression Machine studies. Compared to conventional spark ignition, laser ignition extended the lean misfire limit by about 10 percent at BMEPs of 10 and 15 bar, increased overall burn rates, and improved combustion stability at all test points. Most importantly, laser ignition showed a reduction of brake specific NO_x (BSNO_x) emissions by ~ 70 percent at constant engine efficiency or alternately, an increase in brake thermal efficiencies of up to 3 percentage points, while maintaining BSNO_x emissions constant.

This project was a success at the research level, where for the first time a multi-cylinder engine design of laser ignition system was shown to work effectively in the laboratory. It is recommended that a separate materials research project be undertaken to develop fiber optic laser energy delivery system suitable for engine conditions. The final step, to establish the technical viability of the Advanced Laser Ignition System concept, is performing a series of multi-cylinder engine tests to document the efficiency and emissions benefits of the laser ignition system.

1.0 Introduction

1.1. Background

Reciprocating Internal Combustion Engine are commonly used for Distributed Generation (DG) and Combined Heat and Power (CHP) applications. As shown in Table 1, according to the California Energy Commission’s Advanced Reciprocating Internal Combustion Engine (ARICE) program, the performance and emission targets set for stationary reciprocating engines by year 2010 are brake thermal efficiency greater than 44% and brake-specific nitrogen oxide emissions less than 0.01grams per brake horsepower-hour (g/bhp-hr).

Table 1. Performance Targets for Advanced Reciprocating Internal Combustion Engines

Parameter	2007	2008	2009	2010
Efficiency				
Brake Thermal Efficiency	≥35%	≥38%	≥40%	≥44%
Fuel-to-Electric Efficiency***	≥32%	≥34%	≥38%	≥42%
Overall Efficiency (CHP)	≥85%	≥85%	≥85%	≥85%
Emissions – shaft power (g/bhp-hr)				
Oxides of Nitrogen (NO _x)	<0.015	<0.015	≤0.015	≤0.01
Carbon Monoxide (CO)	<0.02	<0.02	≤0.02	≤0.02
Volatile Organic Compounds (VOCs)	<0.006	<0.006	≤0.006	≤0.006
Particulate Matter (PM ₁₀)	<0.01	<0.01	≤0.01	≤0.01
Emissions – power generation (lb/MW_ehr) *				
Oxides of Nitrogen (NO _x)	<0.07	<0.07	<0.07	<0.07
Carbon Monoxide (CO)	<0.08	<0.08	<0.08	<0.08
Volatile Organic Compounds (VOCs)	<0.02	<0.02	<0.02	<0.02
Particulate Matter (PM ₁₀)	<0.03	<0.03	<0.03	<0.03
Cost**				
FOB Cost (\$/kWe)***	≤700	≤700	≤700	≤700
CO&M Cost (\$/kWeh)	≤0.06	≤0.05	≤0.05	≤0.04
Reliability Availability Maintainability and Durability (RAMD)				
Availability	≥88%	≥90%	≥92%	≥95%
B10 Durability (hours)	≥8,000	≥9,000	≥10,000	≥12,000
Mean Time Between Major Overhauls (hours)	≥35,000	≥40,000	≥45,000	≥50,000

*Distributed generation (DG) emissions standards of the California Air Resources Board (ARB) will apply. Details available at <http://www.arb.ca.gov/energy/dg/dg.htm>.

** Cost expressed in 2006 \$

*** Efficiency and capital cost targets are size dependent. The targets given are averaged industry consensus values.

Primarily, there are three technical approaches to meet California’s DG emissions and performance targets specified in Table 1: Rich-burn (equivalence ratio $[\phi]$ greater than 1.0) operation with exhaust gas recirculation (EGR) and use of three-way catalyst, Low-temperature combustion strategies such as Homogenous Charge Compression Ignition (HCCI), and Lean-burn operation ($\phi \sim 0.6-0.7$).

Rich-burn engine operation ($\phi \sim 1.0$), usually entails the use of an exhaust gas oxygen sensor along with an advanced engine controller. The controller oscillates the combustion equivalence ratio between 0.95 and 1.05 thereby enabling the oxidation and reduction processes in the three-way catalyst. EGR helps keep the combustion temperatures low and the overall efficiency high. However, such a strategy introduces corrosive combustion byproducts and other contaminants back into the engine which compromises hardware life and lubricant quality. Such a strategy could prove to be very competitive with efficiencies as high as 38% and very low emissions. However, as shown in Figure 1, efforts by General Electric–Jenbacher spread over 1.3 million running hours on 17 different engines have shown that engine maintenance costs increase by 42%.

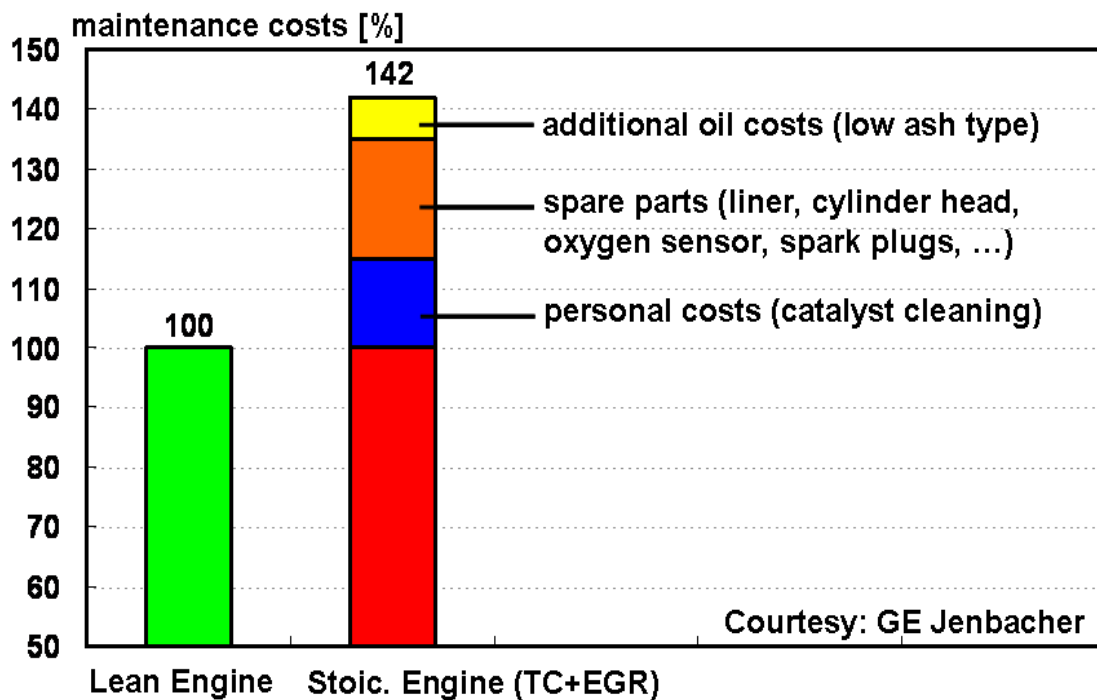


Figure 1. Comparison of Maintenance Costs for Rich-Burn and Lean-Burn Engines.

HCCI and other similar strategies rely on extremely lean fuel-air mixtures ($\phi < 0.3$). In such a system, the inducted fuel-air mixture auto-ignites upon compression usually at very low combustion temperatures. The achievable NO_x emissions are an order of magnitude lower than those achieved using either of the earlier strategies, while at the same time efficiencies are extremely high. However, (i) low specific power for the engine, (ii) difficulty in ignition

timing control and (iii) start ability are reported to be a problem. In light of such issues, the lean-burn technology appears very promising.

Lean-burn operation ($\phi \sim 0.6-0.7$), has remained the primary choice of the gas engine industry. In this strategy, air, far in excess of that required for complete combustion of the fuel, is inducted into the cylinder during each combustion cycle. To offset the energy density, intake air boost is employed with the use of a turbocharger. The resulting low combustion temperatures and high in-cylinder pressures ensure very low NO_x emissions (~ 0.5 grams per kilowatt hour [g/kWh] or 0.37 g/bhp-hr) while simultaneously achieving high fuel conversion efficiencies ($\sim 38\%$). Usually an after-treatment system is not used with lean-burn engines.

Figure 2 shows the typical operation of a lean-burn engine. These engines are operated at the intersection of knock (auto-ignition) limit and misfire (lean-ignition) limit, so as to attain maximum efficiency and simultaneously low NO_x emissions. Boost limit and pre-turbine limit are imposed by the turbocharger construction. Also, as the spark timing is advanced, combustion starts early in the compression stroke and the knock limit is encountered. On the other hand, as spark timing is retarded, the gas density at the time of ignition tends to be higher resulting in misfire. By extending the misfire-limit through judicious choice of an ignition system, substantial benefits in efficiency and emissions can be achieved.

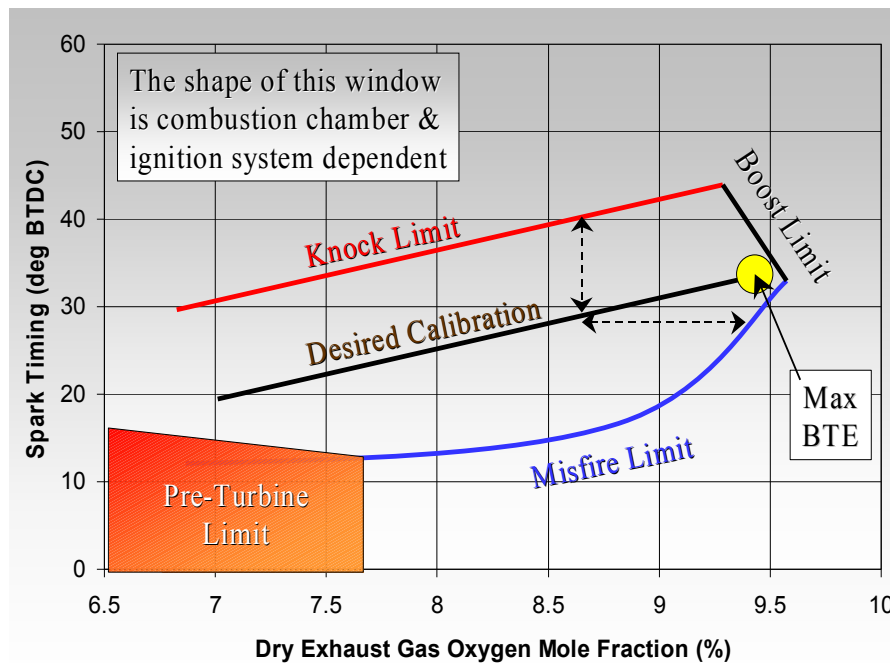


Figure 2. Operational Region of a Typical Lean-Burn Engine. (Courtesy: SwRI)

Figure 2, recast in combustion terminology, is shown in Figure 3. This represents the ignition limits of a typical fuel-air system for $0.5 \leq \phi \leq 1.0$. For rich mixtures, self-ignition occurs above a certain pressure thereby defining the self-ignition limit. Also for a given mode of ignition, a lean limit exists (ϕ_{ll}) for mixtures leaner than which ($\phi < \phi_{ll}$) ignition

cannot be achieved. For methane –air mixtures ϕ_{II} is 5.01%. For achieving maximum combustion efficiency and low NO_x emissions, lean-burn engines are operated at the intersection of lean-ignition limit and the self-ignition limit. Better performance can be achieved by extending the lean-ignition limit by choosing an advanced ignition system.

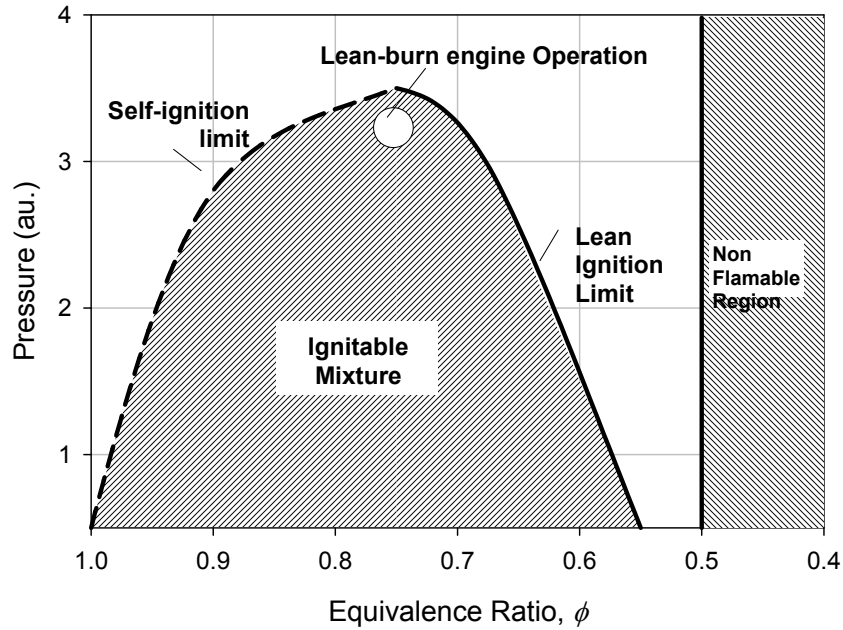


Figure 3. Ignition Limits of a Typical Fuel-Air System.

1.2. Fundamentals of Ignition

In a typical spark plug, successful sparking is achieved when the potential drop across the spark gap exceeds the dielectric breakdown threshold of typical gases. The sparking potential across the electrodes is given by Paschen's law:

$$V_b = f(p, d) \quad (1)$$

where, p is the pressure of the gas and d is the spark gap. The breakdown voltage, V_b , exhibits a linear dependence on the product pd . The electrode shape and material are also found to have significant influence on the spark ignition process [1]. Once gas breakdown occurs and a plasma kernel is established, energy transfer occurs mainly through diffusion on the surface to the surrounding gas. Whether such a diffusion process results in a successful combustion flame front depends upon the kernel energy exceeding Minimum Ignition Energy (MIE), the kernel size exceeding a certain size, turbulence and gas speed [2]. In practice, factors influencing successful spark creation far outweigh those influencing its transformation into a flame front, and it is normally assumed that once a spark is created the mixture is successfully burned.

1.3. Why Laser Ignition?

In present turbocharged of the lean-burn natural gas engines, Capacitance Discharge Ignition (CDI) systems are used as schematically shown in Figure 4. Though these systems are rated at 100-150 millijoules (mJ) per strike, after thermal losses typically 40-60 mJ is transmitted to the spark kernel at rates of voltage rise of 500 Volts per millisecond ($V/\mu s$). In CDI systems, energy stored in a high-voltage capacitor (at ~ 175 Volts Direct Current (VDC)) is discharged through a high-voltage coil resulting in voltages in excess of 28 kilovolts direct current (kVDC) across the spark plug gaps.

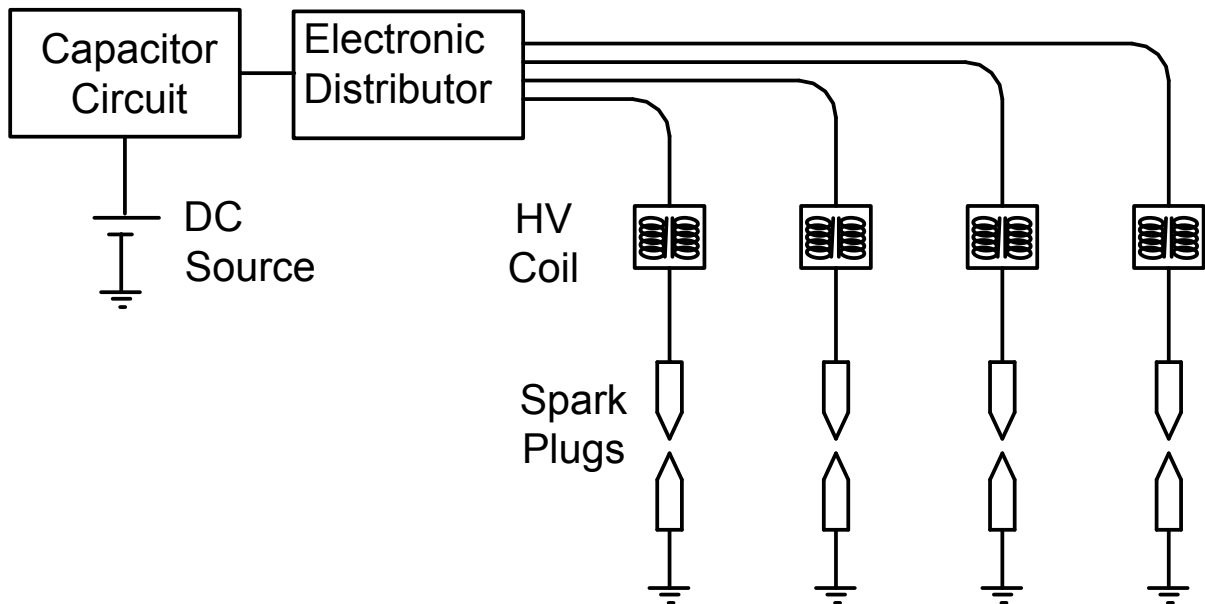


Figure 4. Schematic of a Capacitance Discharge Ignition (CDI) System.

With a push towards lean-engine operation, with a concomitant requirement to maintain engine specific power, the intake air pressure is increased. Lean operation along with high-intake air pressure results in very high charge densities at the time of ignition. Such high gas densities necessitate spark gap voltages in excess of 40 kilovolts (kV) that cannot be achieved using current CDI systems. This often leads to increased misfiring with subsequent loss of fuel efficiency and increased unburned hydrocarbon (UHC) emissions. Higher UHC emissions are essentially volatile organic compounds (VOC), which are currently regulated in California. To address these problems, various research organizations have been exploring alternate ways to achieve ignition [3-6]. Among these alternate methods, laser ignition proves attractive as it offers the following performance benefits:

- Successful ignition of mixtures at *high pressures* ensures reduced occurrence of misfire, and consequently improved fuel efficiency and lower UHC emissions,
- Potentially *lower maintenance* as the requirement to maintain a reasonable spark gap is eliminated,

- Extension of lean operating limits, thereby enabling lower NO_x emissions,
- Shorter ignition delays and enhanced combustion rates, which allow retarded timings thereby *reducing NO_x emissions*, and
- Location of ignition kernel away from the walls, thereby *enhancing overall efficiency* due to reduced heat loss to the cylinder head.

With such potential benefits, an attempt to use laser ignition for reciprocating engines was made by Dale and Smy as early as 1974 [7]. However, the size and cost of laser systems at that time were too large to reduce laser ignition to practice. Over the last two decades, on account of the developments in electro-optic systems, there is a renewed interest in laser ignition for reciprocating engines. The present effort aimed to (i) determine the benefits that accrue with the use of laser ignition, and (ii) develop and integrate systems to reduce laser ignition to practice on commercial multi-cylinder engines. This was carried out in technical tasks, Tasks 2.1 – 2.6, as described below.

As part of Task 2.2, fundamental ignition studies were performed in a Rapid Compression Machine (RCM) to compare the characteristics of laser ignition and conventional spark ignition on methane-air mixtures. The RCM studies demonstrated significant differences between the combustion processes associated with laser ignition and conventional spark ignition. In Task 2.4, the practical implications of the altered combustion behavior with laser ignition were determined through experiments on a single-cylinder research engine. In a parallel task (Task 2.3), various components required for an Advanced Laser Ignition System (ALIS) were developed. In Task 2.5, the successful components developed in Task 2.3 were integrated into a single system and optimized for use with a multi-cylinder engine. Task 2.6, field-testing for performance, is still an ongoing effort. A brief testing on a QSK-19G 6-cylinder engine at Cummins Technical Center was carried out. The progress made in individual tasks is given henceforth. This is concluded with a summary of the overall project.

1.4. ALIS Consortium

At the initiative of the United States Department of Energy (U.S. DOE) Advanced Reciprocating Engine Systems (ARES) program manager, Mr. Ronald Fiskum, and the Energy Commission's ARICE program manager, Dr. Avtar Bining, an ALIS consortium was formed. As shown in Figure 5, this consortium comprised Argonne National Laboratory (ANL), Colorado State University (CSU), National Energy Technology Laboratory (NETL) and Southwest Research Institute (SwRI) as technical partners. Oversight for the program was provided by industrial partners – Caterpillar, Cummins, Waukesha and Altronic Inc. – as well as the funding agencies – U.S. DOE-Distributed Energy Program and California Energy Commission's ARICE Program. Research ideas and progress were discussed and shared through regular technical meetings. Additionally, there was enough interaction among participants through sidebar meetings held at various conference sites. A summary of consortium activities and a list of publications are provided in Appendix A.

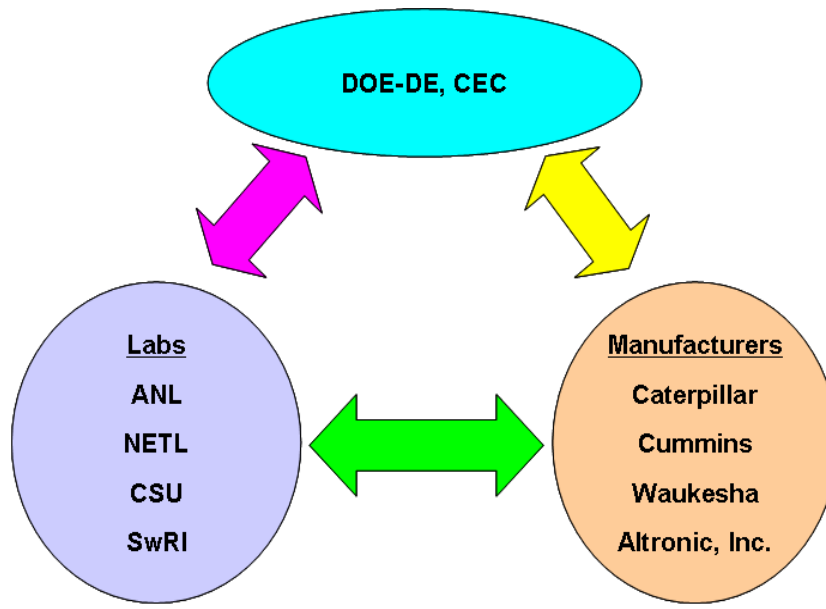


Figure 5. ALIS Development Consortium

1.5. Goals and Objectives

Laser ignition can overcome the ignition problems in lean-burn natural gas engines and further has the potential to improve engine efficiency and lower emissions. The overall benefits due to laser ignition can be summarized as:

1. Improved overall efficiency,
2. Reduced fuel consumption,
3. Lower NO_x and unburned hydrocarbon (UHC) emissions,
4. Enhanced power density, and
5. Reduced overall maintenance requirements.

These performance improvements translate to improving the energy cost/value of California's electricity. Simultaneously, by lowering NO_x and UHC emissions, the environmental and public health costs/risk of California's electricity are reduced.

The overall goals of the proposed ALIS system are:

1. Meet or exceed the current and future California emissions requirements and have other desirable environmental attributes.
2. Improve fuel-to-electricity conversion efficiency.
3. Lower capital costs, installation costs, operation and maintenance cost, and life cycle costs.
4. Enhance reliability, maintainability, durability and usability.
5. Possess multi-fuel use capabilities, such as with sewer gas, landfill gas etc.

In general, the proposed ALIS system is expected to lead to the adoption and use of improved ARICE technologies within California.

Technical and economic/cost performance objectives

The overall technical goal of this project was to develop a Commercial / Production-Ready ALIS integrated ARICE for distributed generation (DG) in California by meeting or exceeding Year 2007 Performance Targets of ARICE (*cf.* Table 1.).

The specific technical objectives of the project were:

1. Completion of experimental studies to determine component design specifications.
2. Development of viable components for high-power laser transmission and their integration into an ALIS.
3. Successful integration and development of ALIS that achieves the technical requirements specified by the industry.
4. Performance evaluation of an integrated ALIS-ARICE system on a multi-cylinder engine.
5. Demonstration of the integrated ALIS-ARICE system in meeting or exceeding 2007 ARICE performance targets.

2.0 (Task 2.2) Natural Gas-Air Ignition Experimental Study

2.1. Rationale for Task 2.2

With the renewed interest in laser ignition, there have been quite a few past studies evaluating laser-based ignition in static chambers [8,9]. As shown in Figure 6, such studies have shown that lasers enable ignition of mixtures at pressures higher than those that can be ignited by conventional coil based Capacitance Discharge Ignition (CDI) systems. However, no significant extension of lean-ignition limit was found with laser ignition. The lean ignition limits for both modes of ignition appeared to coincide at ϕ equal to 0.67.

Similarly, through tests performed on Ricardo-Proteus single-cylinder engine equivalent ration, McMillian et al. [10] report extension of lean ignition to ϕ equivalent to 0.51 with Kopecek et al. [11] reporting the same to ϕ equivalent to 0.42 (useable range ϕ equivalent to 0.46). With most of the lean-burn engines operated close to the intersection of lean ignition limit and self-ignition limit, such a spread in data warrants a systematic study under in-cylinder like conditions. To attain this goal, one needs to perform ignition tests in a Rapid Compression Machine (RCM) that simulates typical natural gas engine conditions. As most of the lean burn engines are operated close to the intersection of ignition limit and knock limit, the self-ignition limit needs to be determined as well. Also, mapping of the minimum laser energies required for successful ignition under different mixture conditions would assist in the development of ALIS.

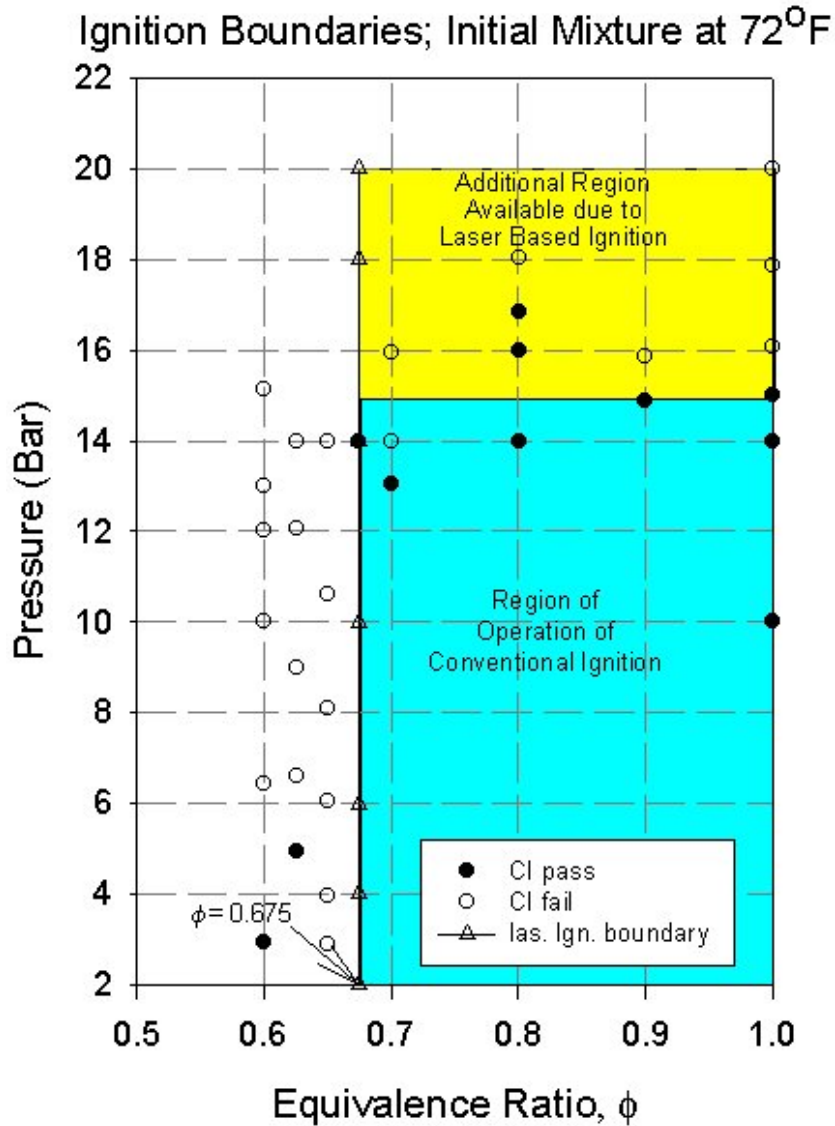


Figure 6. Ignition Limits of Methane-Air Mixtures Established in a Static Chamber (Initial Mixture Temperature ~ 22° C).

2.2. Experimental Setup

2.2.1. Rapid Compression Machine

As most of the current stationary power generation engines are operated at speeds less than 1800 rpm, the rapid compression machine (RCM) was designed with compression time less than 17 milliseconds. Overall the system was designed to withstand conditions at the end of combustion of 362 bar and 3,000 Kelvin (K). Also, with the compression ratio (CR) of typical gas engines being 12.5, the RCM was designed for a CR = 12.

The design concept that was used by Argonne is an improvement over the one developed by Massachusetts Institute of Technology (MIT) [12]. A schematic of the RCM is shown in Figure 7. A picture of the system is shown in Figure 8. This RCM consists of two pistons which, when released, travel towards each other with extremely small resultant vibration. Each side of the RCM consists of three separate chambers each carrying a piston. All the three pistons are mounted onto the same central Titanium shaft that forces their movement in unison. The outermost chamber is a pneumatic chamber carrying a 6 inch diameter aluminum piston. The innermost is a compression chamber wherein a 2.5 inch diameter aluminum piston compresses the experimental gases into the central ignition chamber. In the middle is a hydraulic chamber that contains hydraulic oil pressurized to 165 bar. Special design features within the hydraulic chamber allowed holding the piston in the retracted position even though pressurized air at 20.7 bar was present in the pneumatic chamber. The same design features allowed release of the piston synchronized with an external sparking event. Similar additional features in the hydraulic chamber allowed holding the piston in the compressed position thereby avoiding the piston bounce at the commencement of combustion. Various ports on the compression chambers allowed filling the RCM with dry compressed air and 99.99% pure methane. Fine orifices in the gas lines along with a high-resolution pressure transducer allowed establishing mixtures of the required pressures and equivalence ratios accurately. A port on the combustion chamber allowed ignition with a conventional spark plug (18 mm thread, J-style) powered by the Altronic PM-1 (CDI) ignition system. A second port allowed directing and focusing a laser (focal length 13 mm) to achieve ignition. A third port carrying a Kistler 4073A500 pressure transducer allowed recording the pressure traces. A fourth port carried an exhaust valve. A total of 22 pneumatically driven solenoid valves interfaced to a computer allowed remote operation of the RCM. A computer program written in National Instruments (NI)-Labview driving NI-Field Point system allowed automation of the processes.

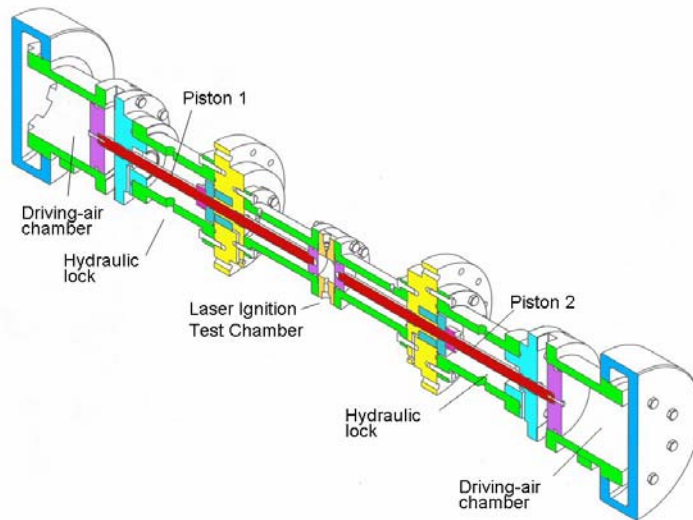


Figure 7. Schematic of the Rapid Compression Machine.

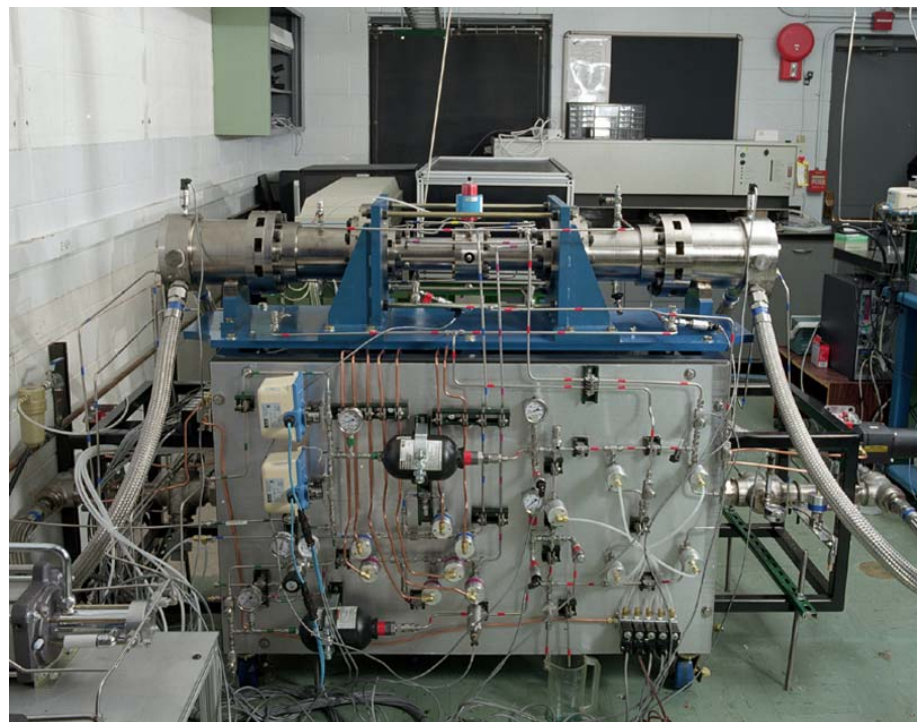


Figure 8. A Picture of Argonne's Rapid Compression Machine.
Photo Credit: Argonne National Laboratory

2.2.2. Laser Ignition System

The laser ignition system is schematically shown in Figure 9. The beam output of a frequency doubled Neodymium: Yttrium-Aluminum-Garnet (Nd:YAG) laser (Spectra Physics GCR 170) was routed through a combination of half-wave plate and polarizer to vary the laser power. A beam-splitter and a power meter allowed monitoring of the laser power. A fast-shutter with 3 millisecond time response allowed incidence of a single pulse from the laser pulse train. All of the timing was controlled by the NI-Field Point system.

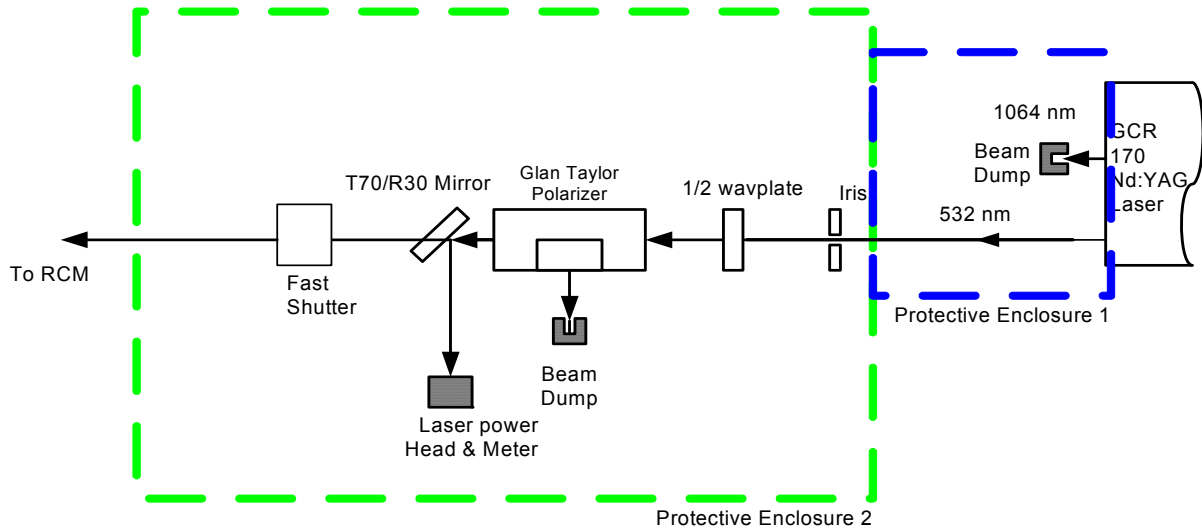


Figure 9. Schematic of the Optical Arrangement in the Laser Ignition System.

2.2.3. Conventional Ignition System

A CDI system, modified for the present tests, was supplied by Altronic, Inc. This system, when activated remotely by a 5 volt (V) pulse supplies ignition energy to the spark plug placed on the wall of the combustion chamber. The arrangement was such that the spark was supplied 30 ms following the end of piston stroke. Such a delay was necessary to allow the locking mechanism to engage completely before the initiation of combustion. Figure 10 shows a picture of this ignition system.

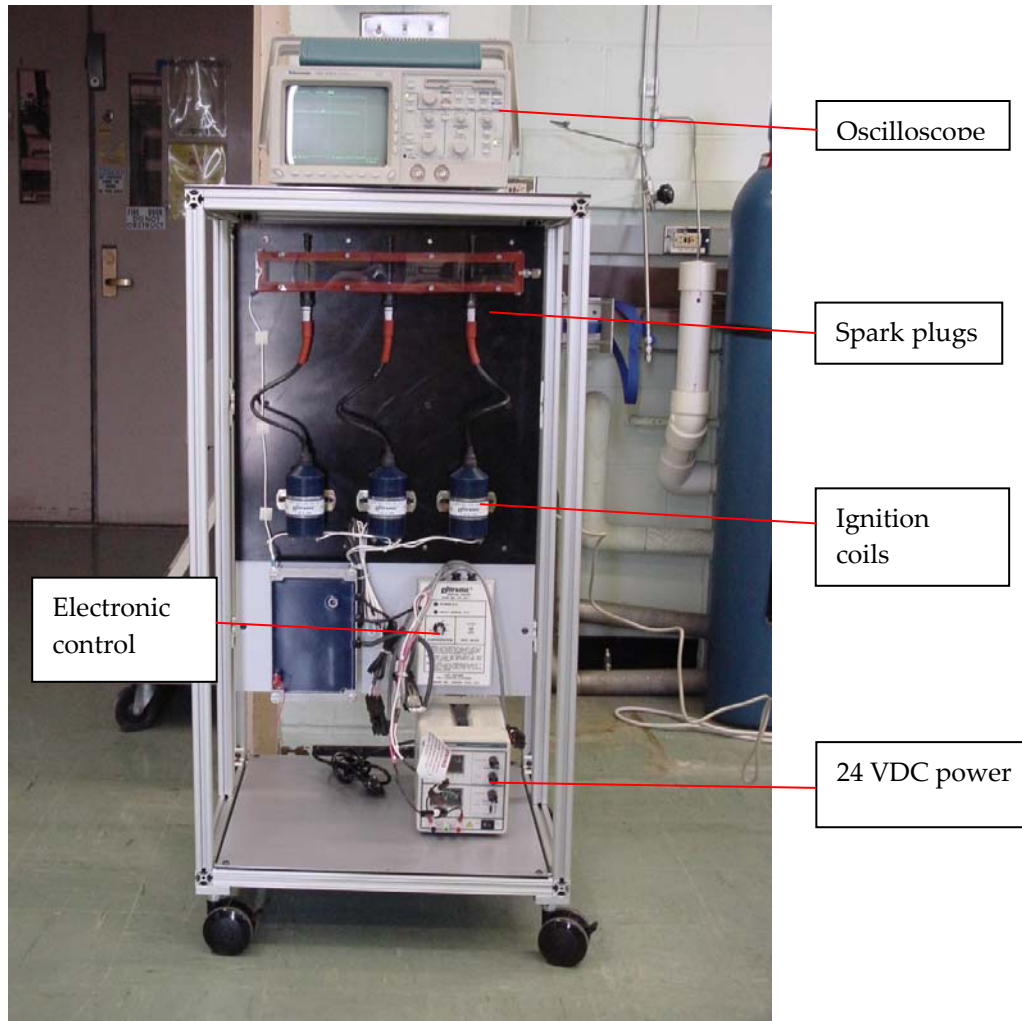


Figure 10. Conventional Ignition System Cart.

Photo Credit: Argonne National Laboratory

2.2.4. Operational Procedure

In a typical experiment, the RCM pistons were retracted and held in the retracted position. Subsequently, a gas mixture of the required equivalence ratio and initial pressure, P_1 , was established in the compression chambers. After allowing 5 minutes for the gases to mix, the pneumatic chambers were pressurized with compressed air at 20.7 bar supplied by a 150 Liter air tank. The pistons were released by activating the appropriate valve sequencing. A photo detector sensing the piston position provided the necessary signal for sequencing the laser pulse or the conventional ignition spark. To allow for locking of the pistons in the compressed position and thereby avoid a piston bounce back at the commencement of combustion, ignition was initiated 30 ms following the end of compression stroke. Also, one second following the end of compression stroke, the exhaust valve was opened. Subsequently, the pistons were retracted and the compression and combustion chambers were purged to prepare for the next experimental run. A typical test run required 20 to 30 minutes for execution.

2.3. Results and Discussion

2.3.1. Test Matrix

With the above setup, tests were performed while varying the initial pressure of the mixture, P_1 , and the equivalence ratio, ϕ . The mixtures established in the RCM were limited to $1.0 > \phi > 0.4$, $3.0 > P_1 > 1.0$ bar and initial temperature, $T_1 = 298$ K. A typical pressure trace obtained during one such test run is shown in Figure 11. As shown in Figure 11, when the pistons are released, the gaseous mixture is isentropically compressed to P_2 . As the ignition (spark) event is sequenced 20 to 30 ms following end of compression, there is a small pressure drop resulting from heat transfer to the combustion chamber walls, (P_2 - P_2'). Following an ignition delay after the incidence of spark, the pressure rises steeply to P_3 due to combustion. Subsequent pressure drop is primarily due to condensation of water vapor and heat transfer to walls of the chamber.

From thermodynamics, one has the relations

$$P_2 = P_1(CR)^\gamma \quad (2)$$

and

$$T_2 = T_1(CR)^{(\gamma-1)} \quad (3)$$

where, CR is the compression ratio and γ is the ratio of specific heat at constant pressure (C_p) to specific heat at constant volume (C_v), which equals 1.4 for air.

A regression analysis performed on the measured values of P_2 assuming γ as 1.4 showed that the compression ratio for the present RCM is 10.0 as opposed to 12.0 that it was originally designed for. With this adjusted compression ratio, calculations were performed assuming adiabatic combustion by using National Aeronautics and Space Administration (NASA) Chemical Equilibrium for Applications (CEA2) program. From such calculations, as shown in Figure 12, it was observed that the measured P_3 values were on an average 83% of the calculated P_3 values, with leaner mixtures exhibiting lower values. Also, it ought to be noted that in the present tests, for all mixture conditions, the temperature at the time of ignition, T_2 was about 765 K (per Equation 3).

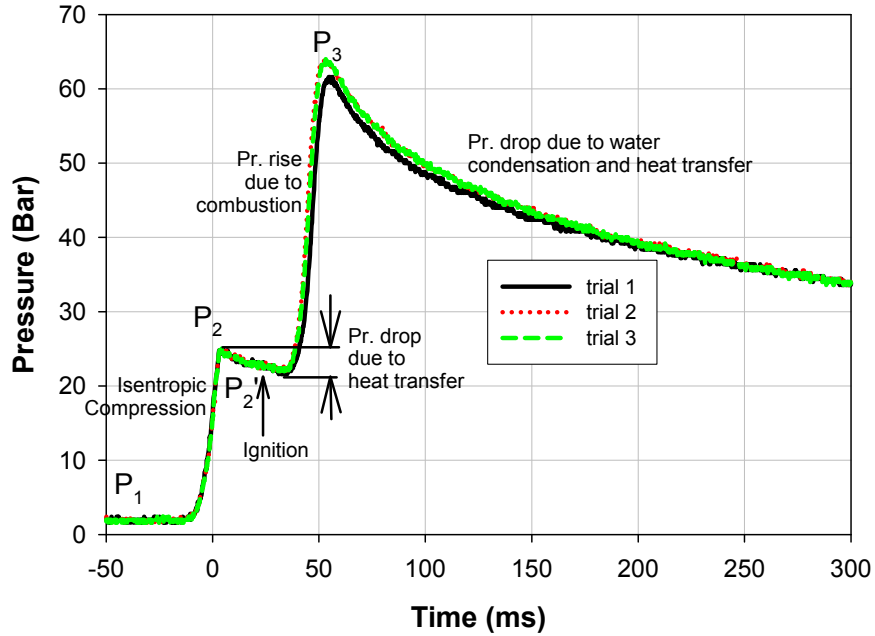


Figure 11. Typical Pressure Traces from RCM Operation; $P_1 = 1$ bar, $\phi = 0.7$

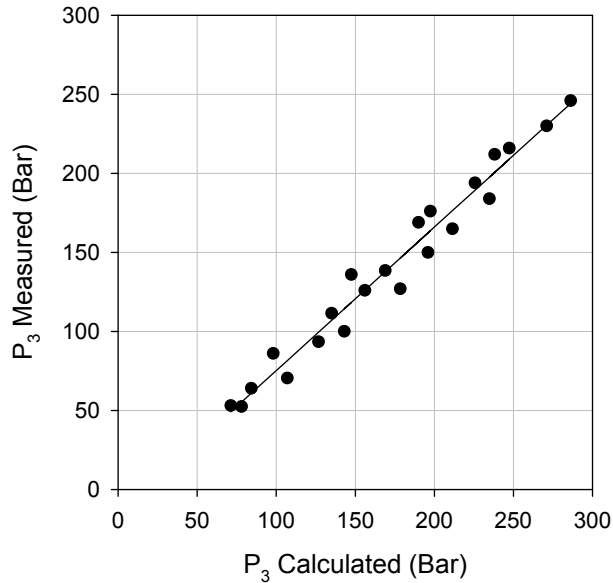


Figure 12. Measured Versus Calculated Peak Combustion Pressures for Various Methane-Air Mixtures, $1.0 < P_1 < 3$ bar and $0.5 < \phi < 1.0$

2.3.2. Ignition Limits

With the above setup, tests were conducted by varying the equivalence ratio, ϕ , between 0.5 and 1.0, and by varying the initial pressure of the mixture, P_1 , between 1.0 and 3.0 bar. For each condition, typically 5 or 6 test runs were executed while varying the laser pulse energy

between the maximum pulse energy of about 75 mJ and minimum pulse energy of 5 mJ. With each test the window within which the threshold energy was present was halved until the final threshold value was determined within an accuracy of ± 2.25 mJ/pulse.

The ignition boundaries determined through such tests expressed as a function of pressure at the time of ignition, P_2' , are shown in Figure 13. It is prominently noticed that self ignition dominates for mixtures with P_2' greater than 63 bar. Also, it is noticed that the lean ignition limit while using the CDI system is ϕ at 0.6. On the other hand, by using laser ignition this could be extended all the way to the flammability limit of ϕ of about 0.5. Such extensions are of significance as the current lean burn engines are operated at the intersection of self-ignition limits and lean ignition limits.

Following such observations, we are not sure of the claims made by researchers at GE-Jenbacher who report extension of lean ignition to ϕ of 0.417 by using a laser.

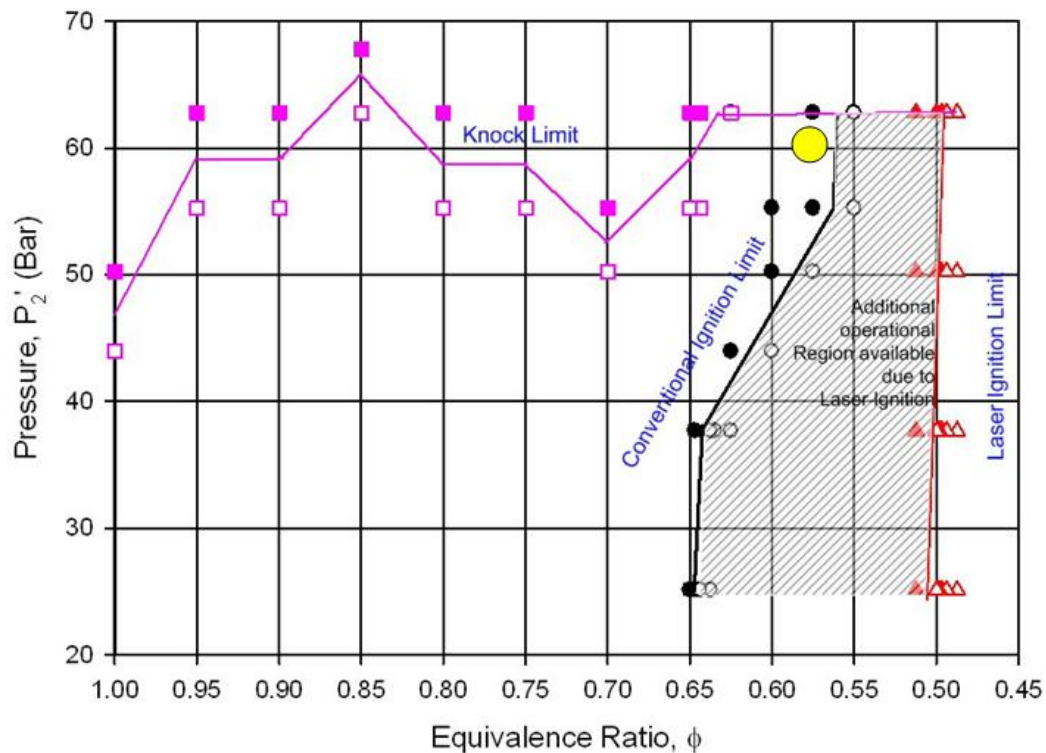


Figure 13. Ignition Boundaries Determined by Using an RCM.

2.3.3. Minimum Required Energy Scans

For the ignition boundaries established above, Minimum Required Energy (MRE) values for successful laser ignition were determined for various mixture conditions. Values determined for a lens focal length, f of 13 millimeters and laser beam quality of $M^2 \leq 5$ are shown in Figure 14. It is observed that except for ϕ of 1.0, MRE values decreased with increase in pressure finally resulting in self-ignition. The values along a cross-section of P_2 of

37.7 bar are shown in Figure 15. For a variation of the equivalence ratio, it is noticed that a minima exists at ϕ of 0.85 for these methane-air mixtures. Also it is noticed that there is a sharp rise in the MRE values for mixtures leaner than ϕ of 0.7. Such a trend was also noticed at other pressures.

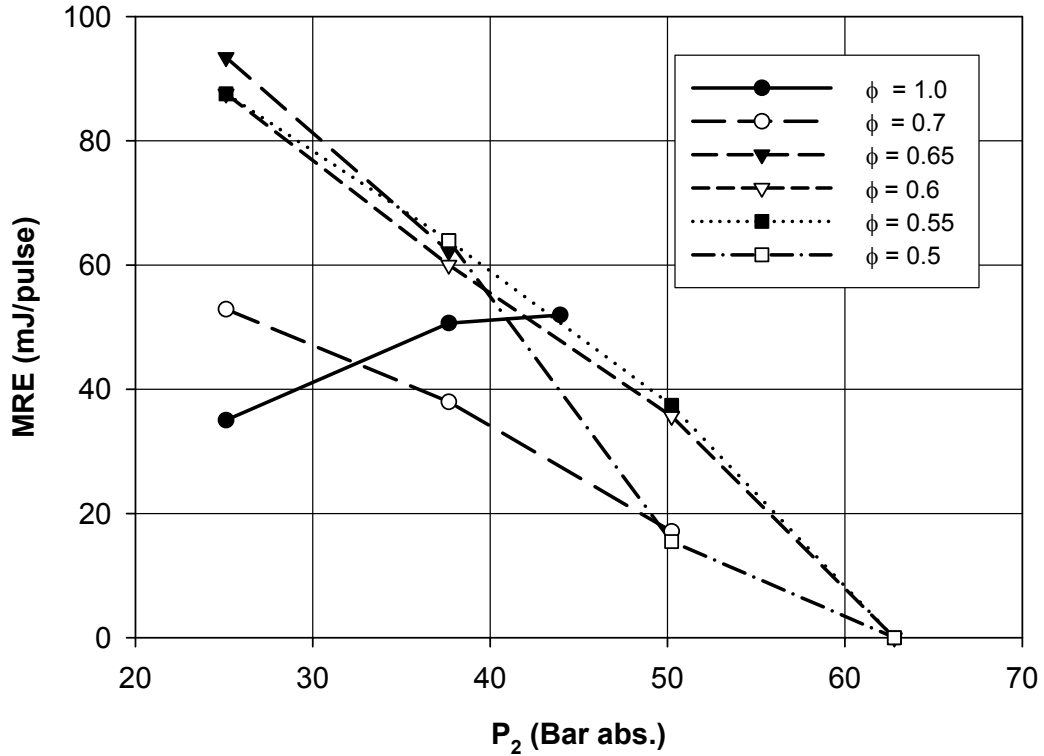


Figure 14. Minimum Required Laser Energies (MRE) for a Lens Focal Length $f = 13$ mm and Laser Beam Quality of $M2 \leq 5$.

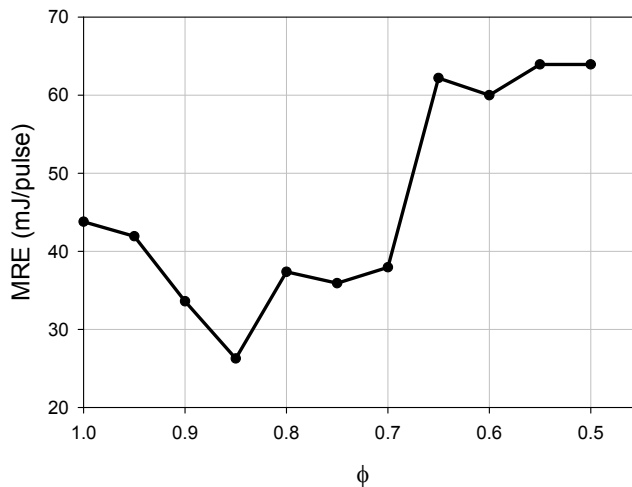


Figure 15. Minimum Required Laser Energies for $P_2 \approx 37.7$ bar.

2.3.4. Ignition Delays and Rates of Pressure Rise

Lean natural gas-air mixtures are characterized by slow flame velocities and longer ignition delays that are of concern for lean burn engine operation. Previous studies in 1-cylinder engines [10, 13] have shown that laser ignition results in smaller ignition delays and faster combustion. As shown in Figure 16, similar tests performed in the RCM showed that ignition delay increased with lean operation for both CDI ignition as well as laser ignition. However, the benefits in terms of smaller ignition delays were only pronounced under lean conditions and at ϕ of 1.0.

Similar comparison of the rate of pressure rise is shown in Figure 17. Again it was found that faster combustion rates occur for lean operation and for ϕ of 1.0 by the use of laser ignition. The reversal of trends for $0.75 < \phi < 0.95$ requires further investigation.

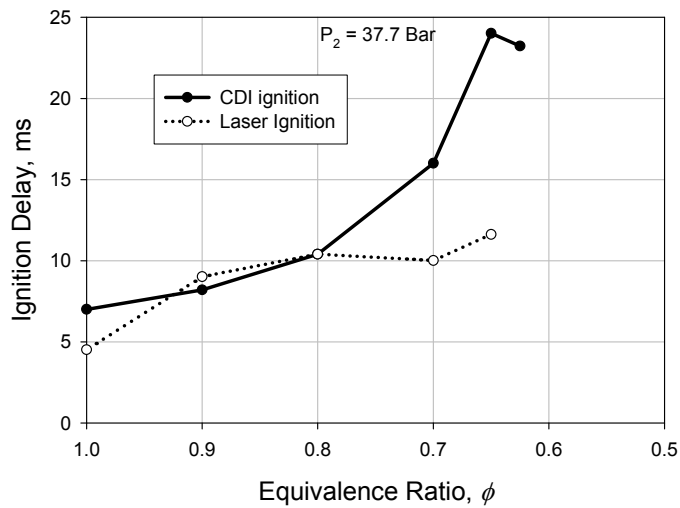


Figure 16. Ignition Delays for CDI and Laser Ignition.

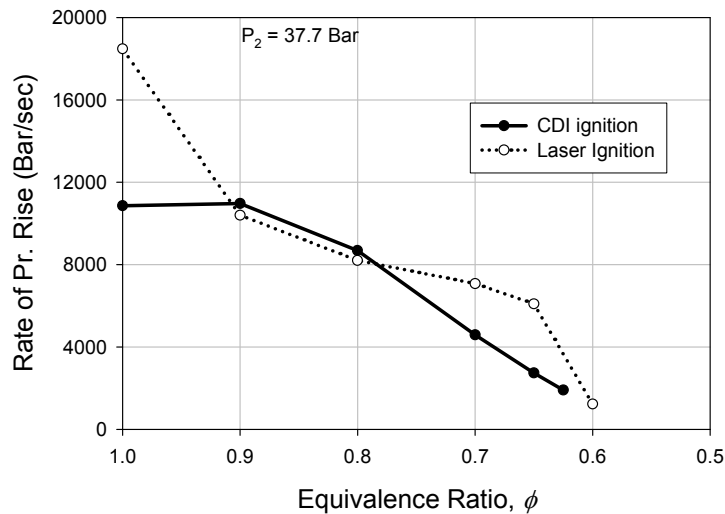


Figure 17. Rates of Pressure Rise for CDI and Laser Ignition.

2.3.5. Conclusions for Task 2.2

Through ignition tests conducted in a Rapid Compression Machine that simulated in-cylinder conditions of a lean-burn natural gas engine, it was observed that laser ignition extends the lean operating limit of methane-air mixtures to the flammability limit (ϕ of 0.5) whereas conventional CDI ignition on an average is limited to mixtures richer than ϕ of 0.6.

Minimum Required Energies for successful laser ignition exhibited a sharp increase followed by a plateau region for methane-air mixtures leaner than ϕ of 0.7. Such a trend shows that a laser ignition system developed to operate at ϕ of 0.65 will successfully operate under all other possible operating conditions.

To reap the true benefits of laser ignition, the required hardware components for the ALIS need to be developed. This was pursued next in Task 2.3.

3.0 (Task 2.3) Design of ALIS Components

From an initial survey of possible configurations for a laser-based ignition system, two promising concepts were identified: (i) The laser-per-cylinder concept, and (ii) The multiplexed laser concept.

In the laser-per-cylinder concept schematically shown in Figure 18, a miniature laser is built directly over the cylinder head. The cost of such a configuration is likely to be very high, as a single laser is required for each cylinder. Also, thermal management in the laser system becomes an issue as the cylinder head temperatures could be as high as 130° Celsius (C). However, this configuration does not require the use of a high-power delivery system (e.g., a fiber). As part of the ALIS consortium, National Energy Technology Laboratory (NETL) has pursued the development of a laser-per-cylinder ignition system, details of which are provided in Reference [14].

Alternately, as shown in Figure 19, the output of a single laser can be distributed among the various cylinders of a multi-cylinder engine. This was primarily pursued by Argonne National Laboratory. This configuration benefits from the cost savings that result from the use of a single laser as lasers are the most expensive components of ALIS. Also, the laser system is isolated from the heat and vibration of the engine. However, this system requires the development of associated high-power components including laser plugs, optical multiplexer and fiber delivery system.

Outside the consortium GE-Jenbacher, and AVL are pursuing both laser-per-cylinder and multiplexed laser approaches or a combination approach of the two [11].

3.1. Goals and Objectives of Task 2.3

The goal of Task 2.3 was to develop various hardware required for ALIS, according to the specifications determined through tests in earlier task, Task 2.2. This entails selection of some candidate technologies and testing them for performance. The successful candidates were sorted further to meet the project objectives.

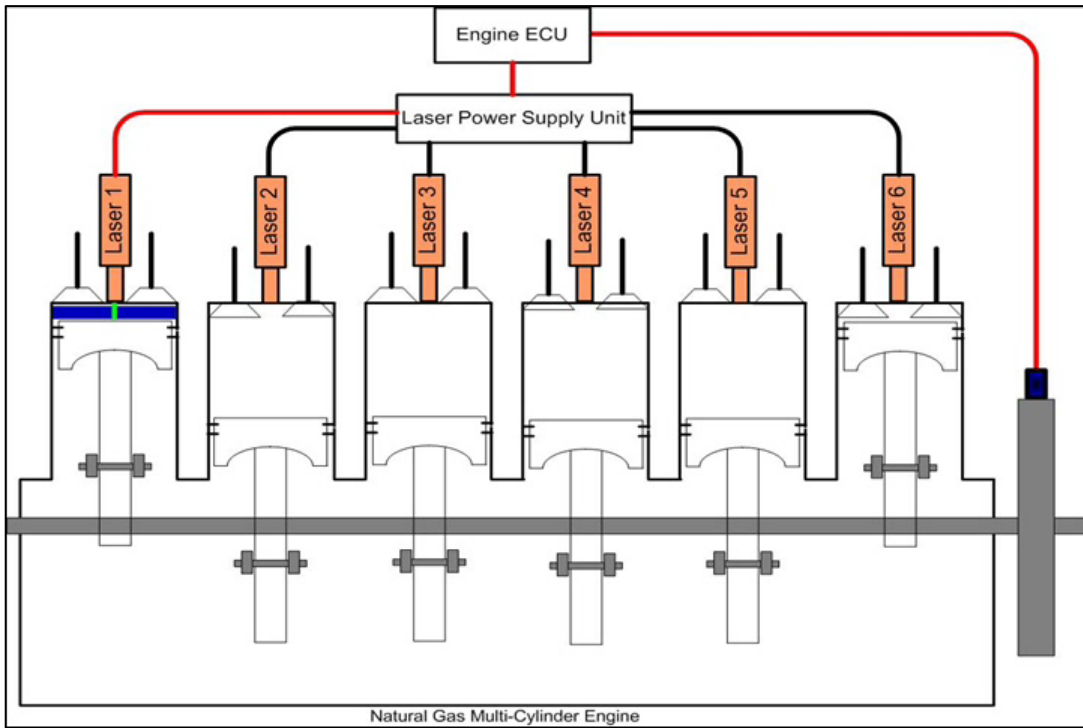


Figure 18. Schematic of the Laser-Per-Cylinder Concept.

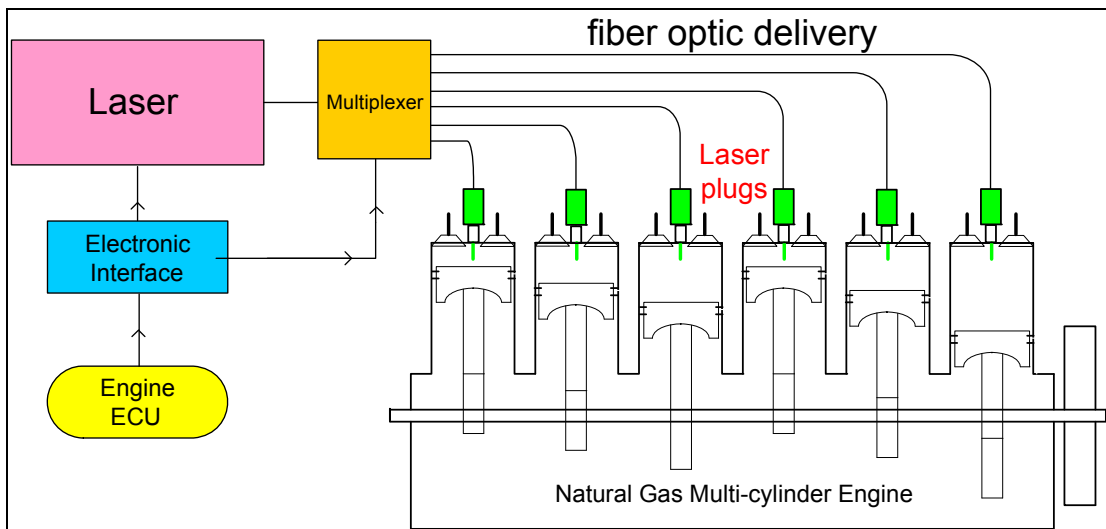


Figure 19. Schematic of the Multiplexed Laser Concept.

The specific objectives of this task are described below:

1. Design and develop laser plugs with the following specifications.
 - i. Have the same thread size as a conventional spark plug, i.e., M18 x 1.5,
 - ii. Provide pressure sealing to 3,000 pounds per square inch (psi).
 - iii. Withstand temperatures as high as 2,400° C.
 - iv. Minimize first and second surface reflections.
 - v. Minimize overall laser energy requirements.
 - vi. Provide sufficient reliability while transmitting laser energies of about 60 mJ per pulse.
 - vii. Be self-cleaning of any deposits.
 - viii. Facilitate coupling to fiber optic transmission.
2. Develop fiber-optic systems that are able to transmit the required laser energies for ALIS operation. In the process, evaluate the performance of the following technologies, among others, for transmissivity, flexibility, and ease of connectivity.
 - i. Conventional silica core of 1 to 2 millimeter(s) diameter fibers with appropriate cladding.
 - ii. Fibers with tapered ends.
 - iii. Hollow fiber systems.
3. Develop an optical multiplexer capable of distributing the laser output among various cylinders of a natural gas engine, while minimizing transmission losses and facilitating the required ignition timing advance or retard. This can be performed by evaluating the following candidate technologies among others.
 - i. Fiber-optic telecommunication multiplexer.
 - ii. Rotating grating-type indexing system.
4. Develop or select a laser system that can
 - i. Provide the required laser energies.
 - ii. Operate with minimal maintenance.
 - iii. Have a small foot print.
 - iv. Provide the aforementioned features at a low cost.
5. Develop an electronic interface in collaboration with Altronic, Inc., which integrates the functions of laser head, Electronic Control Unit (ECU), and indexer into one single unit. This electronic interface should enhance ease of installation, improve durability, satisfy the safety requirements of natural gas engines, have a small footprint, be lightweight, and facilitate manufacturing in large quantities.

In addition to the data gathered in the earlier Task 2.2, guidance in design was also derived from performance requirements of the ignition system as specified by engine manufacturers, as given in Table 2.

Table 2. Performance Requirements of an Advanced Ignition System (Courtesy: Caterpillar, Cummins and Waukesha)

1	Cost (current dollars)	Value	Units
	- First Cost (add \$1/kWe for CSA requirement)	4.00	\$ / kWe
	- Life Cycle Cost (including system replacement at major)	0.25	\$ / MWe-h
2	Performance		
	-Maximum ignition pressure (peak cylinder pressure)	220	bar
	-Minimum air/fuel ratio	0.9	-
	-Maximum air/fuel ratio (with swirl)	2.5	-
	-Minimum methane number (hydrogen capable)	0	-
	- Maximum methane number (landfill capable)	140	-
	- Ignition timing repeatability (non-mechanical)	0.08	° CA
	- Ignition timing accuracy (non-mechanical)	0.08	° CA
	- COV (ARES steady state, 0.5 g/bhp-hr NOx, 25 bar BMEP)	<1.0	%
	- COV (ARICE steady state, 0.015 g/bhp-hr NOx, 25 bar BMEP)	<1.0	%
	- RPM maximum (overspeed)	125	% of rated
	- RPM minimum (cranking)	50	Rpm
	- Full Load range (minimum – maximum)	10 – 25	bar
3	Ignition System Durability		
	- Life to replacement for ignition module and harness	80,000	h
4	Reliability (MTBF*)		
	- Ignition System (continuous duty)	6000	h

*MTBF -Minimum Time Between Failure

3.2. Laser System

From fundamental physics, it is well-known that when a high-power coherent laser beam is focused, multiple photons are absorbed resulting in the generation of free electrons. These electrons are further accelerated by the field gradients and generate more electrons and ions through an inverse *Bremsstrahlung* process. The plasma so generated serves as the ignition kernel for the combustible mixture surrounding it. The energy transfer to the surrounding gas mixture is primarily through diffusion, and depending on its magnitude may or may not result in successful combustion. Overall the process is not wavelength specific and is termed “non-resonant multi-photon ionization.”

An initial literature survey showed that Nd:YAG lasers are ideally suited for laser ignition applications. Based on the configuration of the laser, the output of an Nd:YAG laser can

have wavelengths of 1064 nanometers (nm), 532 nm or 266 nm. The focal spot diameter of a collimated laser beam focused by a lens is given by [15]

$$w_o = \frac{W_o}{M} = \left(\frac{4\lambda}{\pi} \right) \left(\frac{f}{D} \right) \quad (4)$$

where,

w_o = focal spot diameter for ideal Gaussian mode laser (microns),

W_o = focal spot diameter for a typical multi-mode laser (microns),

M = is the mode quality,

λ = laser wavelength (microns),

f = lens focal length (cm), and

D = laser beam diameter (cm).

As evident from Equation 4, smaller wavelengths result in smaller focal spot diameters. As a result, the use of smaller wavelengths is desirable to achieve a laser flux density of about 10^{12} Watts per square centimeter (W/cm^2), which is required for sparking. With the harmonic generation process being at best 50% efficient, theoretically speaking, a factor of two advantage is achieved by going to a higher harmonic. However, a compromise is necessary as the system complexity increases. For the present purpose, a wavelength of 532 nm was chosen.

From a functional standpoint, it was identified that the laser needs to have the following operational characteristics:

- Wavelength = 532 or 1064 nm,
- pulse width < 7 ns,
- repetition rate = 90 Hz (equivalent to the firing requirements of a 6-cylinder, 4-stroke engine operating at 1800 rpm),
- laser energy per pulse = 65 mJ/pulse,
- Base quality, $1.0 < M^2 < 5.0$,
- Operating environment temperature = 10 – 40°C,
- Compact laser head with low power requirement, and
- Lifetime > 10^9 shots or approximately 3000 hours for a 6-cylinder engine.

A survey of current laser technology showed four possible candidates: (i) Passively or actively Q-switched Nd:YAG lasers, (ii) Diode pumped solid state lasers, (iii) Disk lasers, and (iv) Fiber lasers. While all of these could provide the required peak laser powers to achieve sparking, Nd:YAG lasers cannot meet the maintenance requirements because their flashlamps have lifetimes in the range of $10-30 \times 10^6$ shots. Also thermal management of Nd:YAG lasers requires bulky external cooling. The cooling requirements are somewhat

mitigated in the case of disk lasers and fibers lasers due to the large surface area to volume ratio of the lasing media. On account of the rapid advancements in fiber laser technology, it is expected that disk lasers would become obsolete in the near future [16]. However, as of 2005, both fiber lasers and disk lasers were cost-prohibitive for the current application.



**Figure 20. A Commercially-Available Diode Pumped Solid State Laser (DPSSL)
Model: Centurion, Manufacturer: Big Sky Laser, Inc., 100 Hz, 45
mJ/pulse.**

Photo Credit: Argonne National Laboratory

Diode Pumped Solid State Lasers (DPSSL), on the other hand, are ideally suited for the present purpose. With the cost of laser diodes continually decreasing and their power continually increasing, DPSSL are anticipated to make many new applications possible. Most attractive to the current application is the fact that the only component that requires maintenance, the laser diode, has a lifetime greater than 10^9 shots, which for a typical ARICE engine can translate to 2.5 years. An example of a commercially available DPSSL is shown in Figure 20. The performance data of DPSSL from three different manufacturers is tabulated in Table 3 below. The MK-88 laser system from Kigre, has the smallest footprint and has already been shown to achieve sparking in the lab using a 13 millimeter (mm) focal length lens. However, the repetition rate of this laser makes it suitable only for the laser-per-cylinder application shown in Figure 18. On the other hand, the systems from Big Sky laser and JMAR are suitable for the present application.

Table 3 provides a snapshot of the DPSSL technology available as of 2005. This technology is making rapid progress with a very favorable cost and performance trajectory amenable to the laser ignition application. Based on these considerations, it was decided to postpone the selection of a specific laser for the present application. Consequently, all of the demonstrations in the present project are performed using compact Nd:YAG lasers that are already available at Argonne National Laboratory. Except for longevity of the pump source, the performance of these lasers will mimic that of DPSSL in all other respects

Table 3. Performance Specifications of Some Commercially-Available Pulsed DPSSL

Specification	Manufacturer		
	Kigre	Big Sky Laser	JMAR
Model number	MK-88	Centurion	Britelight-24
Wavelength (nm)	1.54	1.064	1.064
Energy/pulse (mJ/pulse)	3-5	45	80
Pulse width (ns)	7	7	7
Repetition rate (Hz)	0 – 20	100	300
Beam quality (M^2)	1.1	*	<1.5
Diode lifetime (number of pulses)	*	>109	>1010
Beam diameter (mm)	0.8	3	8
Laser head size (W x D x L)	0.85" x 2" x 3"	5" x 3" x 9"	18" x 30" x 12"
Laser Power Supply size	10" x 5" x 3.5"	*	19" rack x 38" high

* Information not available

3.3. Laser Plugs

Laser plugs are elements that introduce an optical window so that laser radiation can be focused to create a spark inside the cylinder. Additional requirements for their performance are given below: Foot print similar to that of standard 18 mm spark plug [17], Pressure rating ~ 300 bar, Temperature rating ~ 3,000 K on elements exposed to combustion, and should be self-cleaning of carbon and oil deposits.

After a couple of iterations, a two-lens design was found to be appropriate for ALIS. As shown in Figure 21, the output of a fiber optic cable is collimated using a plano-convex lens. The collimated output is refocused inside the cylinder using a sapphire lens of 13 mm back focal length. Such an arrangement allowed refocusing to a spot size of 240 micrometers (μm). Ray tracing iterations performed using ZEMAX software showed that the use of multi-element lenses does not reduce the final spot size any further.



Figure 21. Ray Propagation Scheme Inside a Laser Plug.

In the arrangement shown in Figure 21, the thickness of the plano-convex sapphire lens was chosen to withstand pressures up to 300 bar. With such a thick lens, it is very important that the curved side of the lens be pointed towards the laser so as to avoid internal reflections that will lead to internal cracking of the lens. Such a lens was also found to withstand typical in-cylinder combustion temperatures.

The physical arrangement of the aforementioned lens configuration is shown in Figure 22. As noticed in this arrangement, the laser plug consisted of a top part and a bottom part separated by an aluminum spacer. The bottom part carried the necessary external threads to fasten the entire laser plug assembly into the cylinder head. A copper crush gasket in the bottom part provided the necessary sealing to prevent leakage of combustion gases beyond the sapphire lens. The top part carried a lens tube, which in turn, housed the collimating plano-convex lens. A fiber optic connector (SMA-type) separated from the collimating lens allowed coupling of the incoming laser radiation.

Through tests performed by incorporating this laser plug in a 4 kilowatts (kW) natural gas engine, it was observed that the laser flux density on the exit face of the sapphire lens was critical. At low laser flux densities distinct carbon deposits were visible on the lens. Above a certain threshold, the laser radiation ablated such deposits and the lens was found to be self-cleaning. Caution needs to be exercised to keep the laser flux densities well below the material damage threshold of 5 gigawatts per square centimeter (GW/cm²). Similar laser ignition tests were performed by GE-Jenbacher and they demonstrated satisfactory performance of the lens arrangement for over 5000 hours of operation [9].

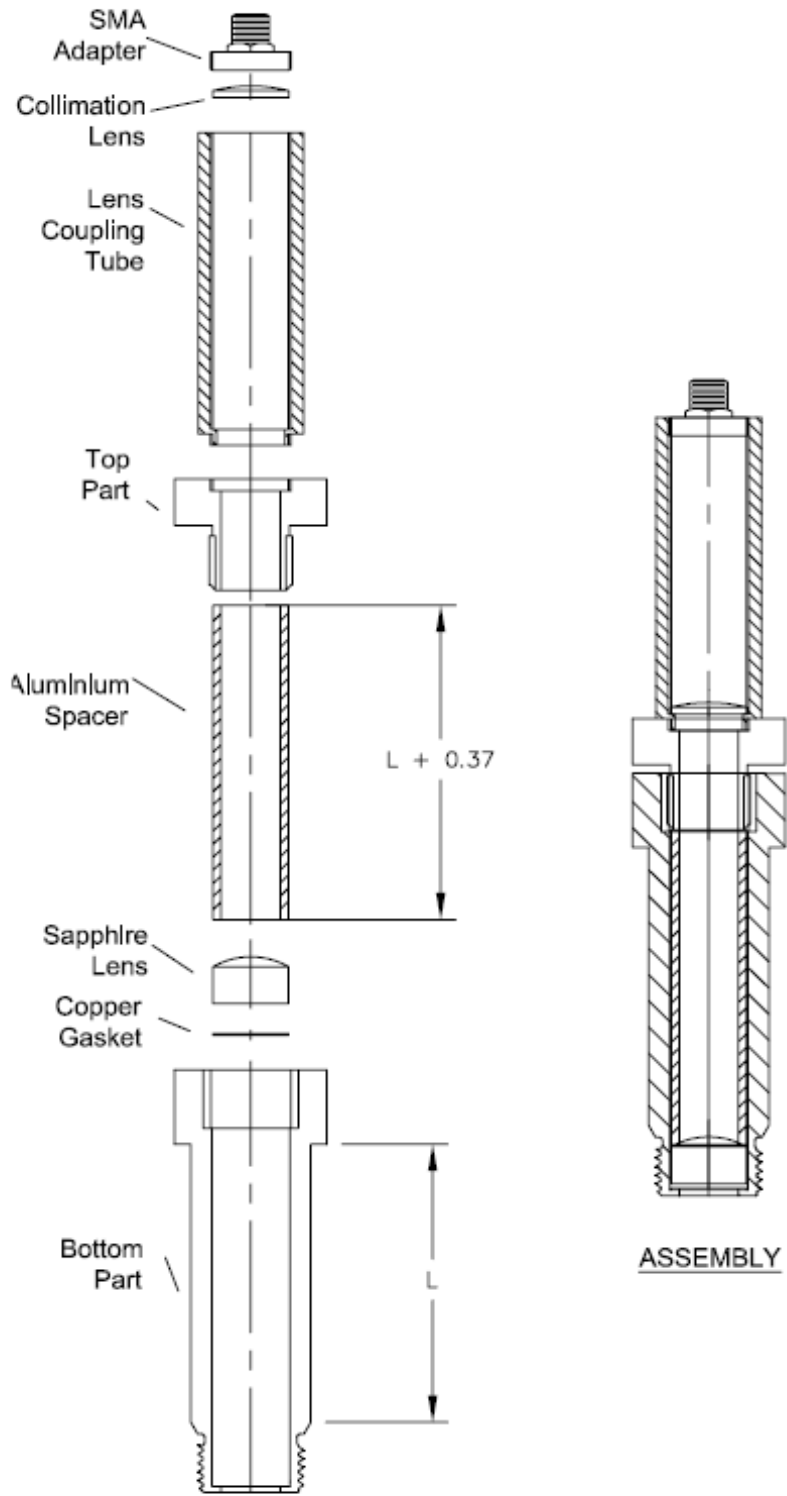


Figure 22. Schematic of a Two-Lens Laser Plug.

3.4. High-Power Optical Multiplexer

The optical multiplexer performs a function similar to the conventional ignition system: It distributes the output of a pulsed laser among various laser plugs installed in different engine cylinders. The functional requirements of such a high-power optical multiplexer are listed below:

- Ignition timing variation of 0-48° crank angle (CA) before top dead center (BTDC).
- Laser trigger pulse generation.
- Individual cylinder ignition timing variation of $\pm 6^\circ$ CA.

Additionally, the system needs to be of low-cost and must conform to the durability targets of the overall system of 80,000 hours.

A survey was performed to evaluate potential technologies that conform to the aforementioned requirements and the following three were identified: (i) Electro-optic switches, (ii) Rotating mirror systems, and (iii) Flip-flop systems. The results from the performance evaluation of prototypes of these systems are discussed below. It ought to be noted that the system designs considered below conform to a 6-cylinder, 1800 rpm, 4-stroke engine. These can be extended to engines with more number of cylinders, if necessary.

3.4.1. Electro-Optic Modulator (Pockels Cell)

A Pockels cell acts as an electro-optic switch because it rotates the polarization of the laser light by 90 degrees when activated. As shown in Figure 23, a polarizing beam splitter can direct the beam one way or the other based on the polarization state of the laser beam incident on it from the Pockels cell. A linear array of such Pockels cell-beam splitter combinations can be used for the present multiplexing purpose. For evaluation, a two-channel system was fabricated at ANL and it demonstrated the required performance (see Figure 24).

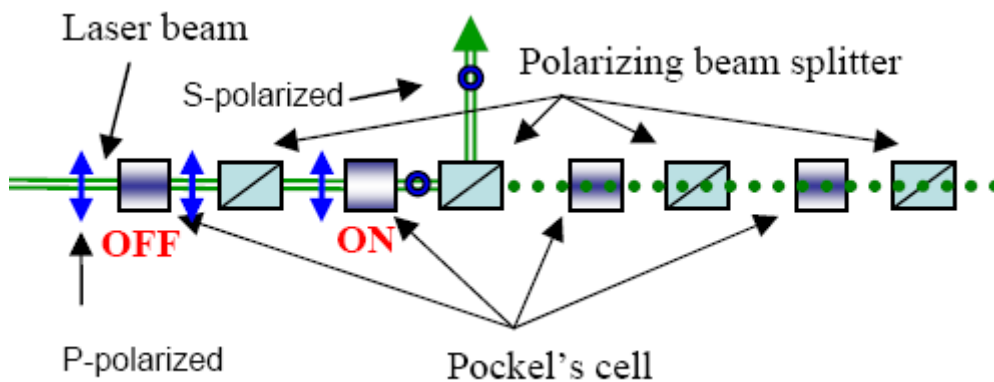


Figure 23. Schematic of a Pockels Cell-Based Multiplexer [18].

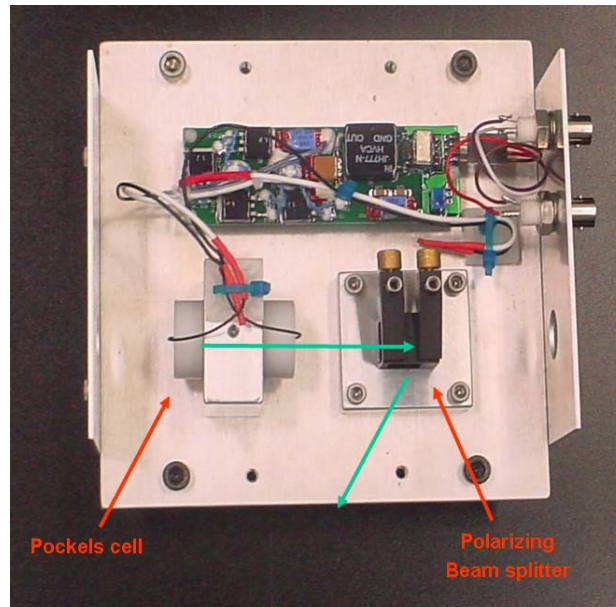


Figure 24. Photograph of a Pockels Cell-Based Two-Channel Multiplexer.
Photo Credit: Argonne National Laboratory

This scheme facilitates manipulation of the laser beam without having any mechanical movement of the components. However, the number of required optical surfaces increases with the number of engine cylinders and eventually becomes too unwieldy. Additionally voltages as high as 5 kV are required for activating the Pockels cell. Under the present market conditions, it was estimated that the cost associated with this scheme amounts to about \$2,000 per cylinder, which is considered to be too high.

3.4.2. Rotating Mirror

This scheme is based on the traditional mechanical distributor system of the 1980's. As shown in Figure 25, a mirror, placed at 45 degrees to the incoming laser beam, is rotated synchronously with the camshaft. As a result, the beam is rotated at 90 degrees about an axis coincident with the incoming laser beam. Laser firing at the appropriate crank angle is facilitated by a timing disk fitted on the shaft. A differential gear system allows ignition timing variation by introducing a phase shift between the mirror and the cam shaft. All of the components required for this system are simple, cost-effective, and offer the required durability. Therefore, a prototype system was designed and assembled. A photograph of the system is shown in Figure 26. Tests performed in the lab using a small electrical motor for driving the system showed that it has the required performance. Through such trials it also became evident that significant performance advantages can be gained by using a mirror inclined at angles $< 45^\circ$ to the incoming laser beam, or alternately, by using a small angle transmissive prism.

When details of this configuration were presented to engine manufacturers, they stressed the requirement of being able to vary the ignition timing of individual cylinders in natural

gas engines. The rotating mirror system does not allow this flexibility. Therefore, development of the flip-flop multiplexing scheme was pursued.

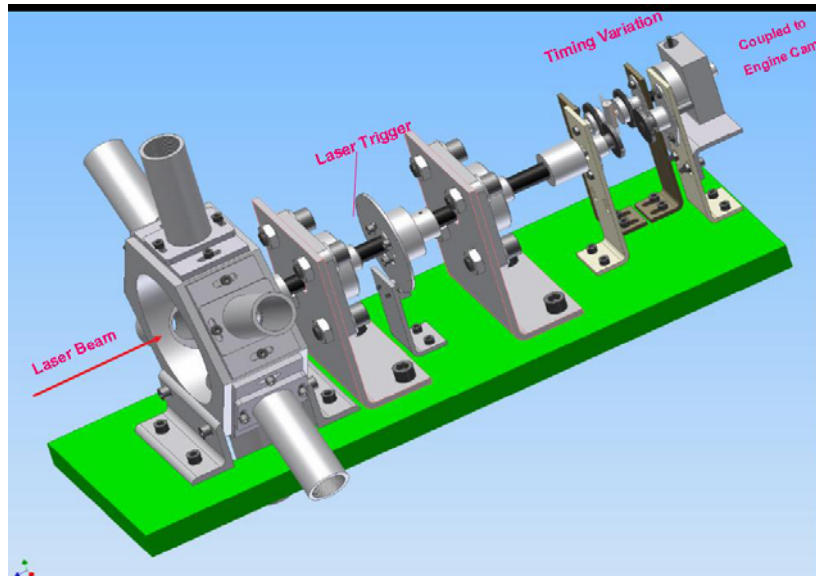


Figure 25. Schematic of a Rotating Mirror Multiplexer.

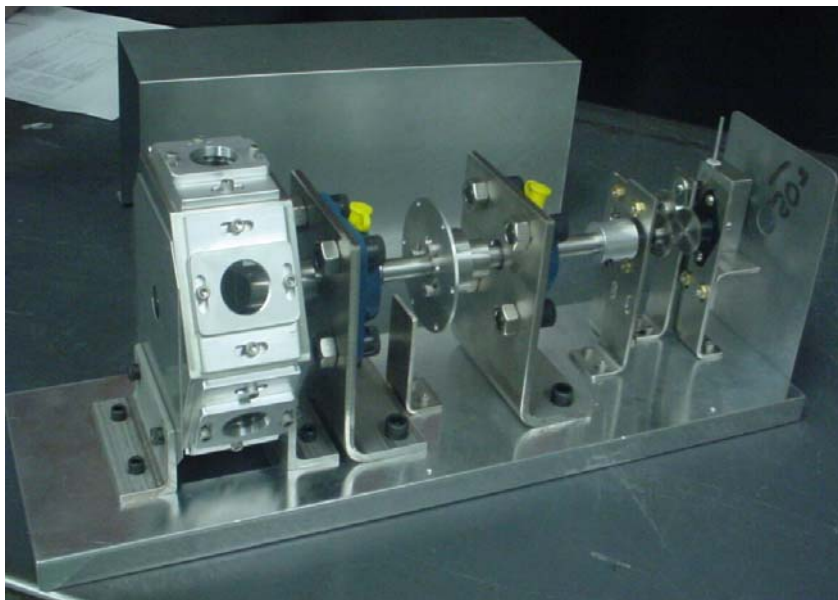


Figure 26. Photograph of Argonne's Rotating Mirror Multiplexer.
Photo Credit: Argonne National Laboratory

3.4.3. Flip-flop

A flip-flop multiplexer consists of a linear array of mirrors. An individual mirror, when activated, moves into the path of the laser beam and deflects it into the respective fiber injection port. This system, schematically shown in Figure 27, facilitates timing variation of individual cylinders. To test the performance of the flip-flop system, a rotary actuator (Model 6EM) was obtained from the Ledex Division of Saia-Burgess, an automotive parts supplier. This actuator, when activated, rotates its shaft by 22.5° and moves the mirror into or out of the path of the beam. In a 4-stroke, 1800 rpm, 6-cylinder engine the target response time for such a system is 11 ms. The time response of a one-channel system was measured using the arrangement shown in Figure 28(a). As noticed in Figure 28(b), the system shows very little bounce and in addition, exhibits a time response of less than 7 ms. Subsequently, efforts were undertaken to develop a six-channel system for use with a 6-cylinder engine.

As mentioned previously, with advances in actuators and micro-electro-mechanical systems (MEMS) technology many other multiplexing schemes, other than those discussed above, are possible. Some of these are discussed in Appendix B. The final choice is likely to be dictated by durability and the cost of these systems.

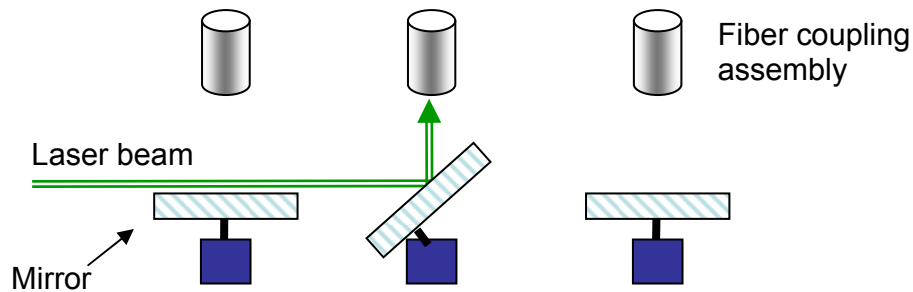


Figure 27. Schematic of a Flip-Flop Multiplexer.

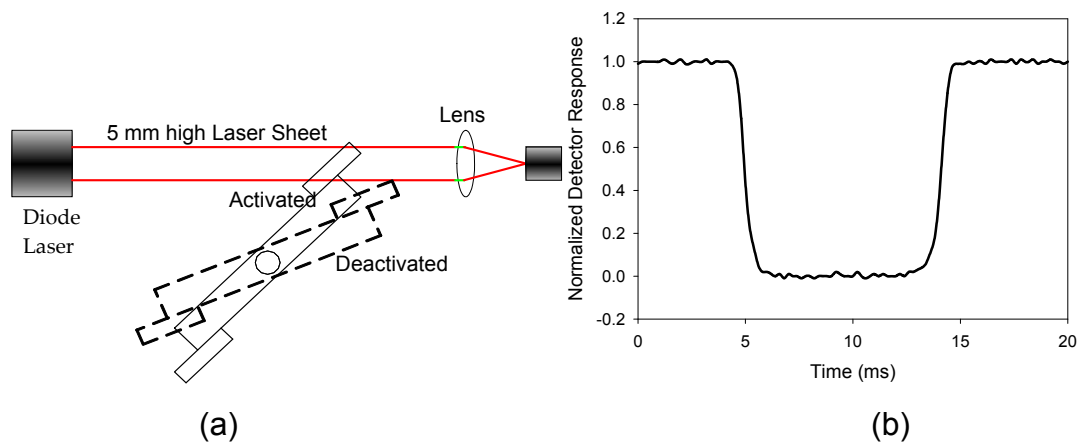


Figure 28. (a): Schematic of Setup to Measure the Time Response of the Flip-Flop (b): A Typical Detector Response Curve.

3.5. Fiber-Optic Delivery

As part of the current ALIS scheme, it was envisioned that the pulsed output of a laser will be transmitted via optical fibers to laser plugs installed in individual cylinders. The functional requirements specified by engine manufacturers for the optical fibers to be used in a multi-cylinder engine are given below:

- Length > 3 m.
- At least one 90° bend with a radius of curvature < 9.
- Operating temperature > 130° C.

Additionally, to achieve sparking at the distal end of the fiber, a laser flux density of 10^{12} W/cm² is necessary when refocused.

For a given fiber and a two-lens system shown in Figure 29, the Lagrange invariant yields

$$a \cdot NA_e = s \cdot NA_s \quad (5)$$

$$\text{As a result, the laser flux density at the focal spot} = \frac{I_{laser}}{s^2} \quad (6)$$

where,

a = core diameter of the fiber (microns)

s = focal spot size (microns)

NA_e = numerical aperture at the fiber exit \approx half cone angle at fiber exit

NA_s = numerical aperture at the focal spot

I_{laser} = intensity of laser (Watts).

Combining Equations 5 and 6, the following equation is obtained:

$$\text{Laser flux density at the focal spot} \approx \left(\frac{I_{laser}}{a^2} \right) \left(\frac{NA_s}{NA_e} \right)^2 \quad (7)$$

In Equation 7, the first term is determined by the fiber core material damage threshold. In the second term, NA_s is determined by the space available for the laser plug. For fibers of short lengths (~ 3 m) the numerical aperture at injection end is approximately equal to that at the fiber exit, i.e., $NA_i \approx NA_e$; in other words, the exit cone angle is determined by the injection scheme used. Hence the laser flux density can be maximized by making a judicious choice of both the optical fiber and the injection scheme.

However, in deriving Equation 7 it has been assumed that the fiber is mode-preserving. For the present case where transmission of high laser power is required, the use of multimode fibers is required. As is usually the case, with the introduction of higher order modes the energy is not equally distributed and is skewed towards the higher order modes. These

aspects of actual physical behavior are not captured by Equation 7. Nevertheless, this equation provides an acceptable basis that assists in the choice of the optical fiber and the injection scheme.

With the insight provided in the aforementioned arguments, different types of fibers were obtained and tested for sparking in the laboratory. The results of such efforts are discussed below.

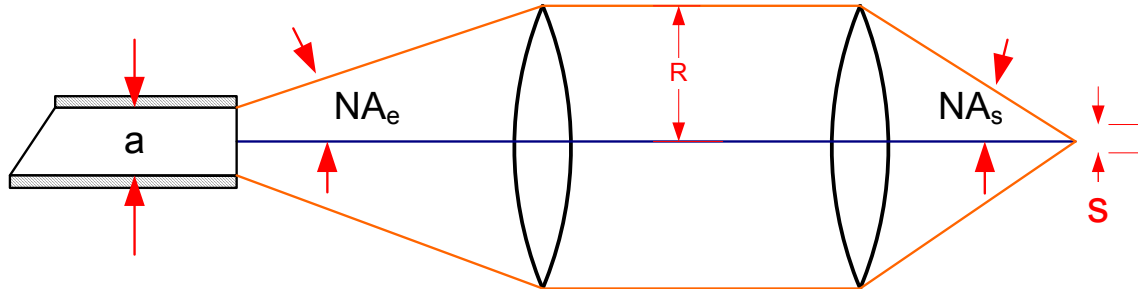
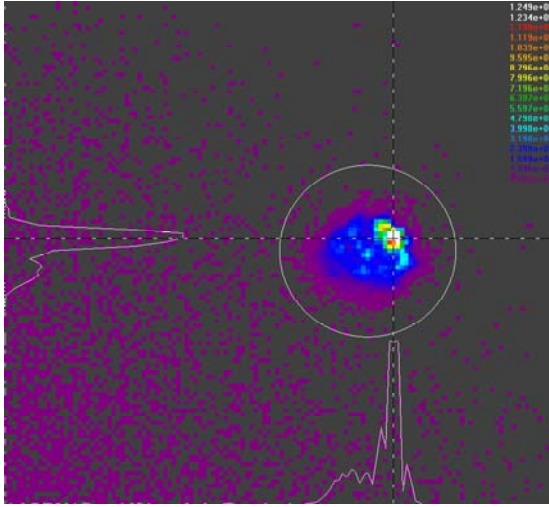
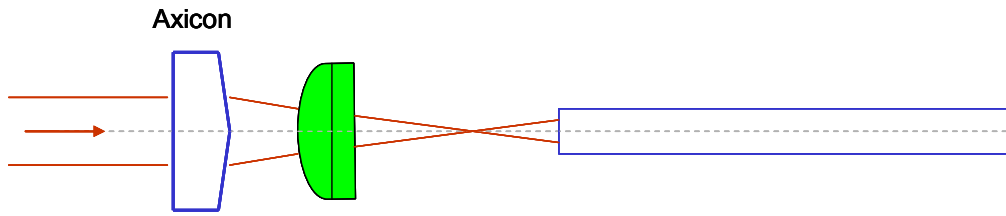


Figure 29. Schematic of Laser Refocusing Scheme at the Distal End of the Optical Fiber.

3.5.1. Solid Core Fibers

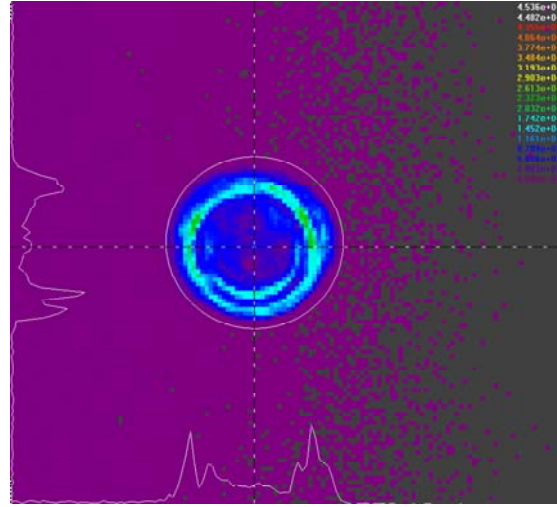
Largely driven by advances in the telecom industry, there have been rapid developments in solid core fiber technology over the past two decades. Currently, step-index (see Figure 31(a)) solid core fibers with 1 mm core diameter and a damage threshold of 5 GW/cm² are readily available. Initial efforts to inject such fibers limited the maximum laser energy transmission to 8 mJ per pulse. The primary mode of failure in such fibers was material damage at the entrance end of the fiber. Analysis showed that significant gains in terms of transmitted laser energy could be obtained by ensuring that the laser beam cross-section profile is incident on the face of the fiber as uniformly as possible. For instance, as shown in Figure 30(a), the beam cross-section incident on the fiber face with the use of a simple plano-convex lens had a Peak-to-Average (P/A) ratio of 15.6. However, a profile that distributed the energy more evenly on the fiber face was achieved using an appropriate axicon-lens combination (see Figure 30(b)). The P/A ratio in such a case was 3.9 and transmitted laser energy was as high as 30 mJ/pulse.

Nevertheless, such advanced injection schemes introduce higher-order modes and the quality of the beam exiting the fiber degrades. Despite the best efforts to counter these effects, the trade-off between the maximum transmittable laser energy and the generation of higher-order modes proved difficult to overcome and sparking could not be achieved. In this respect, the gradient-index fiber shown in Figure 31(b) appeared promising as it had better capability to preserve beam quality. Initial trials in the lab showed that these fibers suffer from low material damage threshold. Ultimately, it was decided to direct the present effort toward strategies with hollow-core fibers.



Simple Plano-convex lens
 $(P/A) = 15.6$
 Max. Transmitted 8 mJ/p

(a)



With Axicon
 $(P/A) = 3.9$
 Max. Transmitted 27 mJ/p

(b)

Figure 30. Fiber Face Laser Intensity Distribution Profiles for an Injection Scheme Using
 (a): Plano-Convex Lens, (b): Combination of Axicon and Plano-Convex Lens.

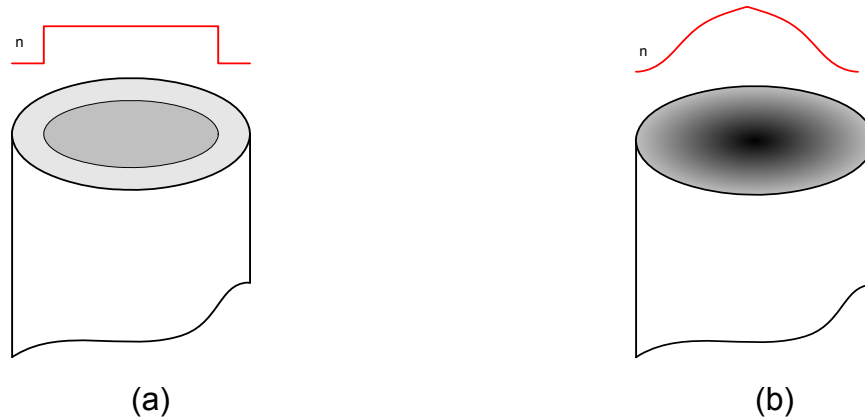


Figure 31. The Refractive Index Distribution in Two Solid Core Fibers: (a) Step-Index Fiber, and (b) Gradient-Index Fiber.

3.5.2. Hollow Glass Waveguides (HGWs)

Hollow Glass Waveguides (HGW) have the structure illustrated in Figure 32(a). They are essentially glass capillary tubes coated on the inside with silver and a reflectivity-enhancing dielectric. The mode of transmission through HGWs is first surface reflection while total internal reflection is the mode of transmission in solid core fibers. As a result of the transmission in air the damage threshold of these fibers is 40 times larger, i.e., ≈ 200 GW/cm². Also, HGWs tend to preserve the mode quality and exit the beam at a low cone angle, both characteristics rendering them ideally suited for spark generation. However, these fibers tend to have higher transmission losses compared to solid core fibers. Additionally, they exhibit certain unique characteristics:

- Transmission losses \propto (core diameter)⁻³.
- Bending losses \propto (bend radius)⁻¹.

Initial evaluations in the lab showed that the 700 μ m core HGWs were ideally suited as they offered the best compromise between flexibility and transmission. Subsequently, 700 μ m core HGWs were obtained from three different sources and tested in the laboratory. Their characteristics are as given below in Table 4.

Table 4. Hollow Glass Waveguides Tested for High-Power Laser Transmission

Source	Coating	Optimized for Wavelength
Polymicro Technologies	Proprietary	3.2 μ m
Rutgers University	Ag/CdS	0.532 μ m
Tohoku University	Ag/ COP	0.532 μ m

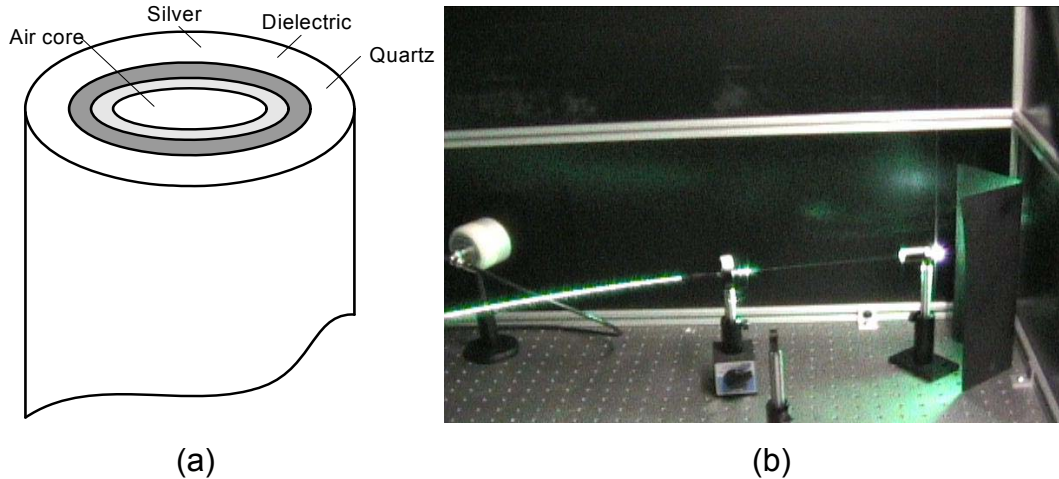


Figure 32. (a) Schematic of the Cross-Section of a Hollow Glass Waveguide (HGW), and (b) A Photograph Showing Spark Generation Using HGW in the Lab.

Photo Credit: Argonne National Laboratory

Sparking was achieved in the laboratory with all three fibers shown in Table 4. In all three cases, the injection was performed with lenses of focal length greater than 250 mm into fibers typically 1-2 meters long. However, the fibers from Tohoku University [19] offered the lowest transmission losses (see Figure 32(b)). Subsequently, a fiber-coupled laser system was developed using these fibers and the operation of a single-cylinder engine was demonstrated [18, 20]. However, the downside with these fibers was that they were very bend-sensitive; for bends $> 45^\circ$, sparking was severely affected [18, 21]. Consequently advanced fibers that are relatively bend-insensitive are desirable, while retaining the favorable characteristics of the HGW fibers from Tohoku University.

3.5.3. Advanced Air-Core Fibers

For future on-engine laser ignition applications, two kinds of advanced fiber technologies appear promising: (i) multi-layer hollow glass waveguides, and (ii) hollow-core photonic band-gap fibers. These are schematically shown in Figures 33(a) and 33(b). Both rely on multiple reflections to confine light to the central air-core, and most importantly both fibers are bend-insensitive. Manufacturing processes of both kinds of fibers are very involved and those that are commercially available – with core diameters $< 10 \mu\text{m}$ – are not suitable for the present purpose. It is expected that fibers with core diameters $\sim 30 \mu\text{m}$ will be required to achieve sparking [22-24]. However, fibers of this size are not readily available.

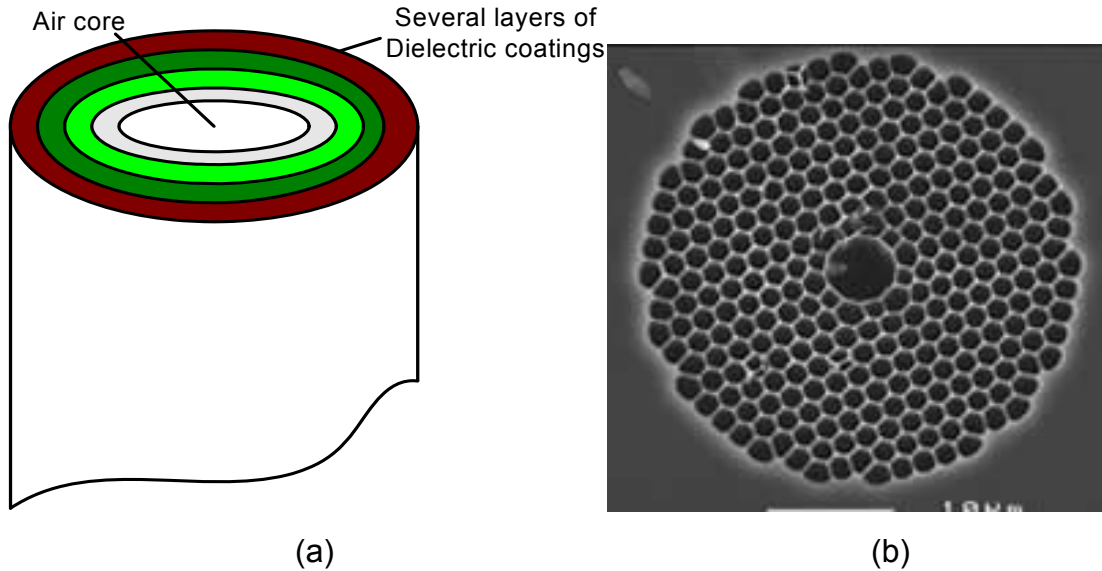


Figure 33. (a) Schematic of the Cross-Section of a Multi-Layer Hollow Glass Waveguide, and (b) Photograph of an Air-Core Photonic Bandgap Fiber

3.6. Electronic Interface

In natural gas-fueled stationary engines, the Electronic Control Unit (ECU) performs two primary functions: (i) providing ignition with feedback from a timing disk, and (ii) speed control with feedback from a governor. In most of the gas-fueled engines, these functions are performed by two separate units. Earlier in the report, as shown in Figure 19, it was envisioned that an electronic interface would be required for the ALIS to communicate with the ignition control part of ECU for ignition timing coordination. In consultation with Argonne's industrial partner, Altronic, Inc., an electronic interface was developed that utilizes commercially available conventional ignition systems.

One such system to drive a flip-flop multiplexer and a laser is schematically shown in Figure 34. The position of a timing disk mounted on the crank shaft is sensed by a magnetic pickup. The signal from the magnetic pickup is processed by the ECU/ Conventional ignition system to provide a 165 VDC pulse that is usually fed to the primary side of the ignition coil. In the present electronic interface such a signal is used to generate a 24 VDC pulse using a resistor step down circuit (represented as a χ box in Figure 34). The 24 VDC signal, in turn, is used to drive a corresponding rotary actuator. The end of stroke of the rotary actuator is sensed by an optical sensor and a trigger signal is provided to the laser after routing it through an OR gate. In such a system, the individual cylinder ignition timing variation is provided by the ECU/ conventional ignition system. One such system was successfully simulated and tested at Argonne using Altronic, Inc.'s CD-200 system. However the basic design of the system is not specific to a particular model or manufacturer.

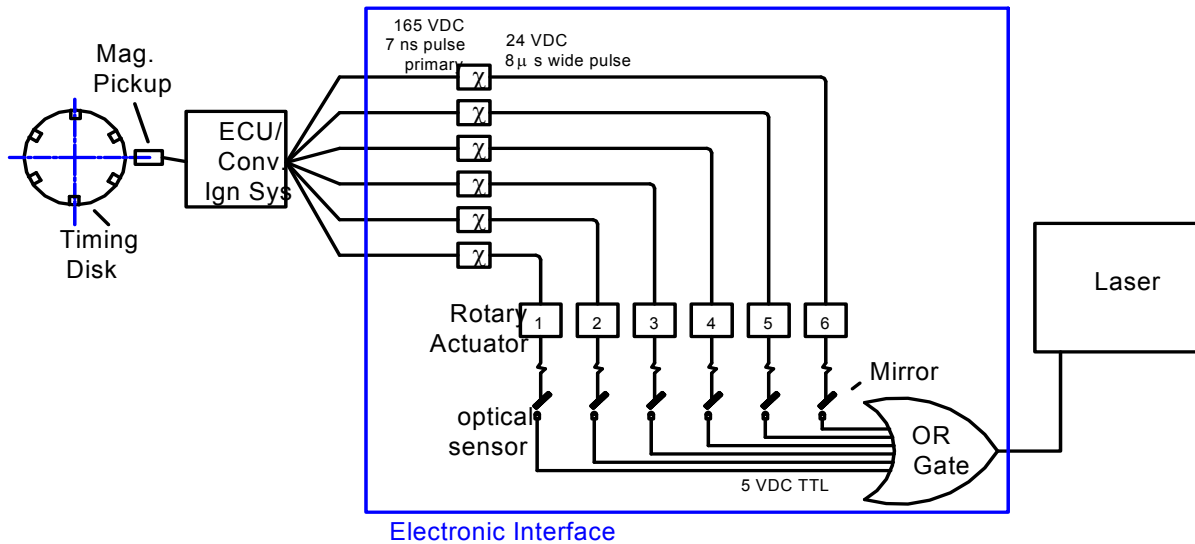


Figure 34. Schematic Diagram of the Electronic Interface

3.7. Results and Conclusions for Task 2.3

From an initial survey of several possible ALIS schemes, two promising configurations were identified: (i) the laser-per-cylinder concept, and (ii) the multiplexed laser concept, wherein the output of a single laser is distributed over various cylinders. The latter concept was chosen as it promised low-cost and simplicity of thermal management. However, this concept required the development of three high-power components, namely, laser plugs, multiplexers and fiber-optic beam delivery. Guidance was derived in the development of such components through (i) data from fundamental studies conducted in an earlier task (Task 2.2), and (ii) requirements of the advanced ignition system as specified by engine manufacturers. Specific details of the high-power components considered in the present task are described below:

Laser Plugs: A two-lens design that successfully meets the physical and functional requirements of a laser plug was easily achieved. Adaptation of this design for various engine geometries can be easily achieved.

Multiplexers: Three schemes that distribute the output of a single laser among various cylinders were pursued: (i) an electro-optic switch, (ii) a rotating-mirror scheme, and (iii) a flip-flop switch. The first two schemes fell short of the requirements either due to high-cost or the inability to provide ignition timing variations in individual cylinders. The flip-flop scheme, however, proved effective in all respects.

High-Power Fiber Optic Beam Delivery: Through tests and analyses it was determined that the fiber optic delivery requirements are (i) low divergence at distal end, (ii) high-power laser transmission, and (iii) preservation of mode quality. Initial tests performed using solid core fibers showed that they are limited by the material damage threshold. Subsequent tests

performed using Hollow Glass Waveguides showed that they are limited by mode shifts introduced by bending of the optical fibers. While photonic band-gap fibers appear promising, they are not readily available for tests and their development is expected to be expensive.

Electronic Interface: An electronic interface is required for the ALIS to communicate with the ECU of an engine for ignition timing coordination. In consultation with Argonne's industrial partner, Altronic, Inc., the timing modules from existing ignition systems were adapted for the present purpose easily.

4.0 (Task 2.4) Single-Cylinder Laser Ignition Studies

Earlier tests performed in an RCM, in Task 2.2, showed that laser ignition extends the lean ignition limit all the way to the lean flammability limit ($\phi = 0.5$) for natural gas-air mixtures. Additionally, it was found that for lean-operation laser ignition accelerates the rate of combustion. The objective of the present task (Task 2.4) is to determine the impact of such altered combustion behavior on the trade-off between brake thermal efficiency and NO_x emissions in a natural gas-fueled engine.

4.1. Statement of Work for Task 2.4

The goal of this task was to perform laser ignition tests on single cylinder natural gas engines of two size classes so as to evaluate the effects of ignition timing, equivalence ratio and intake air pressure on emissions and performance. The following actions were planned to be performed in this task:

- Prepare a test plan for optimizing ignition timing, efficiency and NO_x emissions while avoiding knock in order to determine the performance benefits by the use of laser ignition. Also, advantages by the use of multi point ignition in gas engines needs to be determined. Such tests are to be performed by NETL on a Ricardo Proteus engine.
- Perform the tests on the Ricardo Proteus engine per the approved test plan.
- Prepare a similar test plan for implementation on a large bore engine to determine the performance benefits by the use of laser ignition. Such tests are to be performed by SwRI on a CAT 3401 engine.
- Perform the tests on CAT 3401 per the approved test plan.

In a typical reciprocating engine chemical energy during combustion is converted to mechanical work on the piston. The net shaft power is a result of such work performed on the pistons less the mechanical losses. While the mechanical losses originate at various points of a working engine, the most significant of them (up to 50%) is the friction loss between the piston and cylinder liner. The impact of such losses is diminished in a large-bore engine as the specific surface area is reduced. Also, the reduced heat losses lead to additional efficiency improvements as the combustion cycle approaches the ideal Otto cycle. On account of such factors, the impact of using laser ignition varies in engines of different bore sizes. Field installations of natural gas fueled engines have bore sizes ranging between 130 and 380 mm. For large-bore engines either flame jet ignition or diesel pilot ignition are used to reduce the combustion time. Open chamber spark ignition is limited to bore sizes smaller than 250 mm. To determine the effectiveness of laser ignition in various size classes, it was proposed to perform ignition studies in engines of two sizes.

By the time of execution of the present task, under guidance provided by U.S. DOE's ARES program, the engine manufacturers such as Caterpillar, Cummins and Waukesha had

demonstrated ARES phase-I engines (42% Brake thermal efficiency, 1g/bhp-hr NO_x). Almost all of them have bore sizes of about 160 mm with swept volumes of the order of 3 liters. Both Cummins and Waukesha did not have single cylinder versions of these engines. Caterpillar had a 3501 series single-cylinder engine installed in its Technical Center in Peoria, but it was scheduled for in-house tests. The only alternative was to use research engines of 130 mm bore, mostly supplied by AVL or Ricardo. National Energy Technology Laboratory (NETL), a member of the present consortium to develop ALIS, performed tests in a Ricardo Proteus engine, comparing laser ignition and standard spark ignition. Details of such tests can be obtained from references [5, 6]. Though a high energy spark ignition system was used for comparative purposes, it had a performance similar to an inductive ignition system, which is significantly different from Capacitance Discharge Ignition (CDI) systems typically used with lean-burn gas engines. Also, due to the limitations imposed by their control system, the tests had to be limited to power levels below 12 bar Brake Mean Effective Pressure (BMEP). With the industry trying to achieve 25 bar BMEP by the year 2010, such a limitation could prove too restrictive. Details of such tests are reported in references [25] and [26] and are not reproduced here.

On the other hand, a Bombardier single-cylinder reciprocating engine (BSCRE), with 9.5" bore, was readily available at Southwest Research Institute (SwRI), and was ideally suited to determine the performance benefits in a large-bore engine. Since the engine was equipped with a CDI system that is typical of most field-installed natural gas engines, this readily provided a baseline for performance comparison. Additionally, the system is controlled by a fully flexible control system – Rapid Prototyping Engine Control System (RPECS) – developed by SwRI, which enables varying all operational parameters within the physical limits. This flexibility allowed testing up to 18 bar BMEP. Also, instrumentation to monitor fuel quality and perform emissions measurement was already in place. On account of such benefits, this engine was chosen to be the test platform. Using the 9.5 inch bore engine three sets of ignition tests were performed: baseline tests to determine the performance characteristics of conventional spark ignition using a CDI system, ignition tests with an open-path laser ignition, and ignition tests with a fiber-coupled laser ignition system.

In the following sections, details of the experimental setup are presented first. Subsequently, experimental test results obtained over a range of ignition timings and equivalence ratios are discussed along with the noted benefits of laser ignition.

4.2. Experimental Setup

4.2.1. Single-Cylinder Engine

A large-bore single-cylinder engine at Southwest Research Institute (SwRI) was chosen as the experimental engine for the present ignition tests. The specifications of this engine are provided in the Table 5. The engine was coupled to an eddy-current dynamometer and controlled by SwRI's proprietary RPECS. The dynamometer in turn was coupled to a

synchronous motor that assisted engine startup. The control scheme and the data acquisition scheme are schematically shown in Figure 35.

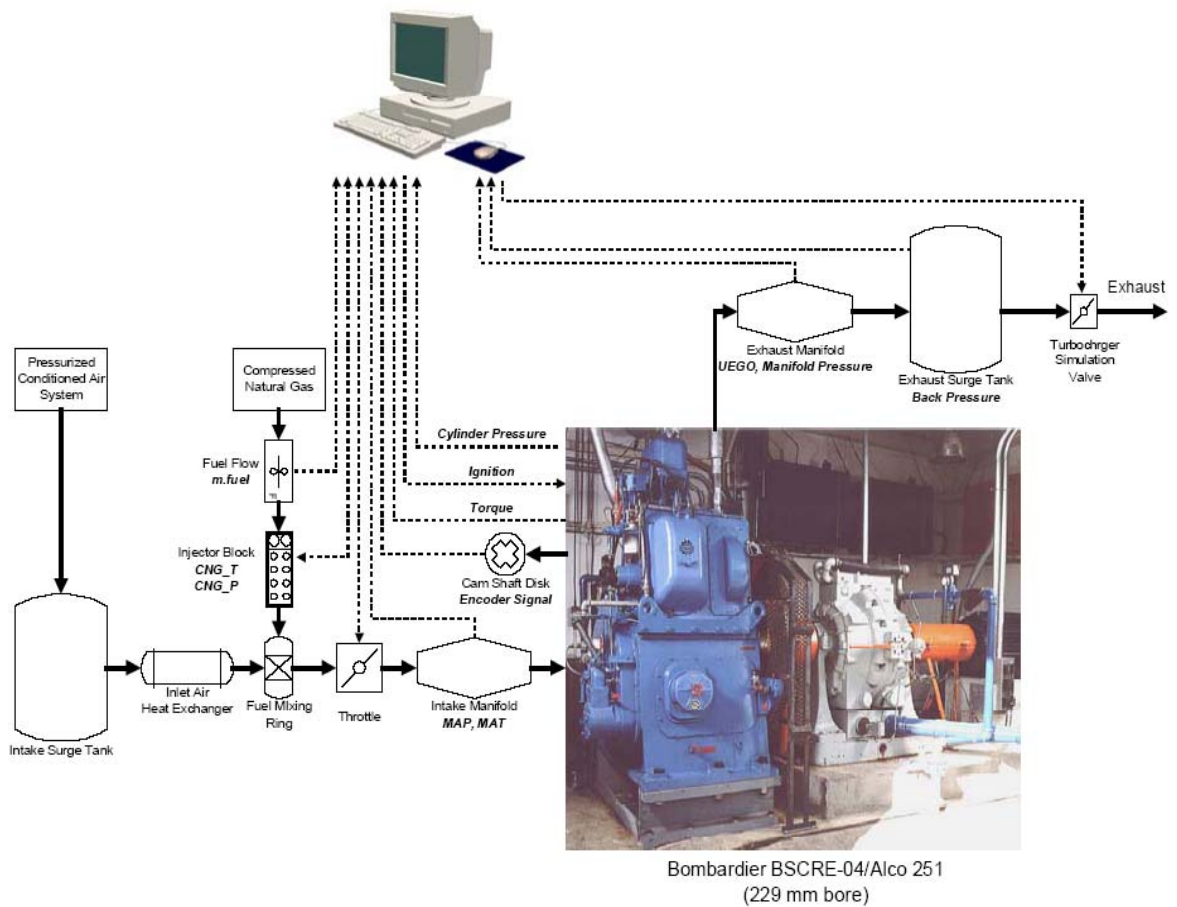


Figure 35. Schematic of the Control Scheme of the BSCRE Single-Cylinder Engine Using SwRI's RPECS.

Photo Credit: Argonne National Laboratory

In-cylinder pressure measurement was performed using a Kistler pressure transducer and combustion heat release analysis was performed subsequently. Emissions measurements were performed using a Horiba emissions bench and the data was analyzed following the standard procedure suggested by Heywood [2]. Natural gas was injected into the intake manifold using an array of low-pressure injectors and the air/fuel ratio was monitored using a Universal Exhaust Gas Oxygen (UEGO) sensor located on the exhaust manifold.

Table 5. Specifications of SwRI's BSCRE Engine

Feature	Specification
Engine Make	Bombardier BSCRE-04
Engine Type	Single-cylinder, 4-stroke
Bore (inches)	9
Stroke (inches)	10.5
Swept volume (liters)	11.5
Compression Ratio	9.3:1
Rated Speed (RPM)	900

The conventional spark ignition system included an Altronic CD-200 module and an 18 mm spark plug. The spark plug had 3 ground electrodes and was located at the same position as the laser plug identified in Figure 36. With this arrangement the following operating variables were identified:

- Intake boost pressure,
- Air/fuel ratio, and
- Spark timing.

4.2.2. Open-Path Laser Ignition Setup

For the open-path laser ignition tests, a compact frequency-doubled Nd:YAG laser was directly mounted over the cylinder head. The output of the laser traveled through the valve cover into a laser plug, from where it was focused into the combustion chamber by a sapphire lens. The sapphire lens was mounted flush with the fire deck and was subjected to combustion pressure and temperature. With this lens, the point of laser ignition was centrally located in the combustion chamber at about 13 mm from the lens face, and about 30 mm from the piston at top dead center. The piston, cylinder head, and laser plug are identified in Figure 36.

Initial experiments showed that the engine cylinder head vibrated sideways at 15 Hz and ± 3 mm amplitude. To minimize the undesirable effects due to these vibrations, the laser was mounted on the ground. The Figure 37 shows the mounting scheme and the spark location.

For these tests, Big Sky's frequency-doubled 'Ultra' Nd:YAG laser was used. The Big Sky Ultra laser was capable of delivering 33.5 mJ of energy per pulse at 532 nm when operating at 10Hz. The pulse duration for the Ultra laser was 8 ns. For the present engine tests, the laser output was adjusted to an energy setting of about 29 mJ per pulse. It should be noted that for an equivalence ratio (EQR; previously referred as ϕ) of 0.6 and BMEP of 15 bar, a laser output of about 9 mJ per pulse is sufficient to ensure consistent ignition of the natural gas-air mixture at normal engine operating conditions. The present application required an operating frequency of 3.75 Hz during engine start-up and the ability to transition to a frequency of 7.5 Hz at rated speed (900 rpm). The external trigger of the Ultra laser was

utilized in conjunction with the RPECS control system to synchronize the laser pulse to the engine cycle in an appropriate manner. Synchronization also provided the flexibility to adjust laser ignition timing during engine operation.

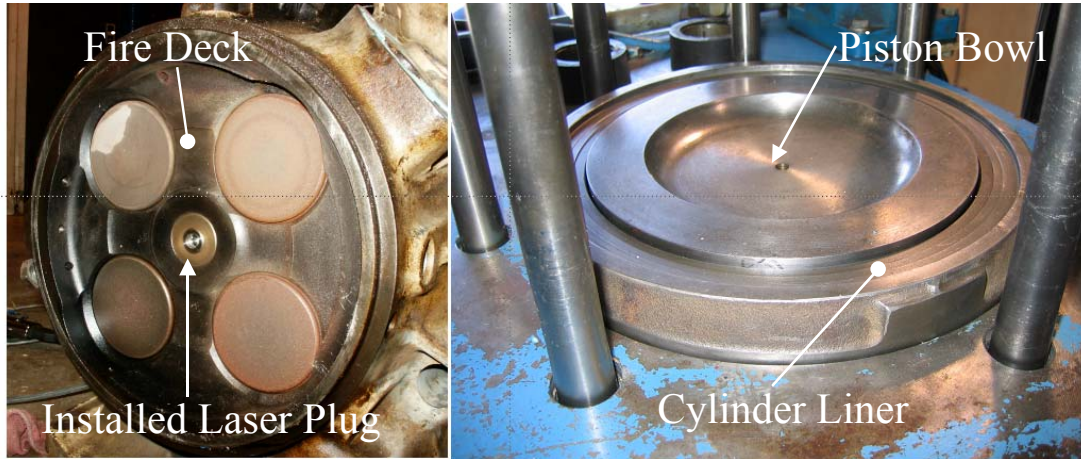


Figure 36. Photograph Showing the Installed Laser Plug in the Combustion Chamber.
Photo Credit: Argonne National Laboratory

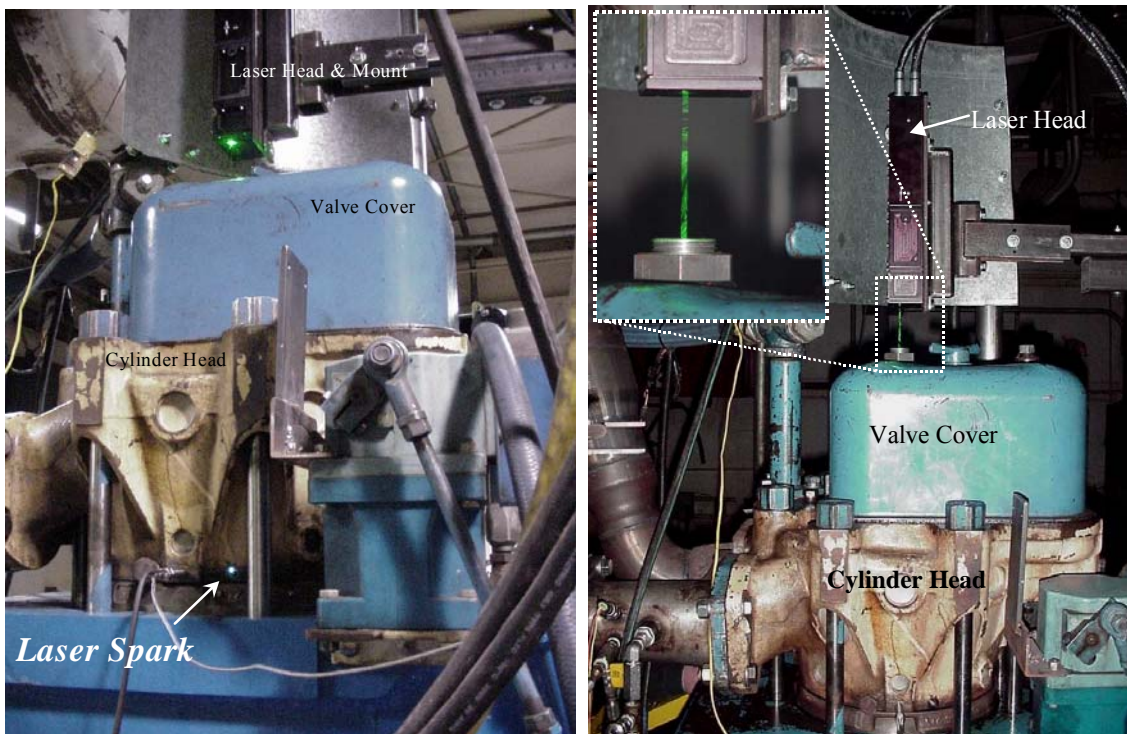


Figure 37. Setup for the Open-Path Laser Ignition Tests on a Large-Bore, Single-Cylinder Bombardier BSCRE-04 Engine.
Photo Credit: Argonne National Laboratory

4.2.3. Fiber-Coupled Laser Ignition Setup

Following the efforts undertaken in Task 2.3, a fiber-coupled laser ignition system, shown in Figure 38, was developed for the present subtask. A compact laser, Model Tempest from New-Wave Research, that had high beam quality and maximum pulse energy of 90 mJ was used for this purpose. The output of this laser was injected into a 28 inch long, 700 μm core silver/ polymer (Ag/COP) hollow glass waveguide (HGW) using a 250 mm focal length lens. At the distal end, the laser emission was collimated and refocused using a combination of lenses with focal lengths of 150 mm and 13 mm. To prevent sparking at the fiber input a nitrogen purge was used. A charge-coupled device (CCD) mounted in the proximity allowed fine mechanical adjustments. All of these elements were mounted on a single 1/2" thick plate for testing on the Bombardier BSCRE-04 engine. Prior to the actual engine tests, engine vibration was simulated in the lab using a shaker table and laser ignition was observed. The fiber-coupled laser ignition system exhibited consistent sparking for over 24 hours. Subsequently, the system was mounted on the engine at 15 degrees from the vertical, as shown in Figure 39. A small port on the side of the cylinder head provided optical access for observing the spark kernel.

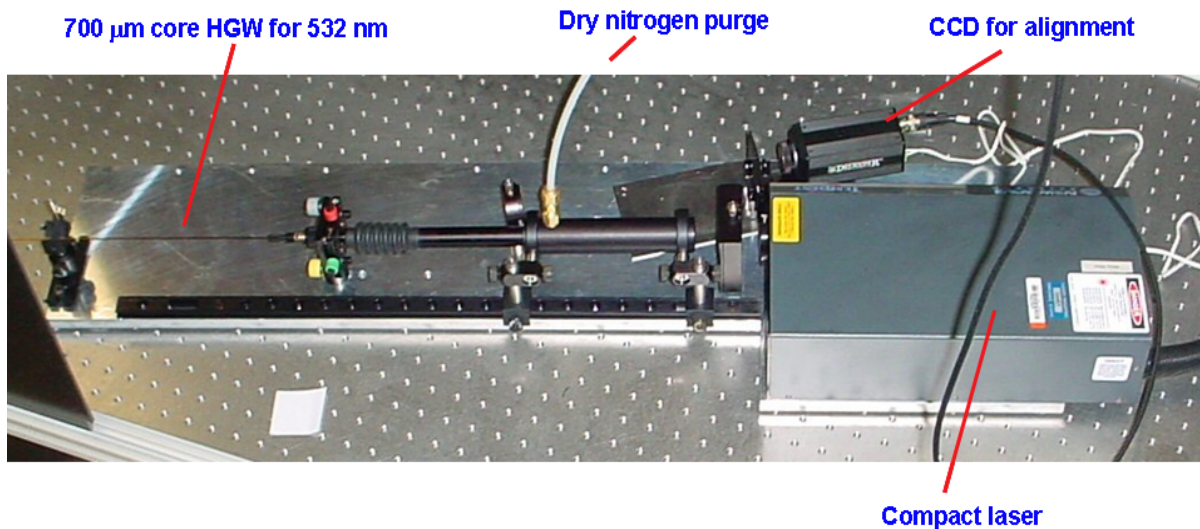


Figure 38. Layout of the Fiber-Coupled Laser Ignition System.

Photo Credit: Argonne National Laboratory

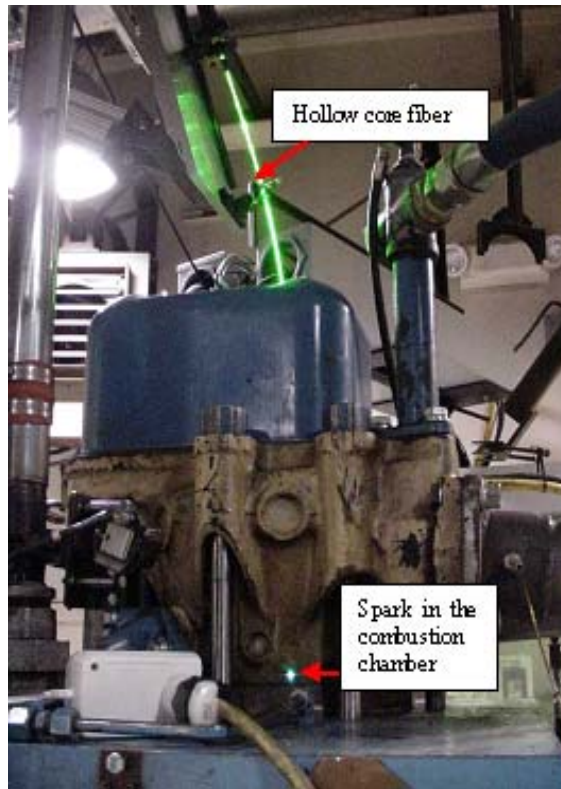


Figure 39. Fiber-Coupled Laser Ignition System as Mounted on the Bombardier BSCRE-04 Engine.

Photo Credit: Argonne National Laboratory

4.3. Test Matrix

Table 6 below shows the test matrix used to compare the laser and conventional spark ignition systems at a BMEP of 15 bar; the matrix was duplicated at the lower load of 10 bar BMEP (~873 Newton meter [N-m] of torque). Engine coolant temperature was maintained at 75° C and lube oil temperature was maintained at 85° C. The intake air temperature was maintained at 55° C for full load operation and at 28° C for part load operation to simulate a turbocharged and intercooled intake charge induction system. The simulated turbocharger efficiency was set at 60 percent by controlling the pressure ratio across the intake and exhaust manifolds. The test matrix shown in Table 6 was expanded to include a comparison between the two ignition systems at a BMEP of 10 bar.

The engine was allowed 5 minutes to stabilize at a given test condition before data was recorded. Ignition timing sweeps were performed to set a baseline vis-à-vis its effects on engine emissions and performance. The lean operating envelope was determined by advancing spark timing from the onset of misfire (at very retarded ignition timings) to an advanced ignition timing, which entailed an exhaust NO_x concentration greater than 2,000 parts per million (ppm) (a typical lean-burn engine would operate well below this NO_x concentration). Engine knock, rather than high exhaust NO_x concentration, often limits ignition advance but the Bombardier engine did not knock during any of these tests. The onset of the misfire regime was defined as an operating condition wherein the coefficient of variance (COV) of the indicated mean effective pressure (IMEP) over 100 consecutive cycles was greater than 5 percent. Single-cylinder engines will often exhibit higher COV of IMEP than their multi-cylinder counterparts because the charge induction process in the former is not continuous. Therefore, a COV of IMEP of 5 percent was used to identify the onset of misfire at retarded ignition timings; however, complete lean misfire was defined as an operating condition wherein 1 percent of engine cycles are devoid of *any* heat release at MBT timing. Indicated parameters and combustion metrics were calculated based on cylinder pressure data acquired with a Kistler piezoelectric pressure transducer that was flush-mounted on the combustion chamber.

With the test matrix described above, three sets of tests were performed:

1. Baseline tests using a conventional CDI spark ignition system,
2. Tests using open-path laser ignition, and
3. Tests using fiber-coupled laser ignition.

Results from tests are presented below. It ought to be noted that a large part of the discussion that follows focuses on results obtained with the open-path laser ignition system. Fiber-coupled laser ignition tests could not be performed for a sufficiently long time to record emissions data. However, based on observations during the short time that the tests were actually performed, it is expected that the results with fiber-coupled laser ignition are likely to be similar to those from open-path laser ignition, so long as similar laser spark characteristics can be maintained in both cases.

Table 6. Test Matrix for Single-Cylinder Laser Ignition Studies

Note	Load N-m	Speed RPM	Phi	Ign.Timing °BTDC	Boost/EBP	Ignition System	Piston
EQR Sweep @ 15 bar BMEP	1,307	900	0.65	PTT Limit***	15 bar, 60% Comp. Eff.	CD200/Open- path laser	Nominal
EQR Sweep @ 15 bar BMEP	1,307	900	0.65	+3	15 bar, 60% Comp. Eff.	CD200/Open- path laser	Nominal
EQR Sweep @ 15 bar BMEP	1,307	900	0.65	+6	15 bar, 60% Comp. Eff.	CD200/Open- path laser	Nominal
EQR Sweep @ 15 bar BMEP	1,307	900	0.65	+...Knock**	15 bar, 60% Comp. Eff.	CD200/Open- path laser	Nominal
EQR Sweep @ 15 bar BMEP	1,307	900	0.625	PTT Limit***	15 bar, 60% Comp. Eff.	CD200/Open- path laser	Nominal
EQR Sweep @ 15 bar BMEP	1,307	900	0.625	+3	15 bar, 60% Comp. Eff.	CD200/Open- path laser	Nominal
EQR Sweep @ 15 bar BMEP	1,307	900	0.625	+6	15 bar, 60% Comp. Eff.	CD200/Open- path laser	Nominal
EQR Sweep @ 15 bar BMEP	1,307	900	0.625	+...Knock**	15 bar, 60% Comp. Eff.	CD200/Open- path laser	Nominal
EQR Sweep @ 15 bar BMEP	1,307	900	0.6	PTT Limit***	15 bar, 60% Comp. Eff.	CD200/Open- path laser	Nominal
EQR Sweep @ 15 bar BMEP	1,307	900	0.6	+3	15 bar, 60% Comp. Eff.	CD200/Open- path laser	Nominal
EQR Sweep @ 15 bar BMEP	1,307	900	0.6	+6	15 bar, 60% Comp. Eff.	CD200/Open- path laser	Nominal
EQR Sweep @ 15 bar BMEP	1,307	900	0.6	+...Knock**	15 bar, 60% Comp. Eff.	CD200/Open- path laser	Nominal
Lean Limit*	1,307	900		MBT from 0.6	15 bar, 60% Comp. Eff.	CD200/Open- path laser	Nominal

4.4. Results and Discussion for Task 2.4

Common metrics for lean-burn engine performance include brake thermal efficiency (η) and brake specific NO_x emissions (BSNO_x). Macro-operational settings that affect these metrics, *ceteris paribus*, include fuel-air equivalence ratio (EQR) and ignition timing. The EQR, also written as ϕ , was controlled globally through a fuel metering block and UEGO sensor feedback, but the EQR values reported here were calculated with a carbon-balance method based on exhaust gas analyses [2]. Crank-resolved engine parameters are plotted versus the crank angle (CA) after top dead center (ATDC) at which 50 percent of the total in-cylinder mass had burned (MFB50). This manner of representing the crank-resolved parameters minimized the ambiguity surrounding actual ignition timing in the two ignition systems. Through combustion analysis of average cylinder pressure (obtained by ensemble-averaging over 100 successive engine cycles), fundamental differences between the two modes of ignition were also compared. Flame development and propagation were quantified through a heat release (burn-rate) analysis. Specific parameters of importance include the crank angle duration for 10 percent, 10 to 50 percent, and 50 to 90 percent of the trapped mass to burn. These parameters are abbreviated as MFB 0-10, MFB 10-50, and MFB 50-90, respectively. Estimating these parameters required an accurate determination of the start of combustion (SOC). For the test results discussed here, SOC was defined as the CA where the heat release becomes non-zero. This method of determining SOC was employed here because in the present laser ignition system the delay between trigger and laser pulse was appreciable ($225 \mu\text{s} \pm 100 \mu\text{s}$). These parameters are delineated in Figure 40.

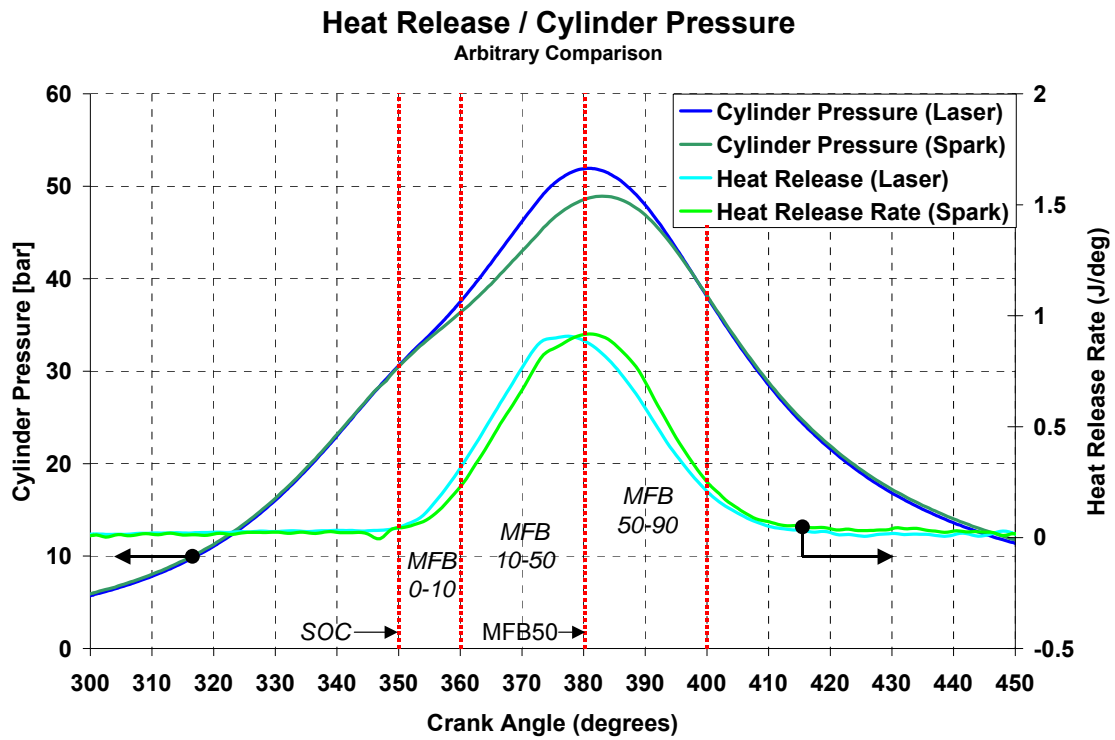


Figure 40. Arbitrary Cylinder Pressure and Heat Release Comparison to Clarify Nomenclature of Combustion Parameters.

4.4.1. Full Load Comparison (15 bar BMEP)

The engine was operated at a BMEP of 15 bar (or 1307 N-m of torque) at 900 rpm, with both a conventional spark ignition system and an open-path laser ignition system for identifying the benefits laser ignition could have on lean-burn natural gas engines. Laser ignition was found to extend the lean misfire limit from an EQR of 0.55 with open-chamber spark ignition to 0.50. Laser ignition also improved combustion stability at retarded ignition timings. The combined effect of these two improvements was a 50 percent decrease in NO_x emissions while maintaining efficiency constant. Figure 41 depicts how laser ignition was capable of extending the lean misfire limit. The various data points represent COV of IMEP over a range of EQR for both laser and spark ignition at different ignition timings. In this plot, increased COV of IMEP correlates to more retarded ignition timings at a given EQR.

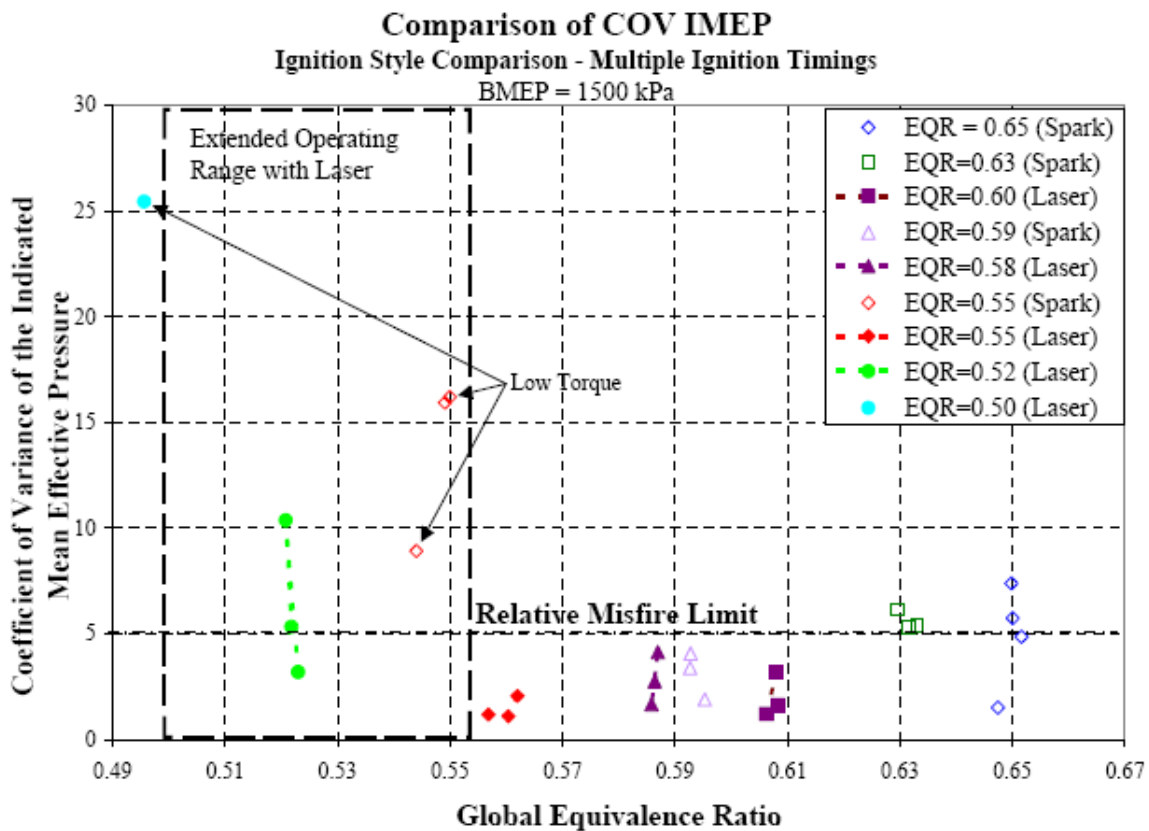


Figure 41. COV of IMEP Versus Equivalence Ratio (EQR) at a BMEP of 15 bar.

When the engine was operated at increasingly lean EQR values with open-chamber spark ignition, complete misfire occurred at an EQR of 0.55 and was detected by a large COV of IMEP (~15%). Even when ignition timing was advanced to 40° before top dead center (BTDC), a steady torque could not be maintained. By comparison, complete misfire occurred at an EQR of 0.50 with laser ignition. As ignition timing was retarded at a given EQR, the COV of IMEP increased (shown by multiple points in a data set). For both ignition systems, Figures 42 and 43 show combustion stability as a function of MFB50 at multiple ignition

timings. Evidently, laser ignition improved combustion stability at any given MFB50 for every EQR tested.

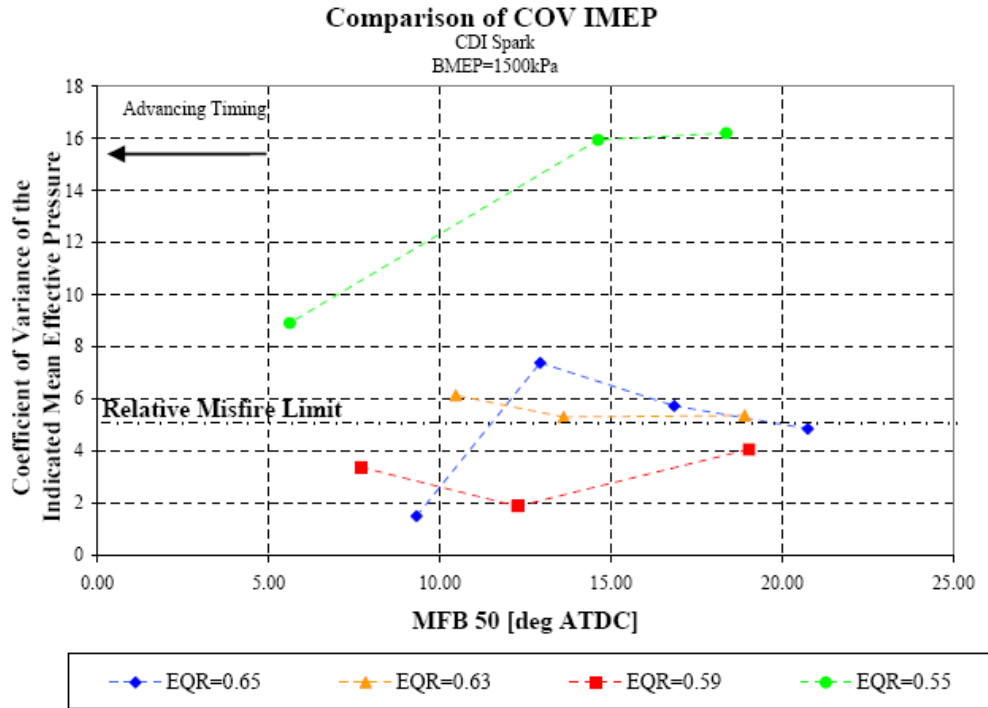


Figure 42. Combustion Stability with Conventional Spark Ignition at a BMEP of 15 bar.

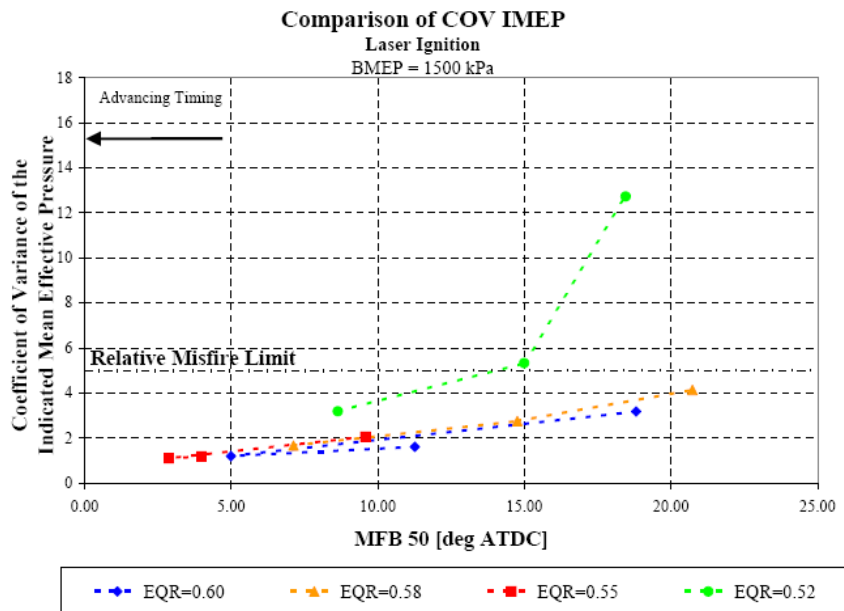


Figure 43. Combustion Stability with Laser Ignition at a BMEP of 15 bar.

Other higher-energy ignition systems for natural gas engines are also capable of extending the lean misfire limit. These include pre-combustion chambers and high-energy spark ignition systems. However, they do not necessarily improve the overall performance of the engine. Pre-combustion chamber ignition systems can ignite leaner mixtures in the main chamber, but the combustion in the pre-combustion chamber may contribute significantly to the overall NO_x emission. High-energy spark ignition systems often accelerate the deterioration of the spark plug, thereby requiring increased maintenance and/or replacement. In addition, they also constrain the flame kernel to the chamber wall where flame growth is often stunted by heat transfer to the metal surroundings. By comparison, laser ignition extended the lean misfire limit, thus gaining the emission and performance benefits without any undesirable side-effects or constraints.

Lean-burn engine technologies are utilized to improve efficiency and decrease NO_x emissions. Figure 44 compares the trade-off between brake-specific NO_x (BSNO_x) emissions and brake thermal efficiency for the two ignition systems. This method of comparing the trade-off between engine performance and BSNO_x emissions is consistent with other such comparisons of lean-burn technologies. As the engine ran leaner, the trade-off leaned toward lower BSNO_x emissions. Laser ignition allowed the engine to run leaner and extended the trend toward lower BSNO_x. With open-chamber spark ignition, a brake thermal efficiency value of 32 percent could be obtained along with 17.7 g/kWh (13.2 g/bhp-hr) BSNO_x emissions when the engine was operated at 90 percent of the misfire limit (typical of lean burn applications). Maintaining the same misfire margin and brake thermal efficiency, the BSNO_x emissions could be reduced to 5.4 g/kWh (4 g/bhp-hr) using laser ignition; this amounts to a 69 percent improvement. From an alternate viewpoint, while maintaining the NO_x emissions level constant at 10 g/kWh (7.5 g/bhp-hr), efficiency improvements up to 3 percentage points are likely with laser ignition.

Combustion characteristics of the two ignition systems were analyzed to examine the reasons behind the benefits observed with laser ignition. Figure 45 shows cylinder pressure data for 100 consecutive cycles for both open-chamber spark ignition (shown to the left) and laser ignition (shown to the right). Spark ignition exhibited complete lean misfire while laser ignition provided relatively stable combustion even at a leaner EQR.

With laser ignition, the COV of IMEP was 5.2 percent at an EQR of 0.52 compared to a COV of IMEP of 16.5 percent at an EQR of 0.55 for conventional spark ignition. Figure 46 shows the ensemble-averaged (over the 100 consecutive cycles) pressure curves for both ignition systems and their corresponding heat release rate profiles. The initial heat release was accelerated with laser ignition and consequently the total burn duration was decreased. As a result of these effects, combustion was more stable and the engine could operate at a lean EQR without misfiring. For the same reasons, good brake thermal efficiency values were also sustainable at more retarded ignition timings with laser ignition compared to spark ignition. This ability to employ more retarded ignition timings further reduced NO_x emissions. The considerable difference in peak pressures between the pressure traces for

laser and spark ignition may be attributed to the higher boost pressure required to achieve the same BMEP value (15 bar) at a leaner equivalence ratio with laser ignition.

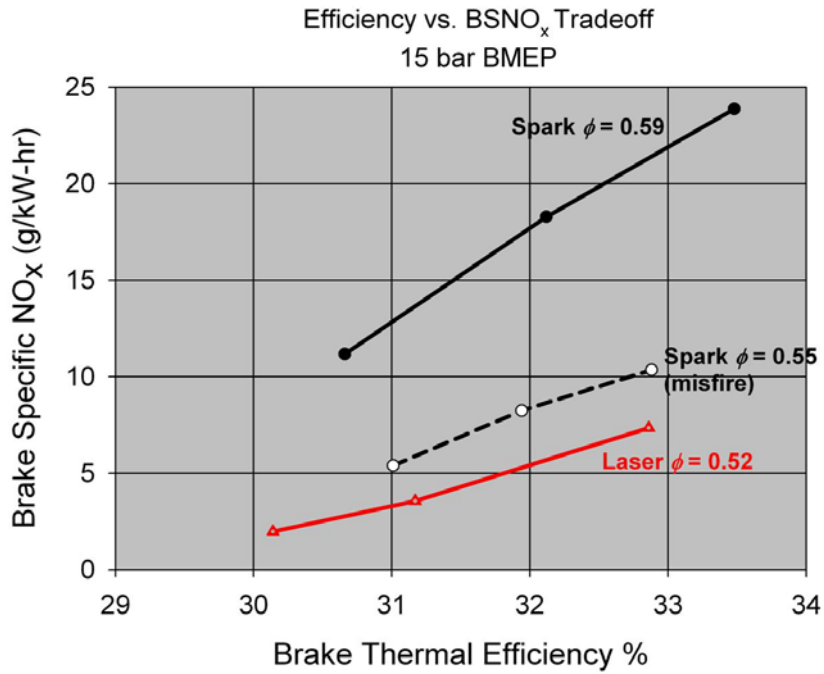


Figure 44. BSNO_x-Brake Thermal Efficiency Tradeoff at a BMEP of 15 bar.

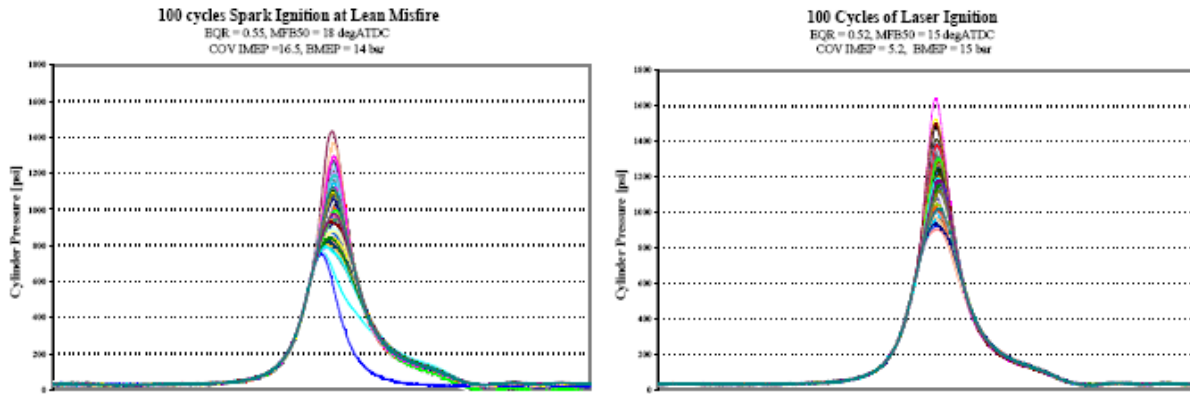


Figure 45. Cylinder Pressure Comparison.

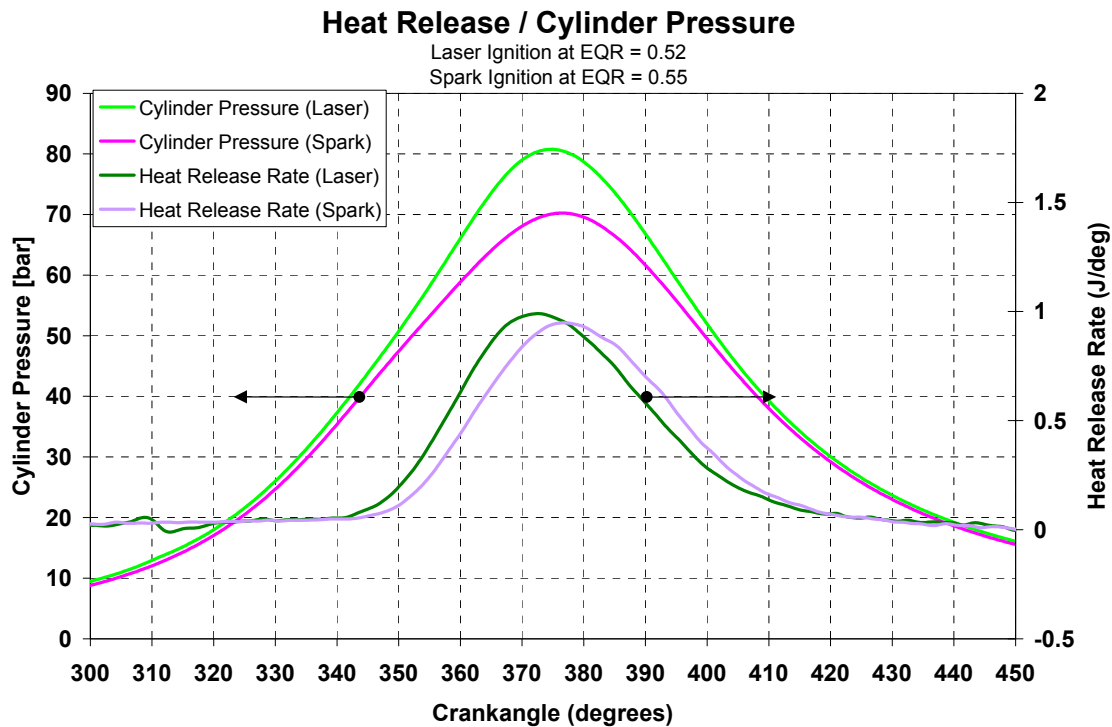


Figure 46. Cylinder Pressure and Heat Release Comparison.

4.4.2. Part Load Comparison (10 bar BMEP)

The performance and emissions improvements shown at full load were also observed at part load. Also, laser ignition was able to extend the lean misfire limit and improve combustion stability; as shown in Figure 47. These test results at a BMEP of 10 bar are comparable and consistent with work published by National Energy Technology Laboratory [14], in which laser ignition extended the lean limit and decreased ignition delay. Using conventional spark ignition, the engine experienced complete lean misfire (COV of IMEP of 15 percent) at an EQR of 0.55. Laser ignition improved combustion stability at the EQR of 0.55 (COV of IMEP of 2.5 percent) and allowed the engine to operate down to an EQR of 0.50, beyond which misfire was observed.

Figure 48 shows the BSNO_x-brake thermal efficiency trade-off at part load illustrates how laser ignition enabled the engine to operate at lower BSNO_x emissions without compromising efficiency. The BSNO_x emissions were reduced by 65 percent while maintaining the thermal efficiency constant at 32 percent.

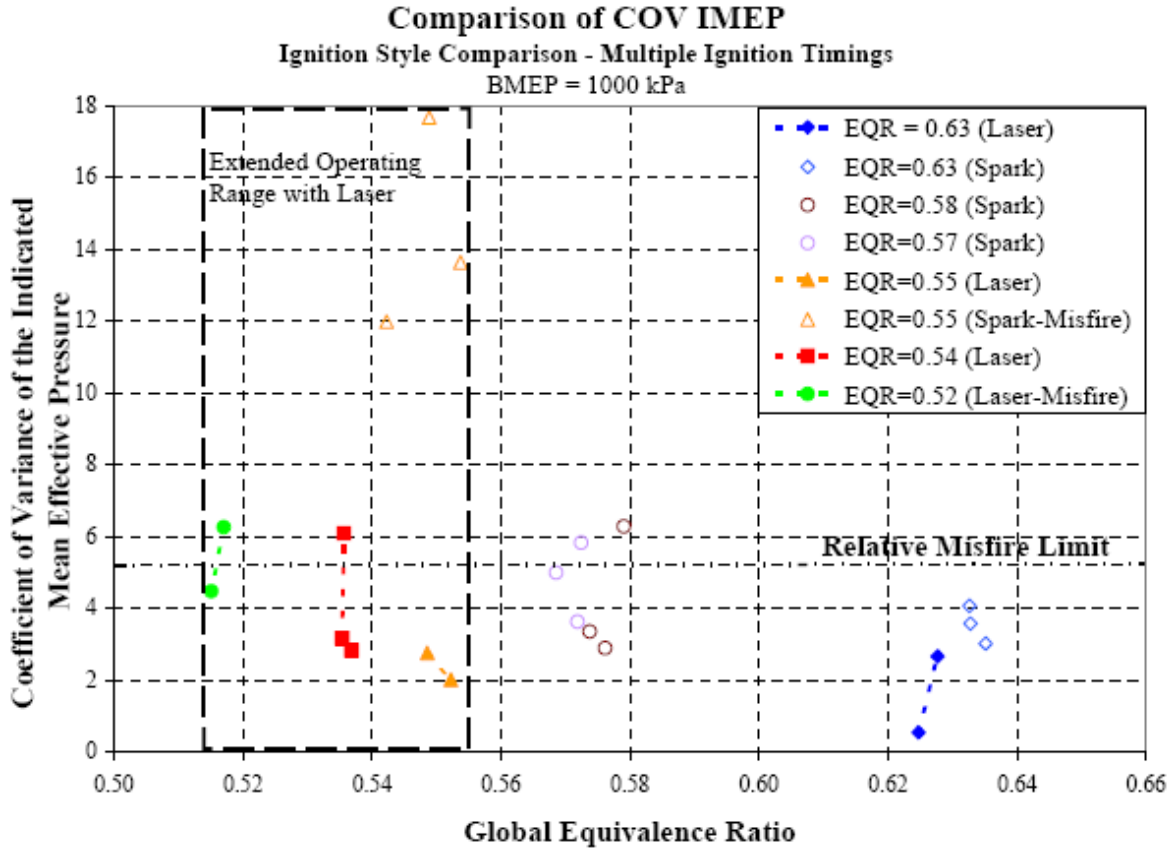


Figure 47. COV of IMEP Versus Equivalence Ratio at a BMEP of 10 bar.

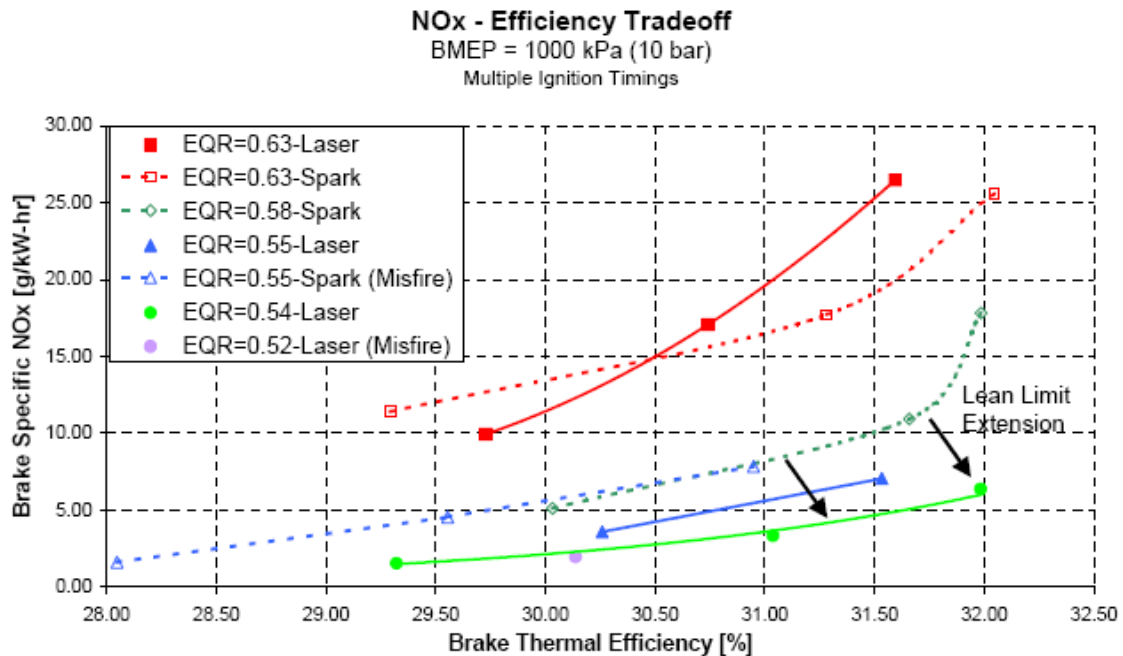


Figure 48. BSNO_x-Brake Thermal Efficiency Trade-off at a BMEP of 10 bar.

4.4.3. Fiber-Coupled Laser Ignition Results

Using the setup shown in Figures 38 and 39, 100 percent ignition probability was achieved with laser ignition and with the engine operating at an EQR of 0.6 and a BMEP of 10 bar. A comparison of the burn durations for different modes of ignition and different percentage mass fraction burns is shown in Figure 49. This plot shows that the apparent advantages with the use of fiber-coupled laser ignition are similar to those obtained using free-space laser ignition, that is, accelerated burn rates during all phases of combustion. This is consistent with the explanation provided by Bradley et al. [27] in that the increased energy content in the plasma kernel generated by laser ignition results in overly reactive species. These species result in the development of a flame front in 'overdrive,' with the associated flame velocities much higher than those typical of conventional spark ignition. The overdriven flame speeds are advantageous to lean-burn engines as the reduced combustion durations can be used to retard ignition, thereby ensuring improved efficiencies and lower NO_x emissions.

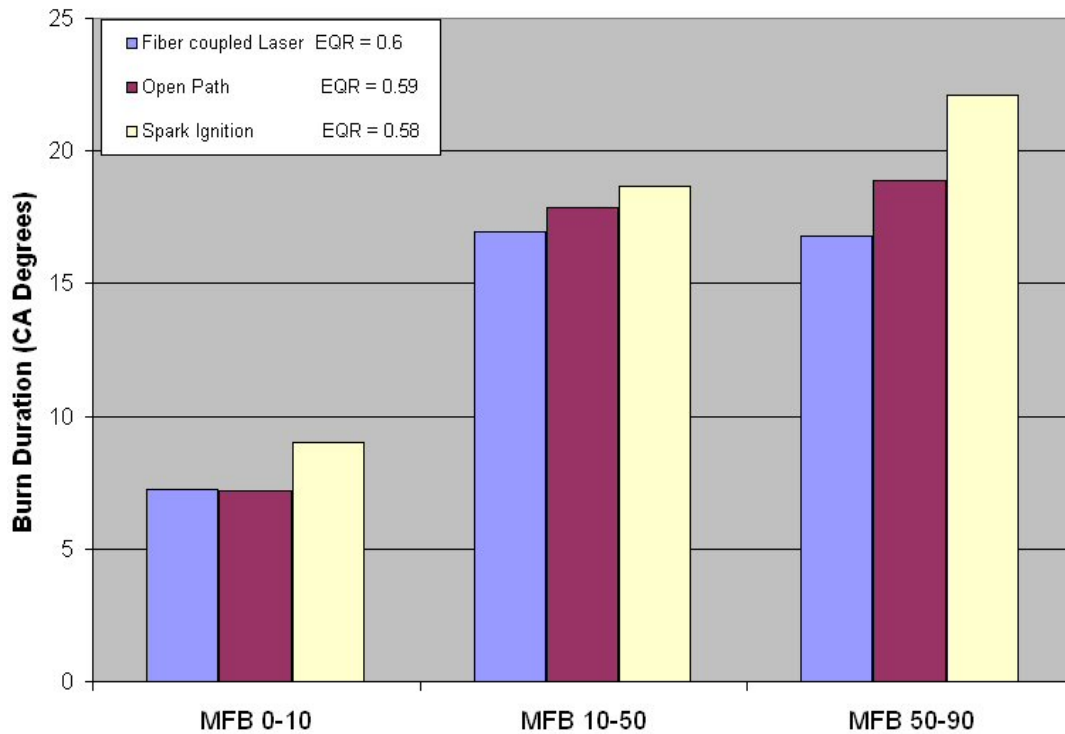


Figure 49. A Comparison of Burn Durations for Different Modes of Ignition.

4.5. Conclusions for Task 2.4

Experiments were performed on a single-cylinder research engine comparing three different ignition systems including:

- i. conventional capacitance discharge spark ignition,
- ii. free-space laser ignition, and
- iii. fiber-coupled laser ignition.

Several benefits were observed with laser ignition including the following:

- Extension of the lean misfire limit by about 10 percent at BMEPS of 10 and 15 bar,
- Increase of the overall burn rate, and
- Improved combustion stability at all comparable test points.

The improved combustion, combined with optimization of engine intake air pressure and ignition timing, was found to result in

- A reduction of BSNO_x emissions by about 70 percent for a given efficiency, or
- An increase in brake thermal efficiencies up to 3 percentage points, while maintaining BSNO_x emissions constant.

Considering all of the perceived benefits of laser ignition, the on-going efforts aimed to develop an ALIS for use with a multi-cylinder engine, which form the essence of Tasks 2.5 and 2.6.

5.0 (Task 2.5) Integrate ALIS and Refine for Performance on a Multi-Cylinder Engine

The goal of this task was to integrate a prototype ALIS from successful individual components and test for its performance on a multi-cylinder natural gas engine. Through these tests, it is envisioned that the design of the integrated ALIS will be refined for superior performance and durability. The following activities were planned in this table:

- Install a small 4-cylinder natural gas generator (Waukesha VSG series) in the engine test cells of Argonne. Also, natural gas fueling system will be procured and installed.
- Integrate the components developed in Task-2.4 into a single ALIS and test it for repeatability and integrity in a lab environment.
- Install the integrated ALIS on the VSG series engine and further check it for integrity.
- Further streamline the ALIS design for enhanced durability, ease of connectivity and operation.

5.1. Engine and Natural Gas Fueling System Installation

5.1.1. Multi-Cylinder Engine

Originally, it was proposed to install a Waukesha VSG 4-cylinder engine for the experiments associated with this task. However, this engine was found to have a 14 mm spark plug port and much higher baseline NO_x emissions than the current goals. In the meantime, under the U.S. DOE's ARES program, the primary US engine manufacturers – Caterpillar, Cummins and Waukesha – developed engines that meet the Phase-I goals (42% brake thermal efficiency, 1 g/bhp-hr NO_x). Therefore, one of the smallest engines in this category – the Cummins QSK-19G engine (in-line 6-cylinder, 4-stroke, 1,800 rpm, lean-burn natural gas operation) – was procured for the present purpose. This engine has a separate head for each cylinder, which is very conducive for conducting engine tests. A photograph of the Cummins QSK-19G engine in one of Argonne's test cells is shown in Figure 50. As shown in this figure, this engine uses an Altronic spark-ignition system with 18 mm spark plugs. Furthermore, Cummins Engine Company promised all the necessary support for installation and commissioning of this engine. This 467 horsepower (hp) engine requires a 600 hp dynamometer for successful operation. The installation of a dynamometer matching the engine power requirements could not be completed on time. This being the case, it was planned to use this engine to check the system integrity during design iterations of ALIS. It was further planned to run experiments on an operating engine in one of the engine test cells of Cummins Technical Center, Columbus, IN. Cummins promised to provide support for the aforementioned activities.



Figure 50. A Photograph of the Cummins QSK-19G Engine in one of the Engine Test Cells at Argonne National Laboratory

Photo Credit: Argonne National Laboratory

5.1.2. Natural Gas Fueling system

Originally, the Cummins QSK-19G engine was expected to be installed in the 362-A102 test cell at Argonne. As this engine required 3,000 standard cubic-feet per hour of natural gas fueling rate at about 15 pounds per square inch (psig) under full-load conditions, enhancements were made to the existing natural gas supply system. The required flow meter and regulator were procured and installed on the natural gas supply system of the building. Also, 3-inch diameter gas lines were extended all the way from the supply system to the test cell. All other utilities – cooling water supply, exhaust and compressed air – were also installed. However, due to lack of funds and certain other unforeseen delays, the installation and commissioning of the required dynamometer was delayed. Consequently, the existing engine was used as a mule engine to check the integrity of the ALIS design and to refine it further. As mentioned, ALIS was demonstrated on an operating engine at Cummins Technical Center.

5.2. ALIS Integration

Through the efforts of Task 2.3, successful designs of the following components were achieved:

Laser: Following a brief survey of available lasers, Diode Pumped Solid State Lasers (DPSSL) were found to have the required performance characteristics. These lasers are commercially available from many laser vendors. However, for the present demonstration, a compact Nd:YAG which is already available in our laboratory was used as a surrogate. Except for the fact that this compact laser does not have the long lifetime typical of DPSSL, it completely mimics the performance of DPSSL.

Laser Plug: The laser plug was designed to have the same footprint as a standard 18 mm spark plug. The plug has a 13 mm back focal length sapphire lens that focuses the incoming laser radiation to achieve a spark. The sealing system was designed in such a way that the laser plug is able to withstand pressures up to 3,000 psig and temperatures up to 3,000 K.

Multiplexer: Out of the many designs that were tested, a flip-flop multiplexer was found to be suitable. In this system, rotary actuators when activated, move mirrors in and out of the laser beam path to distribute the pulsed laser output to individual cylinders. This design proved attractive as it allows ignition timing variation of individual cylinders.

Electronic Interface: A survey showed that commercially available electronic interface systems can be used with minor modifications for the present purpose.

Despite the aforementioned successes, the use of a fiber optic delivery to transmit the laser output from the laser to individual cylinders proved to be a challenge. Further technical developments are necessary for fiber optic delivery to become viable. Therefore, in the integrated design of ALIS, transmission of laser emission in enclosed tubes was envisioned. This is schematically shown in Figure 51. This arrangement consists of a row of mirrors, which move in and out of a laser beam path. When activated, each mirror diverts the beam into a corresponding laser plug installed on each cylinder in the cylinder head.

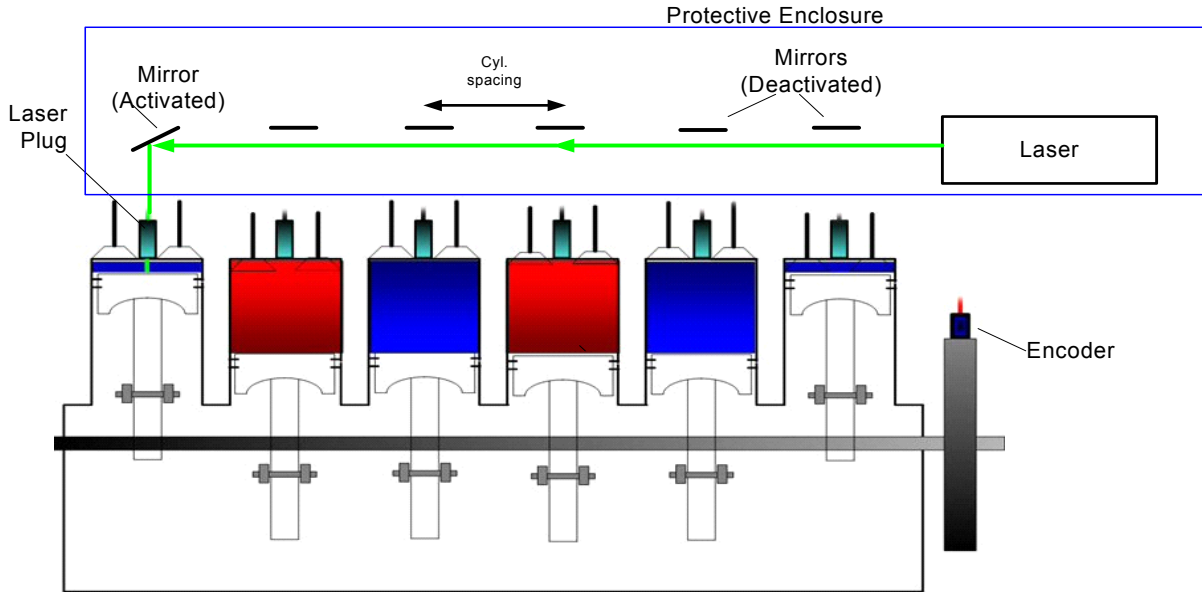


Figure 51. A Schematic of the Integrated ALIS

5.2.1. Mechanical Integration

Functional requirements for the integrated ALIS are:

- i. Vibration insensitivity,
- ii. Electro magnetic insensitivity,
- iii. Operating temperatures up to 100° C, and
- iv. Completely enclosed laser beam, thereby avoiding inadvertent exposure to operators.

To meet the requirements mentioned above, a design shown in Figure 52 was developed. In this system, an arm placed at 22.5° from the horizontal carries a half-inch diameter mirror. This arm is coupled to a rotary actuator by a shaft. When the rotary actuator is activated, it turns the shaft so that the arm is 45° from the horizontal, thereby moving the mirror into the laser beam path. When the actuator is deactivated, it returns the arm back to its original position. For this design to be easily adaptable to the engines of different manufacturers, the overall system needs to be modular to accommodate differences in cylinder-to-cylinder spacing. Each of these modules is interconnected using opaque gas-tight tubes. Besides providing adequate laser safety, they also provide easy installation. The present system was designed for installation and operation on the Cummins QSK-19G without much refinement. Figure 53 shows a picture of the ALIS assembly mounted on Cummins QSK-19G engine (top view) at Argonne. Laser head on the right is out of range.

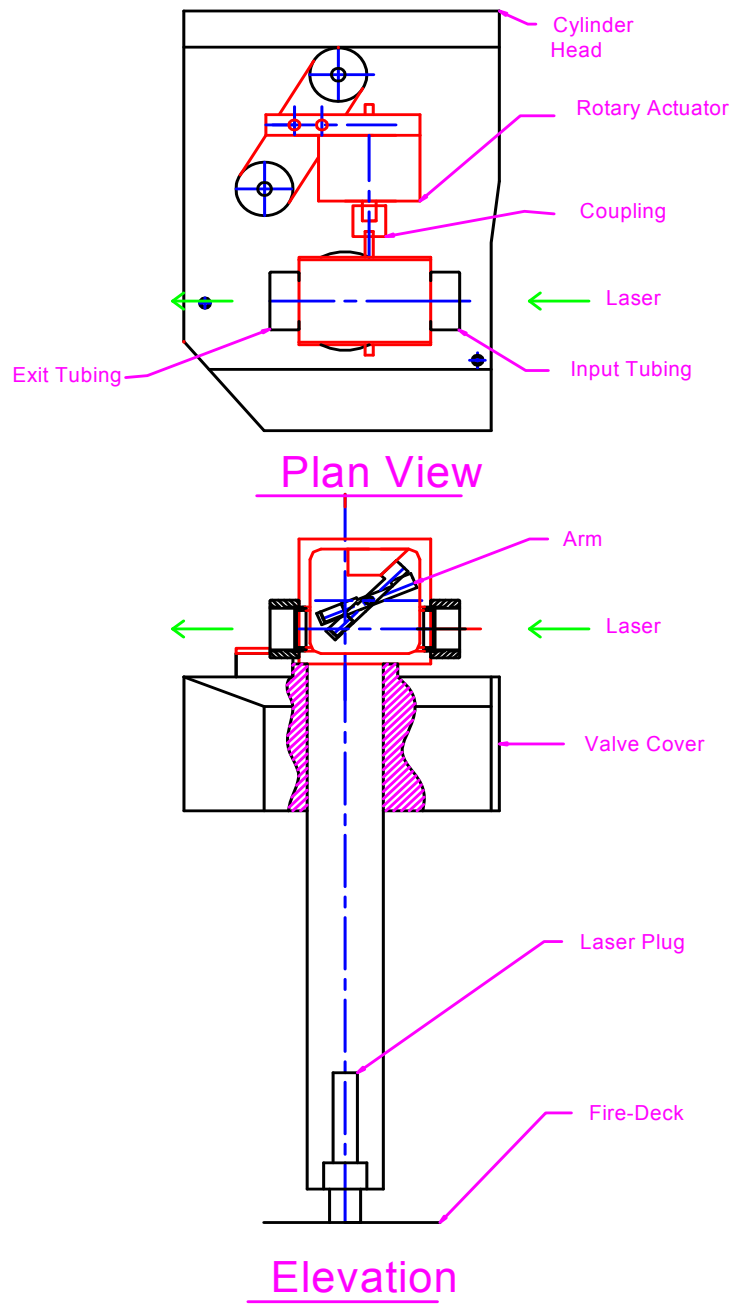


Figure 52. A Schematic of the Integrated ALIS Shown Installed on One Cylinder of a Multi-Cylinder Engine.



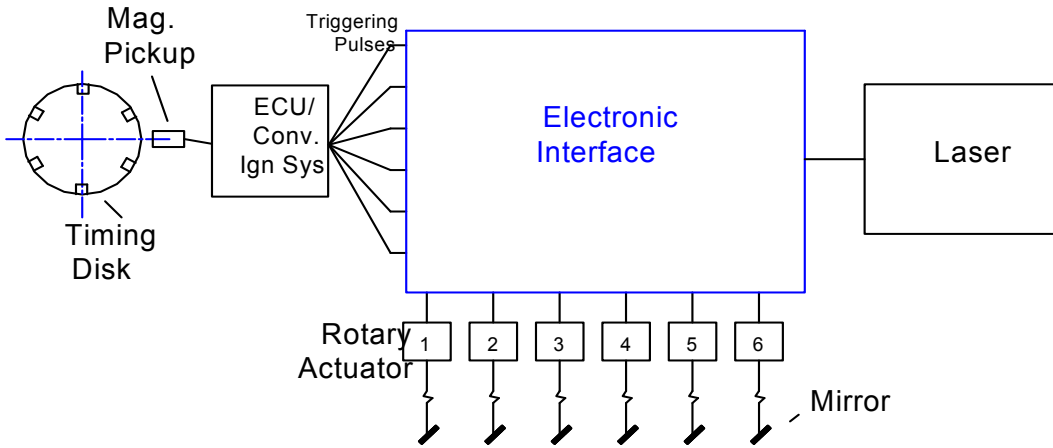
Figure 53. Picture of the ALIS Assembly Mounted on Argonne's QSK-19G Engine (Top View) (Laser Head on the Right is not Shown).

Photo Credit: Argonne National Laboratory

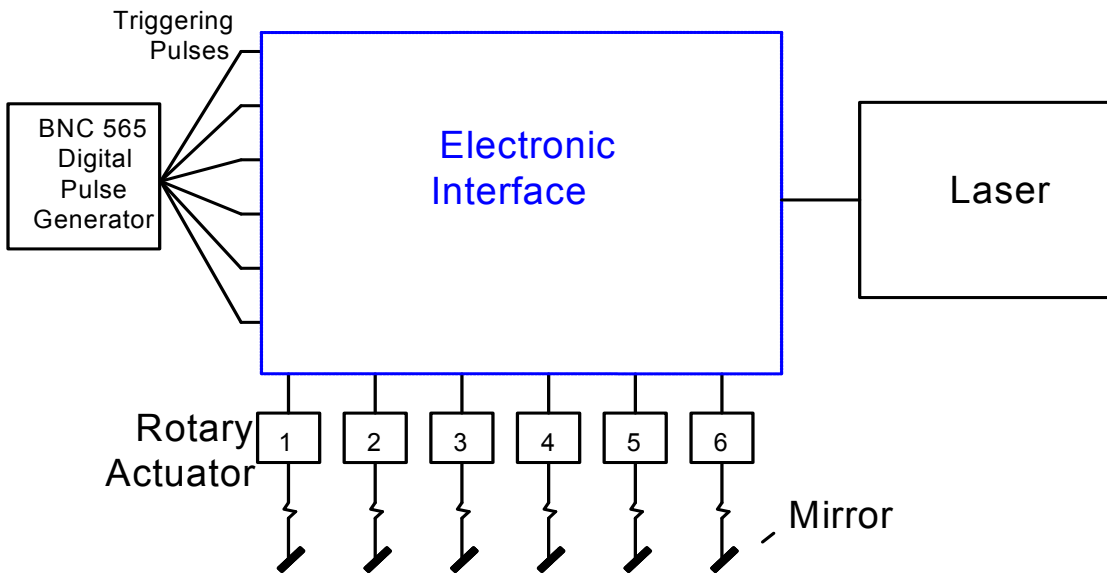
5.2.2. Electronic Integration

The design of the electronic interface was identified through the efforts of a previous task (Task 2.3). Upon completion of these efforts, it was decided to modify existing, commercially available ignition systems for the present proof-of-principle tests. The functional diagram of the electronic interface is shown in Figure 54 (a). In essence, this system (i) activates the rotary actuators, and (ii) provides a firing signal to the laser, coordinated with the activation of the rotary actuator. For the sake of testing the integrated ALIS on a bench scale rig, the triggering signals were supplied by a laboratory digital pulse generator, Model 565 from Berkeley Nucleonics. Such a system provided the flexibility to vary the timing as well as the duration of actuation of individual channels. This is schematically shown in Figure 54 (b).

The functional representation of the electronic interface is shown in Figure 55. In this system the triggering pulses from a digital pulse generator are provided as inputs through 1-6 connectors. Each of these inputs generates a 24 VDC pulse that actuates an individual rotary actuator through outputs connectors 11-16. Additionally, another Transistor-Transistor Logic (TTL) pulse is generated after a delay and routed through an Output Regulator (OR) gate so as to trigger the laser. The delay is adjusted so that the laser output pulse is incident on the mirror at the end of its traverse. Two OR gates are used as the laser has two power supplies each providing a maximum output of 45 Hz. Figure 56 shows timing diagram for 1800 rpm operation where cylinders 1, 3, and 5 are triggered by laser power supply # 1 and cylinders 2, 4, and 6 are triggered by the power supply # 2.



(a)



(b)

Figure 54. (a) Schematic Representation of the use of Electronic Interface in a 6-Cylinder Engine, (b) Schematic Representation of the use of Electronic Interface for Lab-Scale Testing.

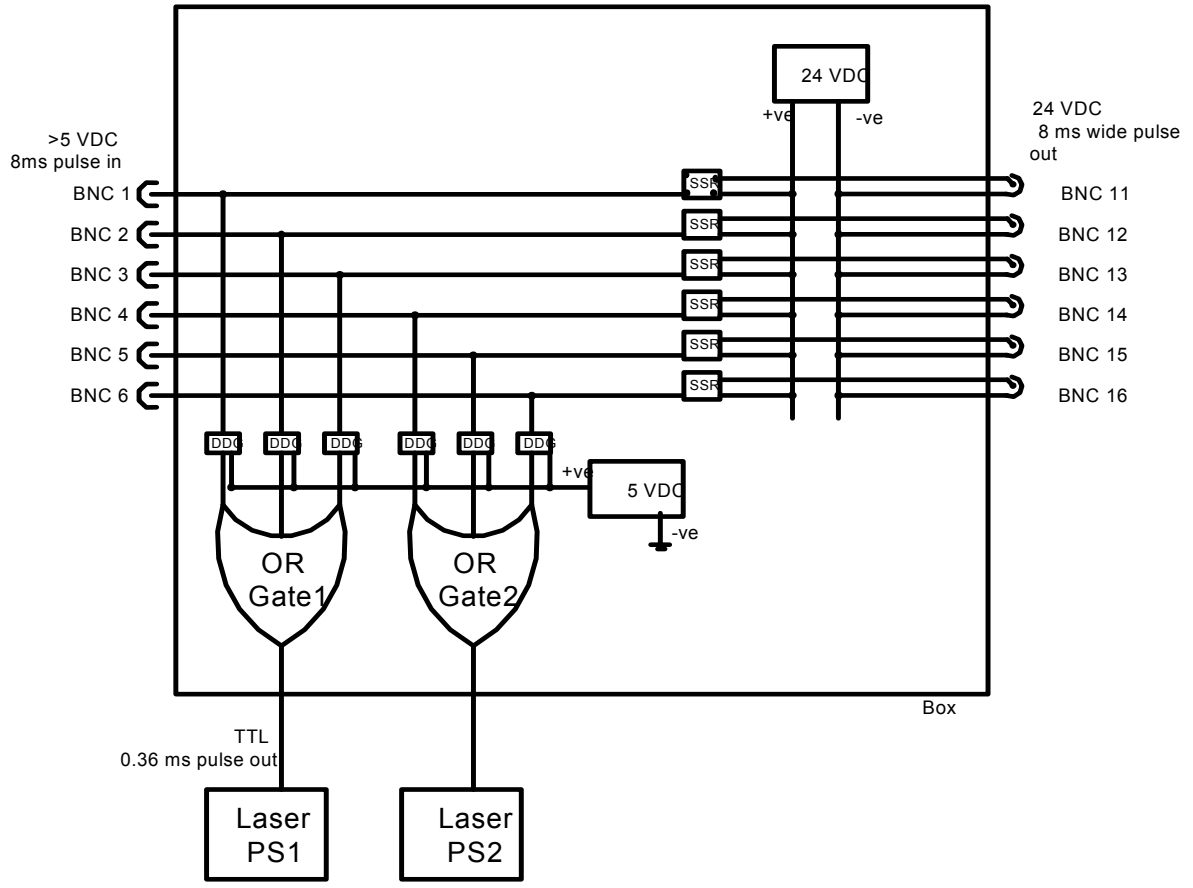


Figure 55. Functional Representation of the Electronic Interface.

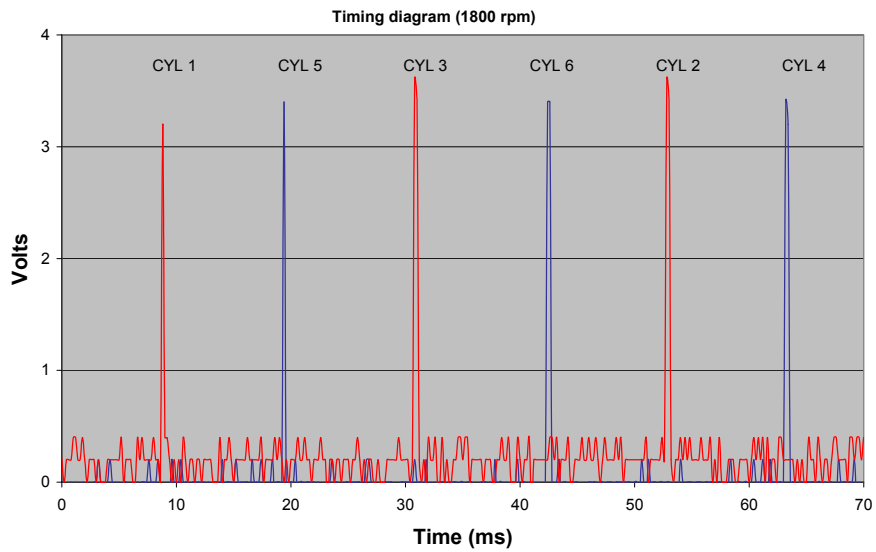


Figure 56. Timing Diagram for 1800 rpm Operation - Red Pulses Trigger Laser Power Supply # 1 While Blue Pulses Trigger Laser Power Supply # 2.

5.2.3. ALIS Testing

The objectives of this testing was to: ensure consistent sparking was achieved on all 6-channels of the system, ensure stability of electronic signals, and check long term durability of the system; minimum 24 hours. Continuous operation was recommended by Cummins before installation on the engine.

With such objectives, the integrated ALIS design was tested for its performance in the laboratory using a test rig that simulates the physical dimensions of the Cummins QSK-19G gas engine. A picture of this rig is shown in Figure 57. TTL pulse signals generated using an 8-channel digital pulse generator, Berkeley Nucleonics 565, were used to simulate the signals from magnetic pickup on the engine. These were used to drive the control box, which in turn, provided the power and driving signals to the actuators and the lasers. The laser plugs used were similar to the ones designed for installation on the QSK-19G engine.

To help in the durability test for 24 hours or more, a misfire detection system was developed (see Figure 58). This essentially consisted of photo detectors (Thorlabs FDS100) placed at the end of 8 inch long plastic tubes. Signals from the photo detectors were screened using voltage comparators and subsequently routed to a counter / timer board (Keithley KPCI-3140) placed in a computer. A visual-basic program helped in data logging.

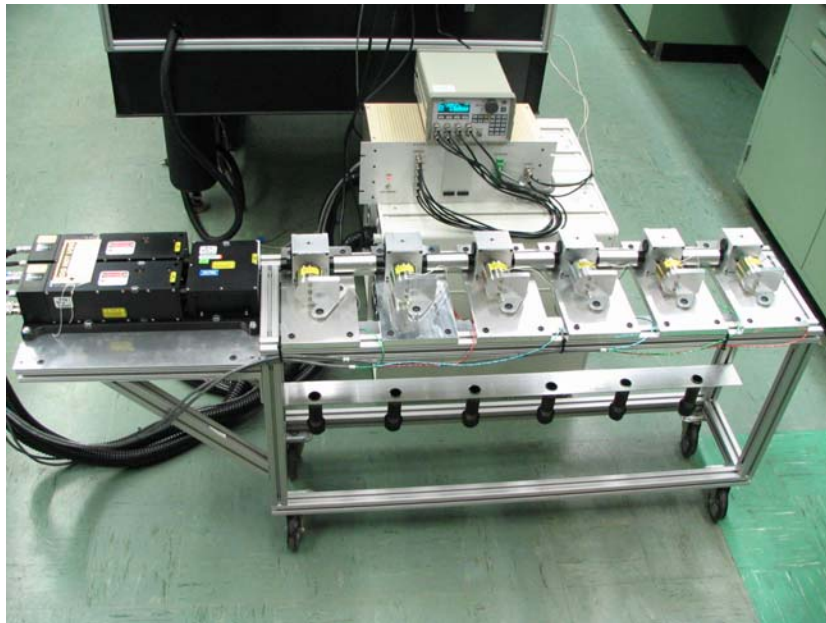


Figure 57. Picture of the 6-Channel ALIS Assembly on the Test Rig (Top View). Also Shown are the Laser, BNC 565 Pulser and the Electronic Interface. Laser Plugs are not Visible.

Photo Credit: Argonne National Laboratory

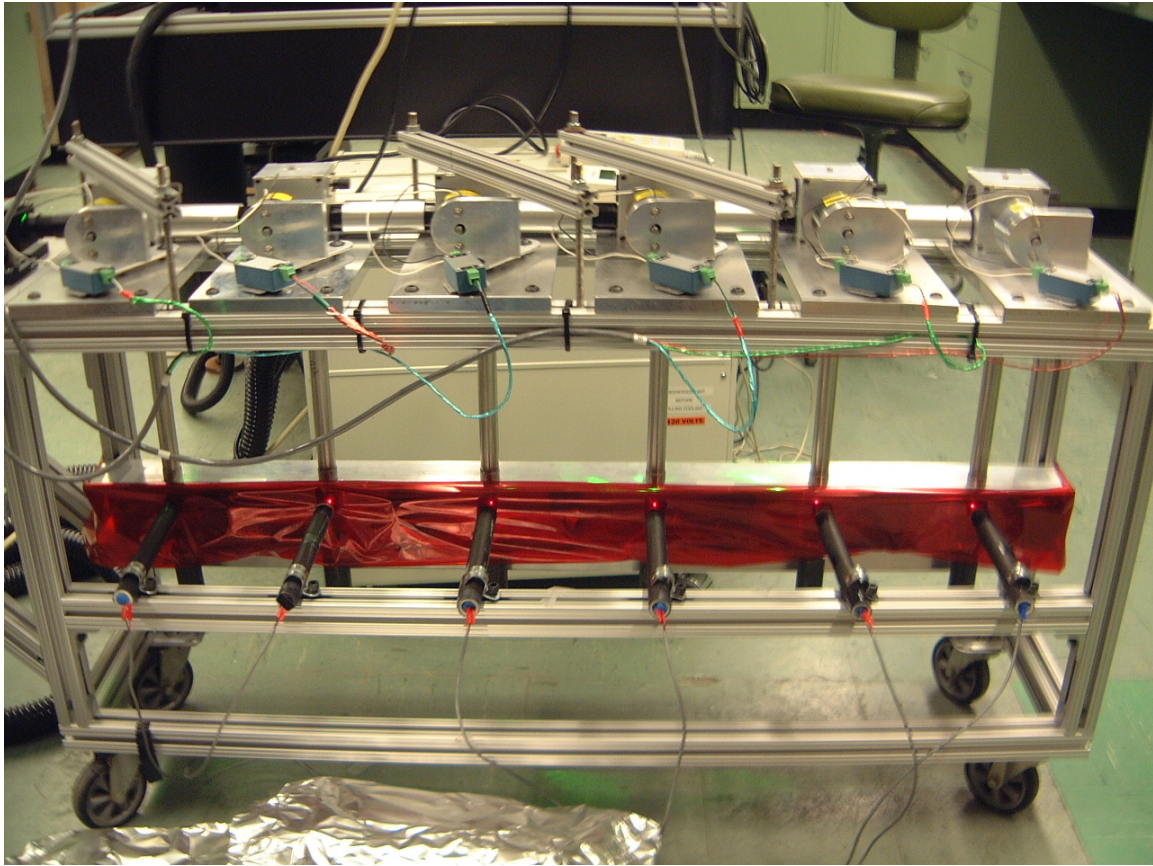


Figure 58. Picture of Misfire Detection System.

Photo Credit: Argonne National Laboratory

Initial trials showed that the signals from the control box drifted over time. This was rectified by using electronic components with higher thermal ratings and the electronic drift/ jitter was reduced to be within ± 3 microseconds. However, consistent sparking could not be achieved on all channels. Subsequently, following a trouble shooting session and analysis, the following changes were made:

- A 2X beam expander was placed in front of the laser (Specialty Optics Company model # 52-25-2X-532),
- The turning optics in the laser head were replaced and the laser was tuned for better performance by BigSky Laser, Inc., and
- Provisions were made to move the mechanical block against which the mirror arm stops to help alignment on the engine.

Subsequent tests performed in the lab showed all 6 channels to be firing consistently over an 8-hour window. Data from a durability test is shown in Figure 59. As seen, the system operated consistently for 8 hours, while operating at an equivalent of 1500 rpm on a 6-cylinder engine. The couplings used between the rotary actuators and mirror arms did not

prove to have the required durability. Efforts are currently being pursued to improve the long-term durability of the system so as to meet the Cummins' requirement of 24 hours or more of continuous operation.

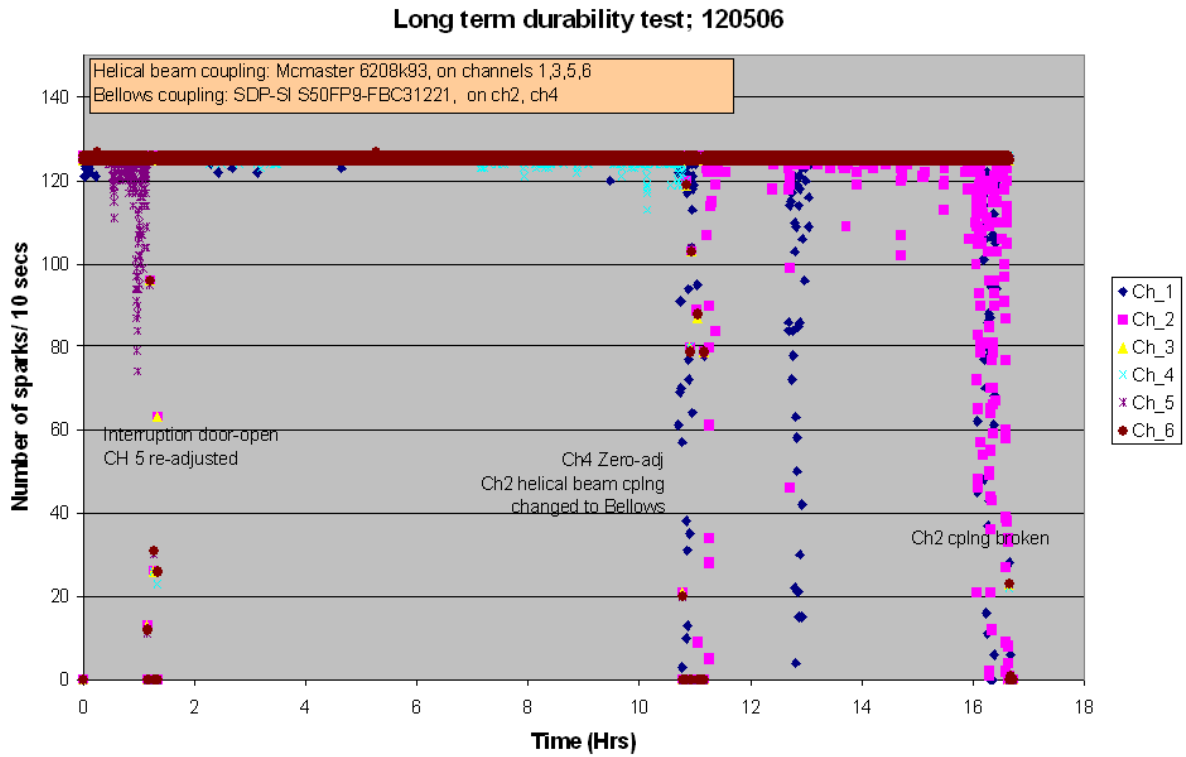


Figure 59. Data From One of the Long-Term Durability Tests.

6.0 (Task 2.6) Performance Testing of Integrated ALIS-ARICE System

The goal of this task is to install the final ALIS design on a multi-cylinder engine and perform tests to quantify the benefits in terms of emissions and performance.

6.1. Statement of Work for Task 2.6

This Task 2.6 included in the installation of the most advanced of the conventional ignition systems from Altronic, Inc. (CPU-95), on a multi-cylinder engine and conduct tests to determine the baseline performance

This was performed at Cummins Engine Company's test facilities, using their production QSK-19G engine which has Altronic ignition system. Since Cummins donated the test cell time to the project, the specific engine that is on the test stand at the time of evaluation was used as baseline. Besides the standard parameters such as engine torque, speed, fuel consumption, temperatures and pressures, the following measurements were made: (i) Combustion pressure trace and analysis, and (ii) Emissions data of regulated species (primarily NO_x).

A test plan in which the engine parameters were varied, to the extent possible, within the ranges mentioned below.

- Load (0–100%)
- Air/ fuel ratio (i.e. λ) (1.0–2.5)
- Ignition timing (0–40° BTDC)
- Intake air pressure (0–45 psig)

Tests were conducted to identify the benefits in terms of performance improvements and reduced emissions.

6.2. Multi-Cylinder Engine Tests

Since the contract with the California Energy Commission was ending on March 31, 2007 and the financial support also ended, this task could not be completed in this contract period. Preliminary tests were completed at the Cummins Engine Company's technical center. In that test, the ALIS worked briefly, firing on two cylinders, but the laser beam could not be focused in other cylinders, due to tolerance stack-up issues of the components. At the suggestion of Cummins designers, a redesign effort will be created to properly assemble the ALIS components in the engine. When and if the financial support from U.S. DOE becomes available.

7.0 (Task 2.7) Economic Evaluation for Feasibility

The goal of this task was to perform an economic evaluation of the feasibility of ALIS in face of its increased initial costs, which are to be offset by the performance and emissions benefits determined in task 2.6. The following activities were planned:

- Estimate the price of a commercially produced ALIS.
- Perform the cost estimates of benefits that account for increased fuel efficiency, higher engine output, lower misfire rate, lower fuel consumption, and lower emissions that result from the use of ALIS.
- Evaluate the viability of ALIS over an engine life cycle on the basis of the above estimates.

The detailed cost analysis at this time is not useful, since all the components have not been finalized yet. However the following discussion gives a brief idea of the order of magnitude of the costs involved.

In a typical laser ignition system, laser plugs and laser system are the prime contributors to the cost of the overall system.

Spark/ laser Plugs: To provide enhanced durability in lean-burn engines, currently iridium tipped spark plugs costing approximately \$200 each are being used. Depending upon manufacturer and engine design, these plugs need spark gap adjustment every 1,000 to 3,000 hours. This being the case, engine manufacturers have expressed interest in obtaining laser plugs up to \$500 provided they have higher durability (up to 6,000 hours). From the designs of the present effort, it can be surmised that the cost target can be achieved, whereas, the durability of the laser plug is yet to be tested over 500 Hours.

Laser systems: The desired first cost of an advanced ignition system, as shown in Table 2 is \$4 per kilowatt-electric (kWe). However, when individually contacted each manufacturer agreed to use a system up to \$20/kWe first cost, provided they have better durability and performance. A DPSS laser system that can drive a 6-cylinder engine is currently commercially available at ~ \$60,000, which translates to \$230/kWe. Technological developments and mass production techniques are anticipated to reduce this cost by a factor of ten to meet \$20/kWe target within the next few years.

8.0 Summary and Conclusions

The project titled: “Advanced Laser Ignition Integrated ARICE System for Distributed Generation in California” produced important results of practical significance toward the development of advanced laser ignition systems for reciprocating engines.

Fundamental RCM studies clearly showed the potential benefits of laser ignition compared to conventional CDI spark ignition: (i) Laser ignition extended the lean operating limit of methane-air mixtures to the lean flammability limit ($\phi_{II} = 0.5$), i.e., much leaner than the lean ignition limit of CDI systems, (ii) Ignition delays were shortened, (iii) Combustion rates were accelerated with laser ignition.

Single-cylinder engine experiments performed with laser ignition realized the potential benefits evidenced in the RCM studies. Compared to conventional CDI spark ignition, laser ignition extended the lean misfire limit by about 10 percent at BMEPs of 10 and 15 bar, increased overall burn rates, and improved combustion stability at all test points. *Most importantly, laser ignition showed a reduction of brake specific NO_x ($BSNO_x$) emissions by about 70 percent at constant engine efficiency or alternately, an increase in brake thermal efficiencies of up to 3 percentage points, while maintaining $BSNO_x$ emissions constant.*

While most of the required components for a successful fiber-coupled laser ignition system were developed, suitable optical fibers for reliable high-power laser transmission were not found. As a result, the ALIS that was finally integrated primarily relied on free-space laser transmission. Tests conducted on a bench-scale system showed that the system has sufficient long-term durability.

In conclusion, this project was a success at the research level, where for the first time a multi-cylinder engine design of an advanced laser ignition system was shown to work effectively in the laboratory. A separate materials research project needs to be undertaken to develop fiber optic laser energy delivery system suitable for engine conditions. The final step to establish the technical viability of the ALIS concept is the performance of an exhaustive series of multi-cylinder engine tests to document the efficiency and emissions benefits of the laser ignition system.

9.0 References

1. Gupta, S. B., Klett, G. M., Biruduganti, M. S., Sekar, R. R., Saretto, S. R., Pal, S., and Santoro, R. J., "Laser Ignition for Natural gas Reciprocating Engines: A literature Review," paper No. 204, CIMAC Congress, Kyoto, 2004.
2. Heywood, J. B., *Internal Combustion Engine Fundamentals*, McGraw-Hill, Inc., 1988, p. 149-150
3. US Patents 5,587,630 and 5,568,801
4. Theiss, N., Ronney, P., Liu, J., and Gundersen, M., "Corona Discharge Ignition for Internal Combustion Engines," ICEF2004-891.
5. Freen, P. D., Gingrich, J., and Chiu, J., "Combustion Characteristics and Engine Performance of a New Radio Frequency Electrostatic Ignition System Igniting Lean Air-Fuel Mixtures" ICEF2004-853.
6. Gao, H., Matthews, R., Hari, S., and Hall, M., "Use of Railplugs to Extend the Lean Limit of Natural Gas Engines," ICEF2004-881.
7. Dale J. D., Smy P. R., Clements R. M., "Laser Ignited Internal Combustion Engine – An Experimental Study," SAE paper 780329, 1978
8. Kopecek H, Wintner E., Pischinger R., Herdin G. R., Klausner J., Basics for a Future Laser Ignition System for Gas Engines, 2000 ICE Fall Technical Conference, ICE-Vol. 35-2, 2000, pp.1-9.
9. Gupta, S. B., Sekar, R., Xu, Z., Leong, K., Reed, C. B., Pal, S., Cramer, J., Santoro, R. J., "Laser Based Ignition of Natural gas-air Mixtures," ASME paper ICES2003-656, Salzburg, Austria, May 2003.
10. McMillian, M.H., Richardson, S., Woodruff, S.D., and McIntyre, D., "Laser-Spark Ignition Testing in a Natural Gas-Fueled Single-Cylinder Engine", SAE Paper 2004-01-0980, March 2004.
11. Kopecek, H., Charareh, S., Lackner, M., Forsich, C., Winter, F., Klausner, J., Herdin, G., Winter, E., "Laser Ignition of Methane-air Mixtures at High Pressures and Diagnostics," ASME-STC 2003-0614.
12. Kitsopanidis, I., and Cheng, W. K., "Auto-ignition Study of Fuel-Rich N-Butane/Air Mixture Using a Rapid Compression Machine," Western States Section/Combustion Institute 2003 Fall Meeting, October 20 & 21, 2003 University of California, Los Angeles Session Paper no. 03F-31.
13. Biruduganti, M. S., Gupta, S. B., Bihari, B., Klett, G. and Sekar, R. R., "Performance Analysis of a Natural gas Generator Using Laser Ignition," ICEF2004-983, ASME Fall Technical Conference, 2004.
14. McMillian, M., Richardson, S., Woodruff, S., McIntyre, D., "Laser Spark Ignition for Natural Gas Fueled Reciprocating Engines," 2005, Gas Machinery Conference GMC2005, Covington, KY, Oct. 3-5, 2005.

15. A.E. Siegman, "New Developments in Laser Resonators," In *Optical Resonators*, SPIE, vol. 1224, 1990.
16. Galvanauskas, A., "High Power Fiber Lasers," *Optics and Photonics News*, pp. 42-47, July 2004.
17. SAE Handbook, 2004.
18. Bihari, B., Gupta, S. B., Sekar, R. R., Gingrich, J. and Smith, J., "Development of Advanced Laser Ignition System for Stationary Natural Gas reciprocating engines," ASME-IC Engines Division Fall Technical Conference, Paper ICEF2005-1325, Ottawa, Canada, 2005.
19. Matsuura, Y., Takada, G., Yamamoto, T., Shi, Y.W., Miyagi, M., "Hollow Fibers for Delivery of Harmonic Pulses of Q-Switched Nd:YAG Lasers," *Applied Optics*, pp. 442-445, 2002.
20. Yalin, A. P., DeFoort, M., Sachin, J., Oleson, D., Willson, B., Matsuura, Y., and Miyagi, M., "Laser Ignition of Natural Gas Engines Using Fiber Delivery," ASME-IC Engines Division Fall Technical Conference, Paper ICEF 2005-1336, 2005.
21. Yalin, A. P., DeFoort, M., Willson, B., Matsuura, Y., and Miyagi, M., "Use of Hollow Core Fibers to Deliver Nanosecond Nd:YAG Laser Pulses for Spark Formation," *Optics Letters*, Vol. 30, Issue 16, Page 2083, August 2005.
22. Konorov, S. O., Fedotov, A.B., Kolevatova, O.A., Beloglazov, V. I., Skibina, N. B., Shcherbakov, A.V., Wintner, E., Zheltikov, A.M., "Laser Breakdown of Millijoule Trains of Picosecond Pulses Transmitted Through a Hollow-Core Photonic-Crystal Fiber," *Journal of Physics D: Applied Physics*, Vo. 36, pp. 1375-1381, 2003.
23. Stakhiv, A., Gilber, R., Kopecek, H., Zheltikov, A.M., and Wintner, E., "Laser Ignition of Engines via Optical Fibers," *Laser Physics*, Vol. 14, pp. 738-747, 2004.
24. Al-Janabi, A.H. and Wintner, E., "High-Power Laser Transmission Through Photonic Bandgap Fibers," *Laser Physics Letters*, Vol. 2, No. 3, pp. 137-140, 2004.
25. Herdin, G., Klausner, J., Wintner, E., Weinrotter, M., Graf, J., "Laser Ignition – A New Concept to Use and Increase the Potentials of Gas Engines," ASME-IC Engines Division Fall Technical Conference, Paper ICEF2005-1352, 2005.
26. Richardson, S., McMillian, M.H., Woodruff, S. D., McIntyre, D. L., "Misfire, Knock and NO_x Mapping of a Laser-Spark-Ignited, Single-Cylinder, Lean-Burn Natural Gas Engine," 2004-01-1853, SAE Fuels & Lubricants Meeting & Exhibition, Toulouse, FRANCE, June 2004.
27. Bradley, D., Sheppard, C. G. W., Suardjaja, I.M., and Woolley, R., "Fundamentals of High-Energy Spark Ignition with Lasers," *Combustion and Flame*, Vol. 138, pp. 55-77, 2004.
28. Yalin, A. P., CSU's Monthly Progress Report to ALIS consortium, August, 2005.

10.0 GLOSSARY

Acronym	Definition
A	Core diameter of the fiber
μm	Micrometers
ALIS	Advanced Laser Ignition System
ANL	Argonne National Laboratory
ARB	California Air Resources board
ARES	Advanced Reciprocating Engine Systems
ARICE	Advanced Reciprocating Internal Combustion Engine
ATDC	After Top Dead Center
BMEP	Brake Mean Effective Pressure (bar)
BSNO _x	Brake Specific NO _x (g/kWh or g/bhp-hr)
BTDC	Before Top Dead Center
C	Celsius
CA	Crank Angle Degrees
CCD	Charge-Coupled Device
CDI	Capacitance Discharge Ignition
CDI	Capacitance Discharge Ignition
CEA2	Chemical Equilibrium for Applications (NASA)
CHP	Combined Heat and Power
COV	Coefficient of Variance
CR	Compression Ratio
CSA	Customer Service Agreement
CSU	Colorado State University
<i>D</i>	Laser beam Diameter as incident on lens
DG	Distributed Generation
DPSSL	Diode Pumped Solid State Lasers
ECU	Electronic Control Unit
EGR	Exhaust Gas Recirculation
EQR	Equivalence Ratio
<i>f</i>	Focal Length
g/bhp-hr	Grams per Brake Horsepower-Hour
g/kWh	Grams per Kilowatt Hour

Acronym	Definition
GW/cm ²	Gigawatts per Square Centimeter
η	Brake Thermal Efficiency (Percent)
HCCI	Homogenous Charge Compression Ignition
HGW	Hollow Glass Waveguide
hp	Horsepower
Hz	Hertz (Frequency)
I_{laser}	Intensity of Laser (Watts)
IMEP	Indicated Mean Effective Pressure (bar)
ϕ	Equivalence Ratio
ϕ_{LL}	Equivalence Ratio Corresponding to Lean Ignition Limit
K	Kelvin
kV	Kilovolts
kVDC	kilovolts Direct Current
kW	Kilowatts
kWe	Kilowatt-Electric
LBI	Laser-Based Ignition
LBIS	Laser-Based Ignition System
M	Laser Beam Mode Quality
MEMS	Microelectromechanical Systems
MFB(#)	Mass Fraction Burn (Percent)
MIE	Minimum Ignition Energy
mJ	Millijoules
mm	Millimeter
MRE	Minimum Required Energy
MTBF	Mean Time Between Failures
MW	Megawatt
$NA_{x=i, e, s}$	Numerical Aperture; subscript: i = incidence, e = exit, and s = at focal spot
Nd:YAG	Neodymium: Yttrium-Aluminum-Garnet
NETL	National Energy Technology Laboratory
nm	Nanometer
N-M	Newton Meter
NO _x	Oxides of Nitrogen
OR	Output Regulator
P/A	Peak-to-Average

Acronym	Definition
ppm	Parts per Million
<u>psig</u>	<u>Pounds Per Square Inch</u>
RCM	Rapid Compression Machine
RPECS	Rapid Prototyping Engine Control System
rpm	Revolutions Per Minute
s	Focal Spot Diameter
SMA	Sub-Miniature – Version A
SOC	Start of Combustion
SwRI	Southwest Research Institute
TTL	Transistor-Transistor Logic
U.S. DOE	United States Department of Energy
UEGO	Universal Exhaust Gas Oxygen
UHC	Unburned Hydrocarbon Emissions
V	Volt
V/ μ s	Volts per Millisecond
VDC	Volts Direct Current
VOC	Volatile Organic Compounds
W/cm ²	Watts per Square Centimeter
w_o	Beam Waist Diameter for a Gaussian Beam
W_o	Beam Waist Diameter for an Actual Beam

Appendix A

Advanced Laser Ignition System (ALIS) Consortium

Argonne National Laboratory (ANL) and National Energy Technology Laboratory (NETL) already had active programs for developing laser ignition for engines applications prior to year 2002, whereas Colorado State University (CSU) proposed laser ignition in response in response to a call for proposals from the United States Department of Energy (USDOE) to Universities. In order to get maximum benefit out of all three independent programs an Ignition Roundtable was held in October 2002 at Argonne National Laboratory and it was decided to pursue ALIS Development as a consortium as proposed by program managers Mr. Ronald Fiskum of USDOE's ARES program, and Dr. Avtar Bining of California Energy Commission's ARICE program.

The consortium comprised of four research institutions (ANL, NETL, CSU and Southwest Research Institute (SwRI)), major engine manufacturers (Caterpillar, Cummins and Waukesha), an ignition system manufacturer (Altronic, Inc.), and funding agencies (USDOE-Distributed Energy Program and California Energy commission).

A.1. Summary of Activities

Various groups in the consortium interacted through monthly conference calls, site visits, and regular meetings until July 2006. The number of such interactions is listed below:

- Monthly teleconference meetings: 19
- Face-to-face meetings: 5
- Site visits: 2 (Argonne National Laboratory and Colorado State University)

During these meetings, research ideas, mutual progress, and plans for future research activities were discussed among the participants. Under the ALIS consortium, a session track "ARES-ARICE Symposium on Gas Fired Reciprocating Engines" was established in the Technical Conferences of the Internal Combustion Engines Division of the American Society of Mechanical Engineers (ASME).

A.2. List of Papers and Presentations by Consortium Members

1. Bihari, B., Gupta, S. B., Sekar, R. R., "High Peak Power and Fiber Optics as Alternative to Spark Ignition: Increasing Efficiencies, Reducing NO_x, and Improving Maintenance schedule," in *High Peak Power and Average Power Lasers*, SPIE Great Lakes Photonics Symposium, June 12-16, 2006, Dayton OH.
2. Bihari, B., Gupta, S. B., Sekar, R. R., Gingrich, J., and Smith, J., "Development of Advanced Laser Ignition System for Stationary Natural Gas reciprocating engines," Proceedings of ASME ICE 2005, Fall Technical Conference, September 11-14 2005, Ottawa, Canada.
3. Bihari, B., Gupta, S. B., Sekar, R. R., "Advanced Laser Ignition System Development Consortium," 2nd Annual Advanced Stationary Reciprocating Engines Conference, March 15 – 16, 2005, Diamond Bar, CA.
4. Klett, G. M., Gupta, S. B., Bihari, B., and Sekar, R. R., "Ignition Characteristics of Methane-air Mixtures at Elevated Temperatures and Pressures," Proceedings of ASME ICE 2005, Spring Technical Conference, April 5-7 2005, Chicago IL.
5. Gupta, S. B., Klett, G. M., Leong, K., Bihari, B., and Sekar, R. R., "Ignition Characteristics of Methane-air Mixtures at Elevated Temperatures and Pressures," A poster presentation at Natural Gas Technologies conference, Jan 30 – Feb 2, 2005, Orlando, Florida
6. Biruduganti, M. S., Gupta, S. B., Bihari, B., Klett, G. M., and Sekar, R. R., "Performance Analysis of a Natural Gas Generator using Laser Ignition," Proceedings of ASME ICE 2004:Fall Technical Conference, Oct 24–27 2004, Long Beach CA
7. Gupta, S. B., Klett, G. M., Biruduganti, M. S., Sekar, R. R., Saretto, S. R., Pal, S., and Santoro, R. J., "Laser Ignition for Natural gas Reciprocating Engines: A literature Review," paper No. 204, CIMAC Congress, Kyoto, 2004.
8. Gupta, S. B., Sekar, R., Xu, Z., Leong, K., Reed, C. B., Pal, S., Cramer, J., Santoro, R. J., "Laser Based Ignition of Natural gas-air Mixtures," ASME paper ICES2003-656, Salzburg, Austria, May 2003.
9. Yalin, A. P., Defoort, M. W., Joshi, S., Olsen, D., Willson, B., Matsuura, Y., and Miyagi, M., "Laser ignition of natural gas using fiber delivery", in Proceedings of ICEF 2005, ASME Internal Combustion Engine Division 2005 Fall Technical Conference, Paper No. ICEF 2005-1336.
10. Yalin, A. P., Reynolds, A. R., Joshi, S., Defoort, M. W., Willson, B., Matsuura, Y., and Miyagi, M., "Development of a fiber delivered laser ignition system for natural gas engines", in Proceedings of ICEF 2006, ASME Internal Combustion Engine Division 2006 Spring Technical Conference, Paper No. ICEF 2006-1370.
11. Yalin, A. P., et. al., "Fiber Delivered Systems for Laser Ignition of Natural Gas Engines", ASME 2006 Fall Technical Conference, ICEF 2006-1574.

12. Yalin, A. P., Defoort, M. W., Willson, B., Matsuura, Y., and Miyagi, M., "Use of hollow core fibers to deliver nano-second Nd:YAG laser pulses for spark formation", *Optics Letter*, 30, 2083-2085 (2005).
13. McMillian, M., Richardson, S., Woodruff, S., McIntyre, D., "Laser Spark Ignition for Natural Gas Fueled Reciprocating Engines," 2005, Gas Machinery Conference GMC2005, Covington, KY, Oct. 3-5, 2005.
14. Richardson, S., McMillian, M., Woodruff, S., McIntyre, D., "Misfire, knock and NO[x] mapping of a laser spark ignited single cylinder lean burn natural gas engine," *SAE transactions* 113:44, 858-865, Society of Automotive Engineers, 2004
15. McMillian, M., Woodruff, S., Richardson, S., McIntyre, D., " Laser Spark Ignition: Laser Development ," *Proceedings of ASME ICE 2004:Fall Technical Conference*, Oct 24-27 2004, Long Beach CA
16. McMillian, M. H., Richardson, S., Woodruff, S. D., and McIntyre, D., "Laser-spark ignition testing in a natural gas-fueled single-cylinder engine", *Society of Automotive Engineers Paper* 2004-01-0980, 2004

APPENDIX B

Future High-Power Optical Multiplexing Technologies

Some additional candidate technologies for high-power optical multiplexing are given below. The performance of these systems is governed by the method of actuation, and hence they are classified accordingly.

B.1. Galvanometer-Based Systems

A photograph of a galvanometer-based system is shown in Figure B1. These systems are primarily used for machining, scanning, and in laser show applications. In these systems, the movement of a magnet is determined by a supplied voltage signal, usually 0-5 VDC. A closed loop control accurately positions the mirror. The optical traverse of such systems is typically 40° with a millisecond time response; however, their lifetime is unknown.

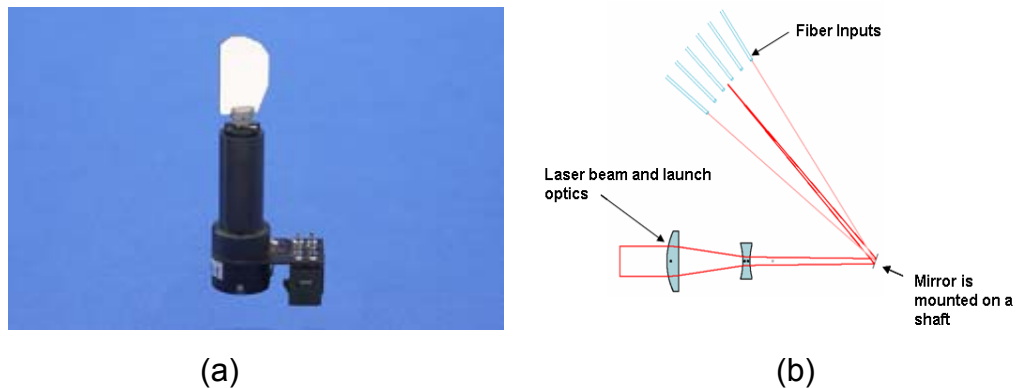


Figure B1. (a) Photograph of a Galvanometer-Based System. Courtesy: Cambridge Technology, Inc. (b) Use of Galvanometer for Laser Scanning [28].

B.2. Piezo-Based Systems

These systems (see Figure B2) operate according to a principle that is somewhat similar to the one shown in Figure B1 (b), except that the actuator is driven by a piezo stack. Though these systems have the required time response, the maximum optical travel is less than 6° . However, they offer relatively higher durability.

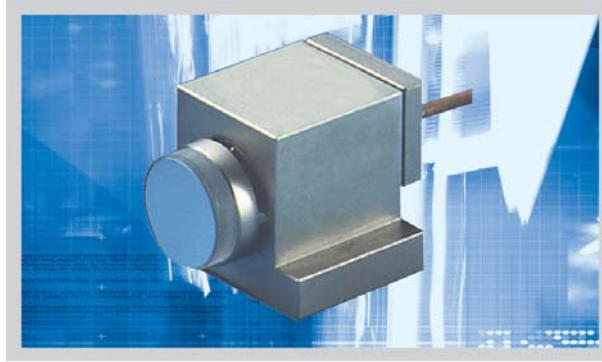
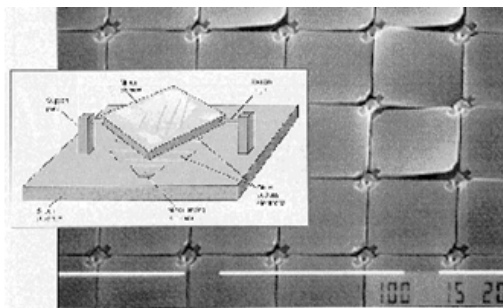


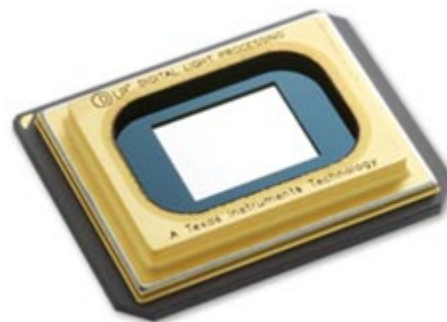
Figure B2. Photograph of a Piezo-Based Laser Scanner. Courtesy: Physique Instrumente.

B.3. MEMS Technology-Based Systems

These systems exhibit several improvements over the two systems discussed above. Using MEMS technology, an array of small mirrors as shown in Figure B3 (a) is manufactured directly onto a small electronic chip. Each of these mirrors repositions itself when activated. The performance characteristics of a readily available chip (see Figure B3 (b)) from Texas Instruments are: (i) array of 2048×1152 mirrors, (ii) response time = $10 \mu\text{s}$, (iii) positions = $\pm 12^\circ$ optical traverse. The inability of these systems to offer more than two positions restricts their use in the case of multi-cylinder engine applications.



(a)



(b)

Figure B3. (a) Photograph of a MEMS-Based Mirror Array, and (b) Texas Instrument's Digital Mirror Device.